

Biophysical Aspects of Single Fluoroalkylamino Acid Substitutions within a Natural Polypeptide Environment



Dissertation zur Erlangung des akademischen Grades des
Doktors der Naturwissenschaften (Dr. rer. nat.)

eingereicht im Fachbereich Biologie, Chemie, Pharmazie
der Freien Universität Berlin

vorgelegt von

Diplom-Chemiker Mario Salwiczek
aus Edderitz (Sachsen-Anhalt), Deutschland

März 2010

1. Gutachterin: Prof. Dr. Beate Korsch (Freie Universität Berlin)

2. Gutachter: Prof. David O'Hagan (University of St. Andrews, Schottland)

Disputation am: 16. Juni 2010

ERKLÄRUNG

Die vorliegende Arbeit wurde auf Anregung und unter Anleitung von Prof. Dr. Beate Kokschi in der Zeit von Juli 2005 bis Dezember 2009 am Institut für Chemie und Biochemie des Fachbereiches Biologie, Chemie, Pharmazie der Freien Universität Berlin angefertigt.

Hiermit versichere ich, die vorliegende Arbeit mit dem Titel „*Biophysical Aspects of Single Fluoroalkylamino Acid Substitutions within a Natural Polypeptide Environment*“ ohne Benutzung anderer als der zugelassenen Hilfsmittel selbständig angefertigt zu haben. Alle angeführten Zitate sind als solche kenntlich gemacht. Die vorliegende Arbeit wurde in keinem früheren Promotionsverfahren angenommen oder als ungenügend beurteilt.

Berlin im März 2010

Mario Salwiczek

Die Dissertation wurde in englischer Sprache verfasst.

Aus dieser Dissertation gingen bisher folgende Veröffentlichungen hervor:

- **M. Salwiczek**, P. K. Mikhailiuk, I. V. Komarov, S. Afonin, A. S. Ulrich, B. Kokschi; Compatibility of the Conformationally Rigid CF₃-Bpg Side Chain with the Hydrophobic Coiled-Coil Interface; *Amino Acids* **2010**, DOI: 10.1007/s00726-010-0581-8.
- T. Vagt, **M. Salwiczek**, B. Kokschi; Molecular Interactions of Fluorinated Amino Acids Within the Hydrophobic Core of a Coiled-Coil Peptide in *Fluorine in Pharmaceutical and Medicinal Chemistry: From Biophysical Aspects to Clinical Applications*; (Editors: V. Gouverneur, K. Müller) Imperial College Press **2010**, in print.
- T. Vagt, E. Nyakatura, **M. Salwiczek**, C. Jäckel, B. Kokschi; Towards Identifying Preferred Interaction Partners of Fluorinated Amino Acids Within the Hydrophobic Environment of a Dimeric Coiled-Coil Peptide; *Org. Biomol. Chem.* **2010**, *8*, 1382-1386.
- S. Samsonov, **M. Salwiczek**, G. Anders, B. Kokschi, M. T. Pisabarro; Fluorine in Protein Environments: A QM and MD Study; *J. Phys. Chem. B* **2009**, *113*, 16400-16408.

- **M. Salwiczek**, B. Kokschi; Effects of Fluorination on the Folding Kinetics of a Heterodimeric Coiled Coil; *ChemBioChem* **2009**, *10*, 2867-2870.
- **M. Salwiczek**, S. Samsonov, T. Vagt, E. Nyakatura, E. Fleige, J. Numata, H. Cölfen, M. T. Pisabarro, and B. Kokschi; Position-Dependent Effects of Fluorinated Amino Acids on the Hydrophobic Core Formation of a Heterodimeric Coiled Coil; *Chem. Eur. J.* **2009**, *15*, 7628-7636.
- **M. Salwiczek**, T. Vagt, B. Kokschi; Application of Artificial Model Systems to Study the Interactions of Fluorinated Amino Acids Within the Native Environment of Coiled-Coil Proteins in *Fluorine in Medicinal Chemistry and Chemical Biology*; (Editor: I. Ojima) Wiley-Blackwell **2009**, 391-409.

Die Ergebnisse wurden des Weiteren auf folgenden Tagungen und Workshops präsentiert:

- **Vorträge**

“Polarität fluorierter Aminosäuren im Kontext von Protein-Protein-Wechselwirkungen“; *ChromForum*, Berlin/Germany, 16.03.2010.

“Biophysical Aspects of Single Fluoroalkylamino Acid Substitutions within a Natural Protein Environment“; *Seminar of the Graduate School #1582 “Fluorine as a Key Element”*, Berlin/Germany, 14.01.2010.

“Fluorinated amino acids: Impacts on the kinetics and thermodynamics of coiled-coil folding“; *Joint workshop of the Physical and Chemical Graduate School Göttingen and the Dahlem Research School “Molecular Sciences”*, Berlin/Germany, 15.09.-17.09.2008.

“Polarity versus hydrophobicity: The impact of fluorinated amino acids on the self-assembly of coiled-coil peptides“; *Young Investigators Mini-Symposium at the 30th European Peptide Symposium*, Helsinki/Finland, 31.08.-05.09.2008.

“Fluorinated amino acids in a native protein environment“; stand-in lecture for Prof. Dr. Beate Kokschi at the Workshop *“Supramolecular chemistry and chemical biology of polypeptides: Synergies towards bio-nanotechnology”*, Kiev/Ukraine, 04.05.-07.05.2008.

“Fluorinated amino acids in native polypeptide environments: Fluorine’s effects on peptide folding and non-covalent protein-protein interactions”; *German-Russian Graduate Student Research School*, St. Petersburg/Russia, 01.09.-02.09.**2007**.

“Fluorinated amino acids: Modulating the metabolic stability and self-assembly properties of peptides and proteins”; stand-in lecture for Prof Dr. Beate Kokschi at the *234th ACS National Meeting & Exposition*, Boston (MA)/USA, 19.08.-23.08.**2007**.

“Fluorine’s effects on peptide folding and non-covalent protein-protein interactions”; Seminar of the *Graduate School #788 “Hydrogen Bonding and Hydrogen Transfer”*, Berlin/Germany, 04.07.**2007**.

- **Poster**

“Biophysical Aspects of Single Fluoroamino Acid Substitutions within the Natural Environment of a Coiled-Coil Peptide”; *19th International Symposium on Fluorine Chemistry*, Jackson Hole, WY, USA, 23.08-28.08.**2009**.

“Fluorinated amino acids in native polypeptide environments: Fluorine’s effects on peptide folding and non-covalent protein-protein interactions”; *XVII International Conference “Horizons in Hydrogen Bond Research”*, St. Petersburg/Russia, 02.09-08.09.**2008**.

“Fluorinated amino acids in native polypeptide environments: Fluorine’s effects on peptide folding and non-covalent protein-protein interactions”; *Tag der Chemie*, Berlin/Germany, 27.06.**2007**.

“Effects of fluorinated amino acids on heterodimeric coiled-coil peptide interactions”; *8th German Peptide Symposium*, Heidelberg/Germany, 14.03.-17.03.**2007**.

For data security reasons the curriculum vitae is not contained in this online version.

For data security reasons the curriculum vitae is not contained in this online version.

For data security reasons the curriculum vitae is not contained in this online version.

PUBLICATIONS, ORAL PRESENTATIONS, POSTER PRESENTATIONS

Publications:

10. M. Salwiczek, P. K. Mikhailiuk, I. V. Komarov, S. Afonin, A. S. Ulrich, B. Koksch; Compatibility of the Conformationally Rigid CF₃-Bpg Side Chain with the Hydrophobic Coiled-Coil Interface; *Amino Acids* **2010**, DOI: 10.1007/s00726-010-0581-8.
9. T. Vagt, M. Salwiczek, B. Koksch; Molecular Interactions of Fluorinated Amino Acids Within the Hydrophobic Core of a Coiled-Coil Peptide in *Fluorine in Pharmaceutical and Medicinal Chemistry: From Biophysical Aspects to Clinical Applications*; (Editors: V. Gouverneur, K. Müller) Imperial College Press **2010**, in print.
8. T. Vagt, E. Nyakatura, M. Salwiczek, C. Jäckel, B. Koksch; Towards Identifying Preferred Interaction Partners of Fluorinated Amino Acids Within the Hydrophobic Environment of a Dimeric Coiled-Coil Peptide; *Org. Biomol. Chem.* **2010**, *8*, 1382-1386.

7. R. Rezai Araghi, C. Jäckel, H. Cölfen, M. Salwiczek, A. Völkel, S. C. Wagner, S. Wieczorek, C. Baldauf, B. Kokschi; A β/γ Motif to Mimic α -Helical Turns in Proteins; *ChemBioChem* **2010**, *11*, 335-339.
6. S. Samsonov, M. Salwiczek, G. Anders, B. Kokschi, M. T. Pisabarro; Fluorine in Protein Environments: A QM and MD Study; *J. Phys. Chem. B* **2009**, *113*, 16400-16408.
5. M. Salwiczek, B. Kokschi; Effects of Fluorination on the Folding Kinetics of a Heterodimeric Coiled Coil; *ChemBioChem* **2009**, *10*, 2867-2870.
4. M. Salwiczek, S. Samsonov, T. Vagt, E. Nyakatura, E. Fleige, J. Numata, H. Cölfen, M. T. Pisabarro, and B. Kokschi; Position-Dependent Effects of Fluorinated Amino Acids on the Hydrophobic Core Formation of a Heterodimeric Coiled Coil; *Chem. Eur. J.* **2009**, *15*, 7628-7636.
3. M. Salwiczek, T. Vagt, B. Kokschi; Application of Artificial Model Systems to Study the Interactions of Fluorinated Amino Acids Within the Native Environment of Coiled-Coil Proteins in *Fluorine in Medicinal Chemistry and Chemical Biology*; (Editor: I. Ojima) Wiley-Blackwell **2009**, 391-409.
2. M. Salwiczek, C. Jäckel, B. Kokschi; Molecular Interactions of Fluorinated Amino Acids in a Native Polypeptide Environment in *Fluorine and Health*; (Editors: A. Tressaud, G. Haufe) Elsevier **2008**, 735-757.
1. C. Jäckel, M. Salwiczek, B. Kokschi; Fluorine in a Native Protein Environment – How Space Filling and Polarity of Fluorinated Alkyl Groups Affect Protein Folding; *Angew. Chem. Int. Ed.* **2006**, *45*, 4198-4203.

Oral presentations at national and international conferences and workshops:

10. "Polarität fluorierter Aminosäuren im Kontext von Protein-Protein-Wechselwirkungen", *ChromForum*, Berlin/Germany, 16.03.2010.

9. "Biophysical Aspects of Single Fluoroalkylamino Acid Substitutions within a Natural Protein Environment"; *Seminar of the Graduate School # 1582 "Fluorine as a Key Element"*, Berlin/Germany, 14.01.**2010**.
8. "Fluorinated amino acids: Impacts on the kinetics and thermodynamics of coiled-coil folding"; *Joint workshop of the Physical and Chemical Graduate School Göttingen and the Dahlem Research School "Molecular Sciences"*, Berlin/Germany, 15.09.-17.09.**2008**.
7. "Polarity versus hydrophobicity: The impact of fluorinated amino acids on the self-assembly of coiled-coil peptides"; *Young Investigators Mini-Symposium at the European Peptide Symposium*, Helsinki/Finland, 31.08.-05.09.**2008**.
6. "Fluorinated amino acids in a native protein environment"; stand-in lecture for Prof. Dr. Beate Kokschi at the Workshop "*Supramolecular chemistry and chemical biology of polypeptides: synergy towards bio-nanotechnology*", Kiev/Ukraine, 04.05.-07.05.**2008**.
5. "Fluorinated amino acids in native polypeptide environments: Fluorine's effects on peptide folding and non-covalent protein-protein interactions", *German-Russian Graduate Student Research School*, St. Petersburg/Russia, 01.09.-02.09.**2007**.
4. "Fluorinated amino acids: Modulating the metabolic stability and self-assembly properties of peptides and proteins"; stand-in lecture for Prof. Dr. Beate Kokschi at the *234th ACS National Meeting & Exposition*, Boston (MA)/USA, 19.08.-23.08.**2007**.
3. "Fluorine's effects on peptide folding and non-covalent protein-protein interactions", Seminar of the *Graduate School #788 "Hydrogen Bonding and Hydrogen Transfer"* Berlin/Germany, 04.07.**2007**.
2. "Interactions of fluorinated amino acids with a native polypeptide environment"; *12. Deutscher Fluortag*, Schmitten/Germany, 06.09.**2006**.
1. "Investigation of OH...FC type hydrogen bonds in peptides using a molecular scaffold"; Seminar of the *Graduate School #788 "Hydrogen Bonding and Hydrogen Transfer"*, Berlin/Germany, 30.11.**2005**.

Posters:

6. "Biophysical Aspects of Single Fluoroamino Acid Substitutions within the Natural Environment of a Coiled Coil Peptide"; *19th International Symposium on Fluorine Chemistry*, Jackson Hole, WY, USA, 23.08-28.08.**2009**.
5. "Fluorinated amino acids in native polypeptide environments: Fluorine's effects on peptide folding and non-covalent protein-protein interactions"; *XVII International Conference "Horizons in Hydrogen Bond Research"*, St. Petersburg/Russia, 02.09-08.09.**2008**.
4. "Fluorinated amino acids in native polypeptide environments: Fluorine's effects on peptide folding and non-covalent protein-protein interactions"; *Tag der Chemie*, Berlin/Germany, 27.06.**2007**.
3. "Effects of fluorinated amino acids on heterodimeric coiled-coil peptide interactions"; *8th German Peptide Symposium*, Heidelberg/Germany, 14.03.-17.03.**2007**.
2. "Concept for the investigation of OH...FC type hydrogen bonds in peptide environments"; *Triple symposium GRK #894/1, GRK #788, and GRK #782*, Freyburg(Unstrut)/Germany, 09.10.**2006**.
1. "Molecular interactions of fluorinated amino acids with native polypeptides"; *Tag der Chemie*, Berlin/Germany, 28.06.**2006**.

DANKSAGUNG

Frau Prof. Dr. Beate Koksche danke ich für die Überlassung dieses sehr abwechslungsreichen und interessanten Themas. Im speziellen möchte ich dafür danken, dass sie mir stets den Freiraum eingeräumt hat, eigene Ideen zu verfolgen und auch umzusetzen. Des Weiteren danke ich ihr für die Bereitstellung finanzieller Mittel für zahlreiche Besuche auf nationalen und internationalen Konferenzen, die meinen wissenschaftlichen Horizont erheblich erweitert haben und es mir ermöglicht haben, mich mit vielen Wissenschaftlern aus unterschiedlichsten Fachgebieten der Chemie und Biochemie auszutauschen.

Ich danke Prof. David O'Hagen (University of St. Andrews, Schottland) für die Übernahme des Zweitgutachtens meiner Dissertation.

In der Arbeitsgruppe möchte ich ganz besonders Toni Vagt, Jessica Falenski und Elisabeth Nyakatura für ihre jederzeit gewährte Diskussionsbereitschaft zu meinem Forschungsthema und allgemeinen Fragestellungen danken. Unsere Gespräche im Kaffeeraum waren immer sehr aufschlussreich und motivierend. Ich danke Harry dafür, dass er unseren Gerätepark im HPLC-Labor gepflegt und instand gehalten hat. In diesem Zusammenhang möchte ich mich auch ganz herzlich bei Carola Feindt (VWR) für die diversen Einführungen in das neue HPLC-System bedanken. Außerdem danke ich Allison Berger und Pamela Winchester für die Korrektur zahlreicher englischsprachiger Manuskripte.

Großer Dank gebührt Dr. Helmut Cölfen und seiner Mitarbeiterin Antje Völkel vom MPI Golm (Potsdam) für die Hilfe bei der Durchführung und vor allem Auswertung der Ultrazentrifugationsexperimente.

Dr. Maria Teresa Pisabarro und Sergey Samsonov vom BIOTEC in Dresden möchte für die Durchführung der Moleküldynamik-Simulationen und die sehr fruchtbare Zusammenarbeit danken.

Weiterer Dank gebührt Prof. Dr. Günther Haufe (Universität Münster) und seinen Mitarbeitern für die Bereitstellung der Aminosäure (S)-2-amino-4-fluoraminobutansäure, die die hier präsentierte Studie sehr bereichert und vor allem vervollständigt hat. Bedanken möchte ich mich in diesem Zusammenhang auch bei Dr. Pavel Mikhailiuk und Prof. Dr. Igor Komarov (Universität Kiev), die mir einen weiteren interessanten Bau-

stein, 3-(Trifluoromethyl)bicyclopent-[1.1.1]-yl glycin, für eine gesonderte Studie bereitgestellt haben.

Ich möchte an dieser Stelle auch ganz herzlich Frau Schmiedtchen, meiner Chemielehrerin in der Oberstufe am Ludwigsgymnasium Köthen, danken. Mit ihrem strengen, aber sehr motivierenden Unterrichtsstil hat sie mein Interesse für die Chemie geweckt und aufrechterhalten. Sie hat mich während meiner Zeit als Zivildienstleistender für die Bewerbung auf ein Stipendium beim Fonds der Chemischen Industrie vorgeschlagen und damit im Prinzip meine Entscheidung zum Chemiestudium getroffen. Ich bin sehr dankbar dafür, dass ich das gelernt habe, was ich immer lernen wollte. Die Grundlagen dafür hat sie gelegt.

Mein größter Dank gilt meiner Familie für den Rückhalt, das Verständnis für meine ständige Abwesenheit und die finanzielle Unterstützung während meines Studiums und der Promotion.

REFERAT

Trotz seiner geringen Häufigkeit als Substituent in natürlichen vorkommenden Biomolekülen ist Fluor auf Grund seines positiven Einflusses auf die pharmakokinetischen und biologischen Eigenschaften von Wirkstoffen ein außerordentlich interessantes Element. Diese Eigenschaften machen die Fluorierung heute zu einem Standard in der Optimierung pharmakologischer Leitstrukturen. Auch fluoriierte Aminosäuren wurden in den vergangenen Jahren in zahlreichen Studien untersucht. Diese Studien zeigen, dass der Einbau von Fluor durchaus positive Effekte beispielsweise auf die Membranpermeabilität, die Strukturstabilität sowie die Stabilität gegenüber Proteasen einiger biologisch relevanter Peptide hat. Jedoch ist das aktuelle Verständnis der Eigenschaften fluorierter Aminosäuren noch begrenzt; das heißt, dass es bis heute nicht ohne weiteres möglich ist, den Einfluss der Fluorierung in der Umgebung nativer Proteine vorauszusagen. Eines der attraktivsten Ziele der biologischen Fluorchemie ist daher eine komplette Charakterisierung der molekularen Wechselwirkungen fluorierter Aminosäuren mit nativen Seitenketten im Kontext von Protein-Protein-Wechselwirkungen.

Im Rahmen dieser Arbeit wurden fluoriierte Analoga der Aminosäure (S)-2-aminobuttersäure hinsichtlich ihrer Hydrophobie mittels HPLC untersucht. Unter Verwendung eines neu entworfenen Proteinmodells auf Basis des α -helikalen *Coiled Coil* Faltungsmotivs wurde weiterhin die Heterodimerisierung verschiedener Peptide, die diese Aminosäuren im hydrophoben Kern enthalten, mit einem ausschließlich nativen komplementären Partnerpeptid charakterisiert. Die Aminosäuren wurden an zwei ausgewiesenen Stellen (a16 oder d19) eingebaut um ihre Effekte auf die Struktur und Stabilität der *Coiled Coils* mittels CD Spektroskopie zu untersuchen. Mit Unterstützung durch theoretische Berechnungen wurde gezeigt, dass sich Unterschiede in Volumen und Polarität der fluoriierten Seitenketten hinsichtlich ihrer Effekte auf die Stabilität in Abhängigkeit von ihrer unmittelbaren Umgebung im hydrophoben Kern unterscheiden. Während in Position a16 das Volumen der Seitenketten die Stabilität des *Coiled Coils* bestimmt, überwiegt in Position d19 auf Grund der unterschiedlichen Orientierung der Seitenketten der destabilisierende Einfluss fluorinduzierter Polarität.

Der Einfluss der Fluorierung auf die Kinetik der Faltung des *Coiled Coils* wurde mittels *Surface Plasmon Resonance* untersucht. Hier zeigte sich, dass Änderungen im Fluorierungsgrad hauptsächlich die Assoziation der Monomere beeinflusst, da diese erheblich von der Hydrophobie abhängt. Wie bereits in früheren Studien gezeigt, scheint ein hoher Fluorierungsgrad trotz erhöhter Hydrophobie die Assoziation zu verlangsamen. Ob dieser Effekt auf der Ausbildung von „Fluorclustern“ im ungefalteten Zustand der Monomere beruht, kann zu diesem Zeitpunkt jedoch nicht eindeutig nachgewiesen werden.

ABSTRACT

Despite its low abundance in naturally occurring biomolecules, fluorine's often favorable impact on their pharmacokinetic and biological properties makes it an outstanding element. In fact, fluorination has become a standard tool in pharmaceutical lead optimization. Peptides and proteins carrying fluorine as an amino acid side chain substituent have also been the topic of numerous studies in recent years. These investigations have revealed interesting results concerning the membrane permeability, structural stability, and stability towards proteolysis of some biologically relevant peptides. However, our current understanding of how these building blocks affect structure formation and thus the biological activity of peptides and proteins is limited. Therefore, it remains difficult to predict the effects of side chain fluorination within natural protein environments. Thus, a complete characterization of the molecular interactions of fluorinated amino acids with their native counterparts in the context of protein-protein interactions is necessary.

In line with the present thesis the hydrophobicity of different analogues of (*S*)-2-aminobutyric acid with increasing fluorine content and side chain volume was investigated by applying an HPLC assay. Furthermore, a newly designed peptide model based on the α -helical coiled coil was used to characterize the heterodimerization of different monomers that present these amino acids within the hydrophobic core with an exclusively native complement. The amino acids were incorporated at two specified positions (either a16 or d19) within the hydrophobic core. With support from theory, the effects on coiled-coil structure and stability were studied by applying CD spectroscopy. It was shown that the impact of size and polarity of the fluorinated building blocks highly depends on the immediate environment of the substitution within the hydrophobic core. At position a16, stability is mainly determined by side chain volume. At position d19, however, the destabilizing impact of fluorine-induced polarity, due to the distinctly different orientation of the side chains at this position, prevails.

The impact of fluorination on coiled-coil folding kinetics was studied by applying a surface plasmon resonance-based biosensor. These investigations revealed that variations in fluorine content mainly affect the association of the monomers, since it highly depends on their hydrophobicity. As has been recognized before, the kinetic data indicate that high fluorine content, despite increasing hydrophobicity, apparently retards association. Whether this effect is based on the formation of 'fluorous clusters' that stabilize the unfolded state of the monomers cannot be concluded at present.

ABBREVIATIONS

AMP	antimicrobial peptides
app.	apparent
BIA	biospecific interaction analysis
CAT	chloramphenicol acetyltransferase
cAMP	cyclic adenosine monophosphate
CD	circular dichroism
CPP	cell penetrating peptides
DBU	1,8-diazabicyclo[5.4.0]undec-7-ene
DIEA	<i>N,N</i> -diisopropyl ethylamine
DNA	deoxyribonucleic acid
DPP IV	dipeptidyl peptidase IV
<i>E. coli</i>	<i>Escherichia coli</i>
EDC	1-ethyl-3-(3-dimethylaminopropyl)carbodiimide
EDTA	ethylenediaminetetraacetic acid
ELE	electrostatic energy
EPL	expressed protein ligation
eq.	equivalent
ESI	electrospray ionization
Fmoc	9-fluorenylmethyloxycarbonyl
FRET	Förster resonance energy transfer
FSPE	fluorous solid phase extraction
GdnHCl	guanidine hydrochloride
GFP	green fluorescent protein
HOAt	1-hydroxy-7-azabenzotriazole
HOBt	1-hydroxybenzotriazole
HPLC	high performance liquid chromatography
MD	molecular dynamics
MM-PBSA	Molecular Mechanics Poisson-Boltzmann Surface Area
MRI	magnetic resonance imaging
mRNA	messenger ribonucleic acid
n.d.	not determined
NHS	<i>N</i> -hydroxysuccinimide
NMR	nuclear magnetic resonance
PDB	Protein Data Bank
PDEA	2-(2-pyridinyldithio)ethane amine
PET	positron emission tomography
PPIases	peptidyl-prolyl isomerases
PTFE	polytetrafluoroethylene
RMSD	root mean square deviation
RP	reversed phase
sec	secondary
SPPS	solid-phase peptide synthesis
SPR	surface plasmon resonance
TBTU	<i>O</i> -(benzotriazol-1-yl)- <i>N,N,N',N'</i> -tetramethyluronium tetrafluoroborate
tert	tertiary

TFA	trifluoroacetic acid
TIS	triisopropylsilane
TOF	time of flight
UV	ultraviolet
VdW	van der Waals
Vis	visible

Abbreviations of the 20 canonical amino acids are consistent with the biochemical nomenclature proposed by the IUPAC-IUB commission (*Eur. J. Biochem.* **1984**, *138*, 9-37).

Abbreviations of non-coded amino acids relevant to the present thesis are given below. Except for alanine, valine, and proline analogues as well as aminobutyric acid, the amino acids are regarded as either alkyl- or arylsubstituted glycines. If not stated otherwise, the abbreviations correspond to the L-amino acids.

Abz	ortho-aminobenzoic acid
3,4CF₃-MePro	(2S)-6-(trifluoromethyl)-3-azabicyclo[3.1.0]hexane-2-carboxylic acid
3-Tfl	3',3',3'-trifluoroisoleucine
4,5CF₃-MePro	(3S)-6-(trifluoromethyl)-2-azabicyclo[3.1.0]hexane-3-carboxylic acid
4CF₃-Phg	4-(trifluoromethyl)phenylglycine
4F-Phg	4-fluorophenylglycine
5-Tfl	5,5,5-trifluoroisoleucine; (S)-2-amino-5,5,5-trifluoropentanoic acid
Abu	aminobutyric acid; (S)-2-aminobutyric acid
CF₃-Bpg	3-(trifluoromethyl)bicyclopent[1.1.1]-1-yl glycine; (S)-2-amino-2-(3-(trifluoromethyl)bicyclo[1.1.1]pentan-1-yl)acetic acid
DfeGly	difluoroethylglycine; (S)-2-amino-4,4-difluorobutanoic acid
DfpGly	difluoropropylglycine; (S)-2-amino-4,4-difluoropentanoic acid
F₃Ala	3,3,3-trifluoroalanine
HfL	5,5,5,5',5'-hexafluoroisoleucine
HfV	4,4,4,4',4',4'-hexafluoroisovaline
MfeGly	monofluoroethylglycine; (S)-2-amino-4-fluorobutanoic acid
TfeGly	trifluoroethylglycine; (S)-2-amino-4,4,4-trifluorobutanoic acid
TfmAla	trifluoromethylalanine, 2-amino-2-(trifluoromethyl)propanoic acid
TfV	4,4,4-trifluoroisovaline; (S)-2-amino-3-(trifluoromethyl)butanoic acid
YNO₂	3-nitrotyrosine

CONTENTS

1	Introduction	1
2	Properties of “Organic Fluorine” and its Relevance in Biological Chemistry	4
2.1	Fluorine as an analytical and diagnostic probe	5
2.1.1	<i>¹⁹F Nuclear magnetic resonance</i>	5
2.1.2	<i>¹⁸F Positron emission tomography</i>	6
2.1.3	<i>C–F Raman spectroscopy</i>	7
2.2	Stereoelectronic consequences of fluorine substitution	8
2.2.1	<i>The size and steric effects of fluorine and fluoroalkyl groups</i>	8
2.2.1	<i>Conformational effects of C–F hyperconjugation</i>	10
2.3	Lipophilicity, hydrophobicity and the ‘fluorous effect’	11
2.4	The impact of fluorination on polar interactions	12
2.4.1	<i>Fluorine’s impact on pK_a</i>	13
2.4.2	<i>Hydrogen bonding</i>	14
2.4.3	<i>Other multipolar interactions</i>	15
2.5	Metabolism and naturally occurring fluorinated organic molecules	16
2.5.1	<i>Metabolism</i>	16
2.5.2	<i>Naturally occurring fluorinated molecules</i>	17
3	Fluorinated Amino Acids in Peptide and Protein Engineering	19
3.1	Incorporation of fluorinated amino acids into peptides and proteins	19
3.2	Fluorinated amino acids as NMR probes	21
3.3	Fluorinated analogues of leucine, isoleucine, and valine in protein engineering	23
3.3.1	<i>Modification of membrane-active peptides by fluorinated amino acids</i>	23
3.3.2	<i>Global fluorination of hydrophobic residues</i>	25
4	Aim of the Work	31
5	Applied Methods	32
5.1	Circular dichroism spectroscopy	32
5.1.1	<i>Physical background</i>	32
5.1.2	<i>Protein structure analysis</i>	34
5.1.3	<i>Thermodynamic analysis of protein folding applying CD spectroscopy</i>	36
5.2	Surface plasmon resonance	39
5.2.1	<i>Physical background</i>	39
5.2.2	<i>Application of SPR in biomolecular interaction analysis</i>	40
6	Results and Discussion	43
6.1	The Coiled Coil as a model for a natural polypeptide environment	43
6.1.1	<i>The coiled-coil folding motif: Structure and function</i>	44
6.1.2	<i>Design of the model system</i>	46
6.2	Hydrophobicity of the fluorinated amino acids	48
6.3	Effects of size and hydrophobicity of fluorinated amino acids at two different positions within the hydrophobic core	52
6.4	Evaluation of the interactions of (S)-4-fluoroaminobutyric acid	55

6.5	Evaluation of the interactions of the newly designed NMR label CF ₃ -Bpg	57
6.6	Helix propensity and coiled-coil stability	59
6.7	Effects of fluorine substitution at position d19 on folding kinetics	62
6.8	Effects of fluorine substitution at position a16 on folding kinetics	64
7	Summary and Outlook	69
8	Literature	74

*Without speculation there is no good
and original observation.*

CHARLES DARWIN

1 Introduction

Life is based upon a precisely scheduled cooperation of biochemical and biophysical processes, most if not all of which depend on the reactions as well as specific interactions, i.e. 'molecular recognition' of biomolecules.^{1,2} Nature has selected one class of molecules - peptides and proteins - to play a key role in controlling the fundamental processes that life depends on. As scaffold molecules they participate in giving different organisms their specific physical appearance. As biocatalysts they perform and host all biotransformations including their own synthesis. They control DNA replication and transcription, as well as the translation of mRNA. Combined with a variety of other, non-peptidic biomolecules they perform and control signal transduction. Their functions include the regulation of food uptake, respiration, reproduction, and for some of the living organisms the modulation of their psychological condition, to name only a few.

Peptides and proteins owe their diverse functions to their tremendous structural versatility. However, although more than 300 naturally occurring amino acids are known, only 20 of them, the canonical α -L-amino acids, have been selected by evolution to be encoded by DNA.³ The primary structure of a peptide or protein, i.e. the sequence with which the amino acids are aligned, predefines its physical and chemical properties. Based on these properties it folds into an individual three-dimensional structure and adopts a specific biological activity. The hypothetical attempt to assemble a tripeptide applying a free choice of genetically encoded amino acids yields 8000 possible peptides. These 8000 hypothetical peptides could in theory each have a specific biological activity. Most naturally occurring peptides and proteins, however, are composed of many more than three amino acids, which may in part explain the vast biological diversity on earth. Each organism is not only characterized by an individual genome but also by a specific set of peptides and proteins, the proteome,⁴ that it codes for. An intact and complete proteome is crucial for an organism to survive. Many diseases arise from protein malfunction due to misfolding⁵ or defective synthesis provoked by mutations at the DNA level.⁶ Also, insufficient secretion of a certain peptide, e.g. insulin, due to organ failure or interactions of external peptides and proteins brought into the body in the course of bacterial and viral infections may be highly pathogenic. It is for these reasons that peptides and proteins are one of the most auspicious molecular entities for developing highly active drugs. Currently, there are 67 therapeutical peptides on the market⁷ including various analogues of human insulin for treatment of type-1 diabetes, which was the first peptide ever to be used as a therapeutical agent. Approximately 150 peptides are in the clinical phase and more than 400 are currently being tested in advanced pre-clinical trials.⁷ One of the most recent highlights is the approval of enfuvirtide (T20), a 36-residue peptide that interferes with membrane fusion mediated by gly-

coproteins on the surface of HIV-1.⁸ Further important targets for peptide based drugs, amongst others, are osteoporosis, cancer, multiple sclerosis as well as cardiovascular diseases.⁹

Peptides as pharmaceuticals stand out due to their very high activity and stringent selectivity; in addition, they accumulate less in tissues and thus exhibit lower toxicity. Furthermore, their metabolic degradation yields non-toxic residues and their tendency to provoke severe immune responses is comparatively low. Unfortunately, there are some major disadvantageous properties of peptides that limit a broad applicability as drugs and are therefore important issues in current pharmaceutical research. Most peptides cannot be administered orally because they are quickly hydrolyzed by the proteases of the gastrointestinal system. Furthermore, their often relatively high polarity impedes delivery through cell membranes, which is especially important for transport through the intestinal membrane as well as the blood brain barrier. These are the main factors that account for peptides' very low bioavailability. To address these issues, research is focused on establishing efficient delivery systems such as liposomes.¹⁰ Furthermore, modifications of their chemical structure are used to stabilize their active conformation and to reduce their susceptibility towards proteolytic degradation.¹¹ To this end, many successful strategies have been established. One of them is the isosteric replacement of the peptide bond by an alkene moiety that mimics its planar character.¹² Another way to prevent hydrolysis is methylation of the amidic nitrogen.¹³ Both chemical modifications may, however, affect hydrogen bond formation at the site of substitution and thus affect folding as well as binding to the target. Proteolytic stability without modification of the peptide bond can likewise be achieved by replacement of native amino acid residues by β - and γ -amino acids,^{14,15} D-amino acids,¹⁶ or α,α -dialkylated residues.¹⁷ In many cases, proteases do not recognize these residues and thus cannot perform cleavage of the adjacent peptide bond. Nevertheless, these modifications have to be carefully placed within a sequence so as to not affect the active conformation of the peptide. One approach that maintains the L-configuration at the α -carbon as well as the native structure of the peptide bond is substitution of amino acids by residues that carry chemically modified side chains that are not found in nature. Ideally, the thereby modified peptide maintains its native conformation as well as its activity and selectivity, whereas binding to the active site of proteases is prevented. In this respect, the substitution of one or more hydrogen atoms by fluorine seems auspicious since fluorination of organic molecules has previously proven useful in the development of therapeutically active molecules as well as in materials science and crop protection. Often, the unique properties of the fluorine atom impart advantageous properties such as increased bioavailability as well as higher biological activity. The great success of fluori-

nation as a strategy in drug development is shown by the fact that to date approximately 20 % of all drugs on the market contain at least one fluorine atom.¹⁸

Fluorination through substitution of native amino acids by fluorine containing analogues has already shown promise in peptide and protein engineering.^{19,20} However, the effects of fluorination on the interactions of peptides with natural protein environments such as receptors are not yet fully investigated. Many reports highlight the often increased hydrophobicity of organofluorine compounds, whereas fluorine-induced polarity and the resulting possibilities to engage in polar interactions within protein environments are less well understood. In this respect, the question of whether carbon-bound fluorine is capable of accepting hydrogen bonds, particularly from protein functional groups, is a matter of scientific controversy. Moreover, there is still no consistent opinion about the so-called 'fluorous effect', a phenomenon that is widely believed to bring about specific self-recognition of fluorinated organic compounds. A complete characterization of the molecular interactions of fluorine as a side chain modification is therefore of great importance. Such studies would enable a directed application of fluorinated amino acids in the *de novo* design of peptides and proteins with new specific functions and selectivity. To this end, systematic investigations based on model systems that mimic natural peptide-protein recognition domains are rather informative. Their characterization provides profound knowledge about the physical and chemical consequences of minor as well as global structural modifications of peptides and proteins by fluorine. Ideally, the observed effects can be generalized and applied to biologically relevant interaction motifs, which then provides the basis for employing fluorination as a new tool in the design of peptide based therapeutical agents.

2 Properties of “Organic Fluorine” and its Relevance in Biological Chemistry

Making up 0.06% of the earth’s crust, fluorine (lat. *fluere*, meaning “to flow”) is three times more abundant than carbon and thus one of the most abundant of all elements.²¹ Despite its high abundance fluorine rarely occurs as a substituent in biomolecules of natural origin,²² which may in part be explained by the extremely low aqueous solubility of fluorine-containing minerals such as fluorite (CaF₂) and cryolite (Na₃AlF₆). Consequently, sea water contains only 1.3 ppm of fluoride resulting in a very low biological availability.²² Furthermore, since its nucleophilicity in water is very low, biotransformations involving the fluoride ion are rare. In a laboratory setting, the unique properties of fluorine and its effects as a substituent in biologically relevant molecules, on the other hand, make it an attractive tool in biological chemistry. Besides its application as an analytical label, fluorine is broadly used as a substituent in biomolecules where the goal is to improve biochemical properties such as metabolic stability, hydrophobicity, and conformation. In many cases chemical modification by fluorine or fluorinated alkyl groups brings about a considerable improvement in biological activity as well as pharmacokinetic properties. These effects are due to fluorine’s unique physicochemical properties: very high electronegativity and electron affinity combined with very low polarizability and high stability in carbon-fluorine bonds (Table 2.1). The most relevant consequences of fluorination in a biological context and especially those that are important for peptide and protein interactions are summarized in the following sections.

Table 2.1 Key physical data of the fluorine atom and the C–F bond compared to other halogens and biologically relevant elements.

X	Ionization potential [kcal/mol] ^a	Electron affinity [kcal/mol] ^a	Polarizability [Å ³] ^a	C–X bond strength [kcal/mol] ^b	VdW-Radius [Å] ^a	Electronegativity [χ _p] ^a
H	313.6	17.7	0.667	98.8	1.20	2.20
F	401.8	79.5	0.557	105.4	1.47	3.98
Cl	299.0	83.3	2.18	78.5	1.75	3.16
Br	272.4	72.6	3.05	65.9	1.85	2.96
I	241.2	70.6	4.7	57.4	1.98	2.66
O	314.0	33.8	0.82	84.0	1.52	3.44
N	335.1	-6.2	1.10	69.7	1.55	3.40
C	240.5	29.0	1.76	83.1	1.70	2.55

^a Ref. 23 ; ^b Ref. 24

2.1 Fluorine as an analytical and diagnostic probe

2.1.1 ^{19}F Nuclear magnetic resonance

Fluorine exists primarily as the ^{19}F isotope, which is NMR-active and has a broad frequency range over roughly 100 ppm in organic molecules.²⁵ Its sensitivity is only marginally lower than that of hydrogen (83% relative to ^1H) and, importantly, a single substitution of fluorine for hydrogen in most cases does not severely alter the conformation or biological activity of the molecule. In addition, the virtual absence of naturally occurring fluorinated biomolecules prevents undesired background signals thus facilitating data evaluation. These properties make ^{19}F an excellent NMR label with numerous and ever emerging applications in medicinal diagnostics as well as protein structure analysis.^{26,27}

The great potential of ^{19}F NMR as a non-invasive diagnostic tool and imaging technique has been shown, for example, by Brix *et al.* They investigated the pharmacokinetics and metabolism of the highly potent anti-cancer agent 5-fluorouracil (Figure 2.1) in an animal model by combining ^{18}F positron emission tomography (^{18}F PET, see next section) and ^{19}F NMR.²⁸ While PET detects ^{18}F with high spatial and temporal resolution, it cannot resolve signals emitted by different metabolites. Due to the broad chemical shift range of ^{19}F and its sensitivity towards even marginal environmental and structural changes, ^{19}F magnetic resonance imaging (^{19}F MRI) was successfully applied here to monitor the metabolism of 5-fluorouracil. However, the usually low *in vivo* concentration of the analytes involves a very low signal-to-noise ratio. Therefore, clinical *in vivo* studies are either very time consuming or require strong magnetic fields that are expensive in energy and also imply a certain safety risk.²⁹ In contrast to magnetic resonance based on ^1H , ^{19}F MRI is, therefore, less commonly used in clinical applications. Nevertheless, ^{19}F NMR is a useful technique to study metabolism²⁷ outside the patient and is, thus, a powerful tool in drug development.

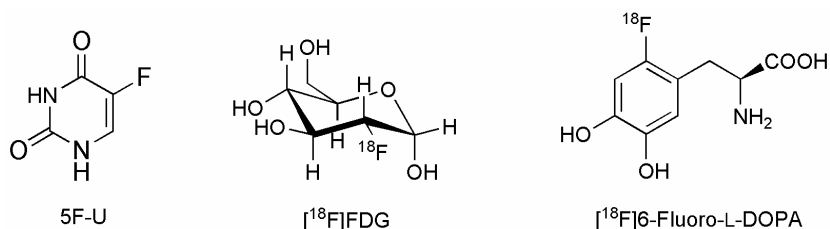


Figure 2.1 From left to right: Structure of 5-fluorouracil, the first pyrimidine analogue to be used as an antitumor agent;³⁰ trade names Fluoroplex, Carac, and Efudex;³¹ and structures of $[^{18}\text{F}]\text{FDG}$ and $[^{18}\text{F}]\text{6-Fluoro-L-DOPA}$.

Besides being used to probe metabolism, ^{19}F NMR has shown outstanding potential in studying the structure and interactions of biological macromolecules such as proteins and DNA. In the context of peptides and proteins, the ^{19}F nucleus is easily incorporated

into primary structures in the form of fluorinated amino acids. As the properties and applications of fluorinated amino acids are discussed in a separate chapter (chapter 3) some recent highlights of ^{19}F NMR application in peptide and protein analysis are summarized there.

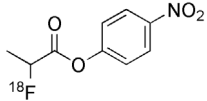
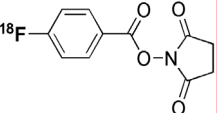
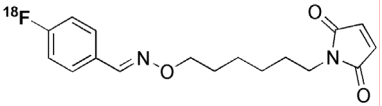
2.1.2 ^{18}F Positron emission tomography

Positron emission tomography is a powerful method in medicinal diagnostics that allows for real-time imaging of drug distribution *in vivo*. It provides spatial and temporal information on metabolic pathways at high resolution and has thus found broad application in neurology, cardiology, and oncology. ^{18}F is the most commonly used radio label in PET because of its low positron energy (0.64 MeV) that accounts for its comparatively low risk to the patient.³² In addition, its half-life of 110 min is sufficient for detailed real-time imaging of drug pathways without needlessly incriminating the patient. Equally important, it suffices to synthesize the tracer molecules. The most successful commercial PET agent is 2- ^{18}F -fluoro-deoxy-D-glucose (^{18}F FDG) (Figure 2.1); it is used for monitoring glucose metabolism.³³ Another prominent example is the amino acid analogue 6- ^{18}F -fluoro-3,4-dihydroxyphenylalanine (^{18}F 6-fluoro-L-DOPA) that is used for imaging cerebral dopamine pathways³⁴ as well as different tumors.³² However, there are many more PET tracers in use today, e.g. nucleosides, phospholipids, and sex hormones.³²

The paramount biological importance of peptides drives the development of peptide-based radiotracers containing the ^{18}F -label. The production of radiotracers requires so-called "hot" fluorination methods, where the active isotope is incorporated shortly prior to use. However, since peptides and proteins carry a large number of functional groups such as amines, carboxylic, guanidine and thiol groups that are crucial for their activity, direct nucleophilic fluorination, which is most commonly used,³⁵ may result in inactivation.³⁶ Therefore, radiolabeling of peptides is usually accomplished by means of bioconjugation with different prosthetic groups (Table 2.2) that are, due to the limited half-life of ^{18}F , incorporated only late in synthesis prior or subsequent to deprotection, depending on the chemistry applied.

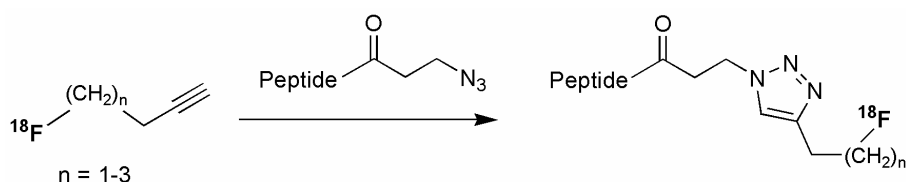
The outstanding properties of peptides, such as high specificity in molecular recognition as well as low toxicity, make them an attractive candidate for radiotracer development. However, despite of all progress that has been made in labeling strategies, the synthesis of peptides and their purification are still rather time consuming, which represents a certain drawback for routine clinical applications.

Table 2.2 Some examples of prosthetic groups used for radiolabeling of peptides.

Prosthetic group	Labeling agent	Method	Peptide
2-[¹⁸ F]-fluoropropionyl		N-Acylation	(D)Phe ¹ -Octreotide ³⁷
4-[¹⁸ F]-fluorobenzoyl		N-Acylation	α-MSH ^{a, 38}
[¹⁸ F]-FBAM ^b		S-alkylation ^c	Glutathione/ LDL ^{d, 39}

^a α-melanocyte releasing hormone, ^b N-[6-(4-[¹⁸F]-fluorobenzylidene)aminoxyhexyl]maleimide, ^c via addition to the maleimide double bond, ^d low-density lipoprotein

In this respect, the application of "click" chemistry to the radiolabeling of peptides⁴⁰ holds great promise as a clinically applicable labeling strategy (Figure 2.2) because it can be carried out in aqueous media under physiological conditions. Furthermore, "click" chemistry yields stable products and tolerates virtually all of the functional groups present in a peptide. The reactive groups (either an azide or an alkyne) are easily incorporated into peptides and product isolation and purification are relatively simple and fast.⁴¹

**Figure 2.2** Labeling of an N-(3-azidopropionyl)peptide applying "click" chemistry according to Marik et al. 2006.⁴⁰

Direct nucleophilic fluorination of some model peptides has been achieved only very recently.⁴² This new approach takes advantage of N-terminally capping peptides with benzoyl moieties that carry electron-withdrawing substituents (cyanide) adjacent to a good leaving group such as trimethylammonium substituents. These modifications allow for quick and efficient labeling of peptides under mild conditions by means of nucleophilic fluorination at the aromatic ring.

2.1.3 C–F Raman spectroscopy

Although the body of literature dealing with C–F Raman spectroscopy in pharmaceutical chemistry and medical diagnostics is still rather small, this newly developing meth-

odology shows great promise in drug development. Since C–F exhibits unique emission bands in the range of 500 to 800 cm^{-1} , this method also profits from the virtual absence of naturally fluorinated biomolecules.⁴³ Trifluoromethyl groups, aromatic C–F bonds, and difluoromethylene groups are easily distinguishable based on their specific vibrational emission bands.⁴⁴ Furthermore, the method is highly sensitive enabling qualitative and quantitative analysis of, for example, fluorinated drugs in pure samples as well as mixtures. Therefore, C–F Raman spectroscopy represents one more tool to investigate the metabolic fate and pathway of drugs.⁴⁵

2.2 Stereoelectronic consequences of fluorine substitution

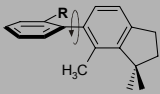
The steric properties of a molecule or substituent, i.e. its size and conformation, to a great extent determine specificity in molecular recognition. One aspect of the optimization of pharmaceutical lead compounds is variation of substituents in an attempt to mimic a natural substrate. The goal is to endow the newly developed molecule with substituents that are isosteric to those of the natural analogue while imparting higher (metabolic) stability, activity, or ideally both. The concept 'bioisosterism', thus, comprises not only the steric properties of a molecule but also its biological activity.^{46,47} Substituents or molecules are termed 'bioisosteric' when they are chemically and physically similar and, most importantly, exhibit equal or improved biological properties compared to the original lead compound or natural analogue.

2.2.1 The size and steric effects of fluorine and fluoroalkyl groups

The van der Waals radius of fluorine (1.47 Å) lies between that of hydrogen (1.20 Å) and oxygen (1.52 Å).²³ Single substitutions of fluorine for hydrogen, hydroxyl groups, or carbonyl oxygen in biologically relevant molecules are, in many cases, conservative in terms of structure and activity.⁴⁸ Therefore, especially the substitution of one fluorine atom for hydrogen is widely considered bioisosteric. While this is true only for single fluorine substitutions, the size of multiply fluorinated alkyl groups such as trifluoromethyl frequently faces scientific controversy. This may in part be attributed to the fact that results from different studies are often exclusively interpreted in terms of steric size neglecting electronic contributions, rotation, and shape of the residues considered. Additionally, the parameters used to evaluate steric properties may be highly specific for the model under observation.⁴⁹ Thus, estimates of the size of CF_3 in the literature vary from methyl⁵⁰ up to *sec*-butyl and phenyl.⁵¹ Comparison of the van der Waals volumes (Table 2.3), however, clearly shows that the actual volume of CF_3 lies halfway

between that of methyl and isopropyl. Rotational barriers of substituted 6-aryl-1,1,5-trimethylindanes studied by NMR⁵² (Table 2.3) further suggest that the trifluoromethyl group indeed most closely resembles an isopropyl group, although the latter is bigger and dissimilar in shape. The fact that both groups nevertheless impart almost identical rotational barriers to the aryl substituted indane demonstrates that steric interactions depend on the shape and flexibility of a substituent in addition to its volume. Thus, comparing steric *effects* rather than steric *size* itself may be more meaningful and one has to keep in mind the participation of electronic effects, especially in the case of the highly electronegative fluorine.

Table 2.3 Rotational barriers of substituted 6-aryl-1,1,5-trimethyl indanes.

	V_{VdW} [Å]	$\Delta G^{\#a}$ [kcal/mol]
R = CH ₃	21.6	19.3
CF ₃	39.8	21.9
CH(CH ₃) ₂	56.2	22.2
Phenyl	91.6	17.6

^a free energy of activation at 340 K

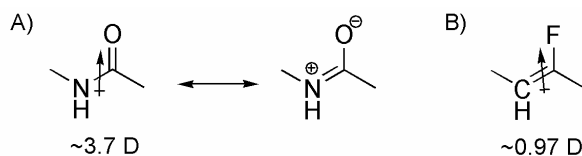


Figure 2.3 A) Resonance structures of the peptide bond and B) a fluoroethylene isostere. The arrows represent dipole orientation.⁵³

The strong inductive effect of fluorine becomes especially important when it is used as a replacement for oxygen. In peptides, a fluoroethylene unit can replace a peptide bond both sterically and electronically.⁵⁴⁻⁵⁷ Here, the double bond imitates the peptide bond's planar character while being stable to hydrolysis by enzymes. Meanwhile, fluorine mimics the carbonyl oxygen thus maintaining dipole orientation (Figure 2.3). Besides conferring hydrolytic stability to a peptide, the fluoroolefine peptide bond isostere is fixed in either a *cis* or *trans* configuration and accordingly can be used to alter or stabilize the conformation of a peptide, respectively.⁵⁸ While native peptide bonds are usually found in the more stable *trans* configuration, 10-30% of the acyl-proline bonds in small peptides are *cis*-configured, which results from steric hindrance due to *N*^α-alkylation.⁵⁹ Since *cis-trans* isomerization is crucial for the three-dimensional structure of proline-containing peptides and proteins but slow compared to folding, peptidyl-prolyl

isomerases (PPIases) have evolved in nature. Some of these enzymes regulate the function of proteins related to immunosuppression as well different diseases such as AIDS, Alzheimer's, and cancer. Therefore, efforts towards specifically inhibiting these and other proteins by applying fluoroolefine-based peptide bond isosteres show great potential in medicinal chemistry.^{58,59} Recently, alkene and fluoroalkene peptide bond isosteres have also been used to probe the importance of intrahelical hydrogen bonds on the activity of anti-HIV fusion peptides.⁶⁰ It was found that the fluoroalkene is a better mimic of the peptide bond, since the modified peptides have a higher activity than those containing the hydrocarbon alkene.

2.2.1 Conformational effects of C–F hyperconjugation

The C–F and C–O bond are similar in length (~ 1.4 Å) and dipole orientation. In addition, both have a low energy σ^* antibonding orbital that may undergo hyperconjugation. One prominent consequence of this is the anomeric effect (Figure 2.4). The methoxy and fluorine groups prefer the axial position in 2-methoxytetrahydropyran and 2-fluorotetrahydropyran, respectively.⁶¹ This effect can be explained by hyperconjugation, i.e. lone pair donation from the pyran oxygen nonbonding orbital (HOMO) into the $\sigma^*_{\text{C-O}}$ / $\sigma^*_{\text{C-F}}$ orbital (LUMO), which would be impossible for the equatorial conformer. Fluorination of sugars has, therefore, gained much recognition in recent years. Many analogues of furanoses and pyranoses are described and hold great potential as enzyme inhibitors (e.g. glycosidases), nucleoside mimics with antitumor activity, and radio imaging agents⁶² (see section 2.3).

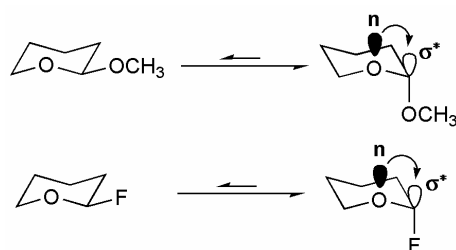


Figure 2.4 Anomeric effect of fluorine compared to oxygen in tetrahydropyran.

Another conformational consequence based on hyperconjugation⁶³ is the *gauche* effect. Other than intuitively expected, 1,2-difluoroethane prefers the *gauche* over the *anti* rotamer despite the steric clash and electronic repulsion of the two fluorine atoms (Figure 2.5), which is in contrast to equally disubstituted chloro- and bromoethanes. Chlorine and bromine atoms both have a bigger VdW-radius (see table 2.1) and, therefore, unfavorable steric interactions should make larger contributions as compared to fluo-

rine. Furthermore, due to the high electronegativity of fluorine, the C–F σ^* orbital is a much better electron acceptor than the respective C–Cl and C–Br σ^* orbitals. In the case of 1,2-difluoroethane, and accordingly in difluoroethyl subunits of any other alkyl chain, electron density from the C–H σ orbital is donated into the C–F σ^* orbital, which is only possible in a *gauche* conformation. Apparently, the hyperconjugative stabilization overrides the steric and electronic repulsion of the fluorine atoms.

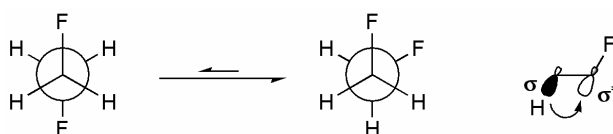


Figure 2.5 *Gauche effect in 1,2-difluoroethane through hyperconjugation.*

It should be added that another explanation for the *gauche* effect in 1,2-difluoroethane has been proposed. The bent bond model⁶⁴ reasons that the *anti* conformer is destabilized by electron density building up on opposite sites of the C–C bond thus reducing orbital overlap. In the *gauche* conformer electron density is build up on the same side of the C–C bond, which results in a slight bending of the bond and enables a better overlap of the orbitals. However, more recent calculations show that the overlap increase is too small to effectuate the high energetic preference (~ 1 kcal/mol) of the *gauche* over the *anti* conformer.⁶³

The *gauche* effect has also been observed for fluorinated amides,⁶⁵ esters,⁶⁶ β -fluoroalcohols, and protonated amines.⁶⁷ All of these linkages and functional groups are very common in biologically active molecules and, therefore, the fluorine *gauche* effect holds promise as a tool to modulate their activity based on conformation. Moreover, it has strong implications for the conformation of fluorinated amino acids, especially proline where it affects the *cis-trans* isomerization of the peptide bond as well as the conformation of the pyrrolidine ring.⁶⁸ Thus, a single fluorine atom can be used to alter the conformation of an entire peptide chain.

2.3 Lipophilicity, hydrophobicity and the 'fluorous effect'

Lipophilicity is considered key to membrane permeability and thus to a great extent determines the bioavailability of drugs. Consequently, it is an important issue in pharmaceutical lead optimization. Many investigations are motivated by the general notion that fluorination increases lipophilicity and is thus a useful tool to improve receptor-ligand interactions as well as membrane permeability. There are, however, two problems with such a generalization. First, some but not all fluorinated compounds are

more lipophilic than their hydrocarbon congeners. This statement holds true for aromatic and olefinic compounds, while a decrease in hydrophobicity is often observed for partly fluorinated aliphatic hydrocarbons.⁶⁹ The impact of fluorine furthermore highly depends on the number of fluorine substitutions and their position relative to certain functional groups. For example, fluorination reduces the basicity of amines, which renders them less easy to protonate. Consequently, the molecule more readily penetrates a membrane.⁷⁰ Second, the terms ‘hydrophobicity’ and ‘lipophilicity’ are sometimes confused or considered synonymous. Usually both properties correlate very well but, as stated above, some fluorinated compounds share the interesting property of being more hydrophobic and at the same time less lipophilic than hydrocarbons of equal structure. This arises from fluorine’s high electronegativity and low polarizability. Fluorine strongly withdraws electron density from its surroundings and renders a molecule reluctant to interactions with water thus making it more *hydrophobic*. Based thereon, fluorinated compounds show a greater preference for the organic phase in partitioning experiments, which is then often interpreted in terms of greater lipophilicity. The partitioning coefficient $\log P$ of a compound, however, is a measure of relative solubility and expresses the reduced solubility in water, i.e. hydrophobicity, rather than lipophilicity. On the other hand, the lowered polarizability also diminishes favorable dispersion interactions between the fluorinated compounds and other hydrocarbons. This is shown, for example, by the lower boiling points of perfluorocarbons relative to hydrocarbons.⁶⁹ Thus, as far as aliphatic hydrocarbons are considered, fluorination also makes the molecule more *lipophobic*. This character is especially pronounced for perfluorocarbons that tend to form a third, fluorous phase in addition to the aqueous and organic phase. This phenomenon is often referred to as the ‘fluorous effect’. The ‘fluorous effect’ has some interesting technical implications as a phase separation and immobilization technique.⁷¹ For example, it can be utilized for extracting fluorinated products in synthesis. On the other hand, when perfluoroalkyl capping reagents are used in peptide synthesis, undesired byproducts can easily be separated by employing fluorous solid phase extraction (FSPE).⁷² Furthermore, fluorous biphasic chemistry is used for the surface immobilization of catalysts,⁷³ construction of microarrays,⁷⁴ fluorous HPLC purification of, for example, amino acids,⁷⁵ and, as will be discussed later, the stabilization of protein structure (see chapter 3).

2.4 The impact of fluorination on polar interactions

The high electronegativity of fluorine results in a considerable ionic character of the C–F bond and, through induction, affects the polarity of neighboring functional groups.

Nevertheless, fluorine itself is only weakly polarizable so that direct polar interactions involving the fluorine atom are usually weak. By far the most controversial discussions evolved around fluorine's properties as a hydrogen-bond acceptor. The controversy even led to reconsideration of the role of hydrogen bonding in base pair recognition during DNA replication (because fluorinated nucleobases that presumably do not form strong hydrogen bonds are easily accepted in replication).⁷⁶ Fluorine's high partial negative charge in C–F bonds was furthermore found to mediate other multipolar interactions with functional groups of proteins or the peptide bond itself.⁷⁷ In this section some important examples of indirect as well as direct polar interactions involving the C–F bond are summarized.

2.4.1 Fluorine's impact on pK_a

Due to fluorine's strong electron withdrawing nature, it increases the acidity of, for example, COOH, C–OH, and C–H. Conversely, the basicity of amines is reduced⁷⁸ (see Table 2.4). Since hydrogen-bonds and electrostatic interactions involving these functional groups play an important role in molecular recognition, fluorination may strongly affect receptor-ligand interactions. For example, the cimetidine analogue mifentidine (Figure 2.6), a histamine H₂ receptor antagonist that reduces secretion of gastric acid, exhibits increased potency (~ 20-fold) upon substitution of the terminal methyl group by a trifluoromethyl group.⁷⁹

Table 2.4 pK_a values of some selected carboxylic acids and amines.^{69,78}

Carboxylic Acid	pK_a	Amine	pK_a
CH ₃ COOH	4.8	CH ₃ CH ₂ NH ₂	10.7
CF ₃ COOH	0.2	CF ₃ CH ₂ NH ₂	5.9
C ₆ H ₅ COOH	4.2	C ₆ H ₅ NH ₂	4.6
C ₆ F ₅ COOH	1.8	C ₆ F ₅ NH ₂	-0.4

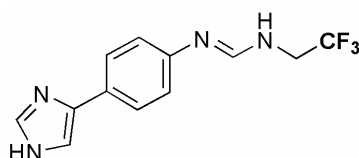


Figure 2.6 Structure of the cimetidine analogue mifentidine.

This finding is explained by the fact that mifentidine preferably acts in its neutral form. Fluorination reduces the percentage of the protonated amidine ($pK_a=8.7$ for the CH₃- and 6.1 for CF₃-analogue) from 93.2% to 5.1% thereby increasing receptor affinity. In

addition, it may be noted that despite the distance to the trifluoromethyl group the pK_a of the imidazole is also reduced by one pK_a unit, which points to the strong impact of fluorine's electronegativity. It has furthermore been shown that lowering the basicity of amines by fluorination may enhance bioavailability by increasing hydrophobicity, lipophilicity, and thus membrane permeability.^{70,80}

2.4.2 Hydrogen bonding

Despite the pronounced ionic character of the C–F bond, the resulting partial negative charge at the fluorine atom, and the three lone pairs that it provides for potential interactions, carbon-bound fluorine is rarely found as a hydrogen-bond acceptor in small molecule crystals or protein-ligand complexes.⁸¹ Conventional $X\cdots H-Y$ hydrogen bonds, where X and Y are N or O exhibit $X\cdots H$ distances of less than 2.2 Å. This distance, being roughly 0.5 Å shorter than the sum of the respective van der Waals radii (H: 1.20 Å, O, 1.52 Å, and N: 1.55 Å) is therefore considered an important criterion for strong hydrogen bonding, in addition to an $X\cdots H-Y$ angle larger than 90°. Thus, when X is carbon-bound F, a hydrogen bond may be present if its distance from H is smaller than 2.3 Å. However, these short distances are rare. A survey of crystal structures by Dunitz *et al.* in 1997 showed that merely 0.6% of the crystals considered exhibit such short C–F \cdots H–X contacts.⁸¹ Taking the angle criterion as well as distances of hydrogen to other, better acceptors into account finally revealed that out of 5947 only two unequivocal C–F \cdots H–O and 12 possible C–F \cdots H–N type hydrogen bonds were present. All the remaining short contacts, apparently, are imposed onto C–F as a result of stronger ‘classical’ hydrogen bonds in close proximity.

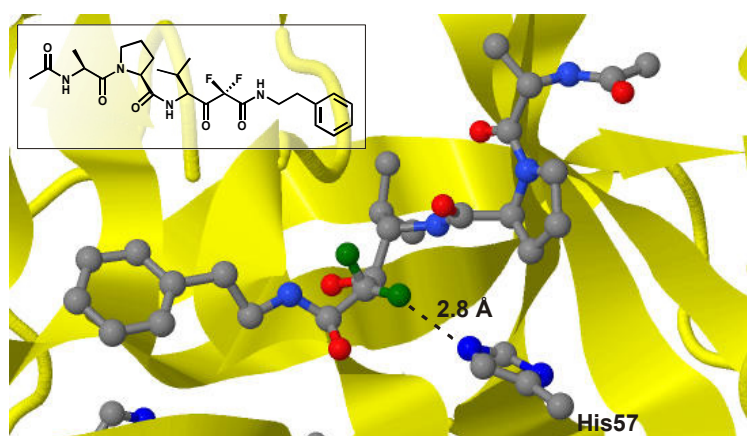


Figure 2.7 Crystal structure of the complex between elastase and its inhibitor Ac-Ala-Pro-Val-difluoro-N-phenylethylacetamide (PDB code 4EST).⁸² The structure shows a very close contact between F and the imidazole NH of His57 (F \cdots N distance 2.8 Å, hydrogen is not shown) indicating a C–F \cdots H–N hydrogen bond.

Evidence for hydrogen bonds in protein-ligand co-crystals involving fluorine is even poorer. Dunitz *et al.* did not find any unequivocal example and only two structures, in which weak H \cdots F hydrogen bonds are possible (see, for example, Figure 2.7).⁸¹ A more recent screening of the PDB in 2004, in contrast, suggests that 10% of the C–F bonds in protein crystals involve fluorine in hydrogen bonding.^{81,83} This finding may first of all be explained by the continuously growing body of high resolution structures published in the PDB and second by the slightly less constrained criteria applied by the authors. As opposed to Dunitz *et al.* they did also include H \cdots F distances just at or below the sum of van der Waals radii (~2.7 Å for H and F) with a 15% tolerance. At this point it may be noted that the findings of such data base screenings highly depend on the individual definition of hydrogen bonding, which in turn may be one reason for the controversy.

In general, hydrogen bonds involving carbon-bound fluorine as an acceptor are weak, approximately 2-3 kcal/mol as opposed to the 5-10 kcal/mol in conventional hydrogen bonds. In addition, a recent theoretical investigation has shown that there is only marginal electron transfer between hydrogen and fluorine upon interaction.⁸⁴ This may again be explained by fluorine's reluctance to donate electrons because, due to its low polarizability and high electron affinity, they are strongly bound to the nucleus. Several authors therefore suggest referring to these interactions as *weak dipolar interactions* rather than *hydrogen bonds*.

2.4.3 Other multipolar interactions

As opposed to O–H and N–H or any other equivalent, polarized X–H bond in organic molecules, the positively polarized carbonyl carbon atoms in protein backbones and side chain amides (glutamine, asparagine) as well as guanidyl groups (arginine) were found to provide a 'fluorophilic' environment.^{18,85} In contrast to the geometry of hydrogen bonds, however, the C–F bond (mainly but not exclusively aromatic) does not linearly but orthogonally approach the positively polarized sp² carbon (see, for example, Figure 2.8). Such interactions may stabilize enzyme inhibitor complexes as has been shown for tricyclic thrombin inhibitors.⁸⁶ Fluorination at the *para*-position of the phenyl ring (Figure 2.10) results in a roughly five-fold increased binding affinity ($\Delta\Delta G=1.1$ kcal/mol) compared to the non-fluorinated analogue. This finding is explained by a favorable interaction of fluorine with the backbone amide carbon of Asn98. In addition, C–F makes very short contacts with the α -carbon.

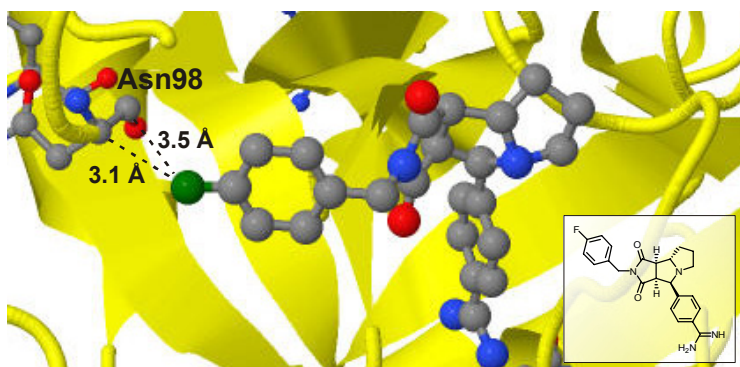


Figure 2.8 Crystal structure of (3aS,4R,8aS,8bR)-4-(2-(4-fluorobenzyl))-1,3-dioxodecahydropyrrolo[3,4-a]pyrrolizin-4-yl)benzaminidine bound to its target thrombin (PDB code 1OYT).⁸⁶

The distance to the α -hydrogen has been calculated to be as short as 2.3 Å, further indicating polar, probably hydrogen-bond like interactions. In addition, aromatic fluorination increases hydrophobicity thereby promoting desolvation and adding to binding affinity.⁸⁷ Such orthogonal multipolar interactions as described above were shown to be abundant in protein-ligand complexes⁷⁷ and apparently play an important role in orienting and binding of fluorinated ligands to their targets.

2.5 Metabolism and naturally occurring fluorinated organic molecules

2.5.1 Metabolism

In pharmaceutical lead optimization, modulating the metabolism of biologically active compounds is of equal importance to altering its activity. Slowing down metabolism through structural modifications on the one hand is desirable since it extends the *in vivo* half-life of the drug. On the other hand, it may also prevent the formation of potentially toxic metabolites. Fluorine has proven especially useful in blocking oxidation sites of aromatic rings that are normally hydroxylated at the *ortho* and *para* positions by cytochrome P450.⁸⁸ It is often stated that the metabolic stability of fluorinated compounds results from the strength of the C–F bond compared to C–H (see Table 2.1). As for cytochrome P450 it is also believed that the difficulties in forming an F–O bond (as opposed to H–O) during metabolism account for the stabilizing effect.⁸⁹ Thus, the C–F bond stability is not the only factor. In addition, the presence of fluorine atoms in a molecule may result in alternative metabolic pathways that the drug goes through.

Hydrolysis does similarly account for the deactivation of pharmaceutically active compounds. Fluorine decreases the basicity of adjacent functional groups and thus tends to destabilize cationic intermediates that usually occur under acidic hydrolysis. Accordingly, it may be used, for example, to stabilize enol ether bonds as has been

shown for fluorinated analogues of the platelet aggregation inhibitor prostacyclin (PGI₂) (see, for example, Figure 2.9).^{90,91}

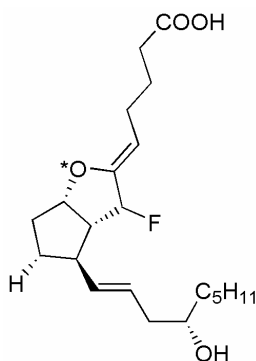


Figure 2.9 Structure of the PGI₂ analogue 7-fluoroprostacyclin. While exhibiting an identical inhibitory activity compared to original PGI₂ its chemical half life at pH 7.4 is increased from 10 minutes to more than a month.⁹¹ The protonation site that is deactivated by fluorine's electron withdrawing effect is marked with an asterisk.

The stability of fluorinated pharmaceuticals notwithstanding, it should be noted that biotransformations involving defluorination reactions are as well very common. Frequently, carbon atoms adjacent to C–F bonds in aliphatic compounds are hydroxylated and HF elimination will occur in such cases. In addition, the elimination of fluoride has also been observed during oxidative metabolism of aryl fluorides.⁸⁸ Thus, man-made fluorinated biological molecules are readily recognized by metabolic enzymes. While these versatile catalysts perform diverse chemical reactions and accept a large number of substrates, enzymes that *form* C–F bonds are rarely found. However, there are a few tropical plants that are able to produce fluorinated biomolecules. A brief account of these rare compounds is given in the next sub-section.

2.5.2 Naturally occurring fluorinated molecules

Considering the notorious toxicity of many tropical and subtropical plants it is maybe not surprising that the first fluorinated biomolecule, the highly poisonous 2-fluoroacetate, was isolated from an African plant (*Dichapetalum cymosum* known as 'gifblaar' or 'poison leaf') in 1943.²² Since then 12 natural organofluorine compounds have been isolated, all of which, except for one (nucleocidine), very likely are secondary metabolites of 2-fluoroacetate (Figure 2.10). Some plants that produce fluoroacetic acid also accumulate high levels of fluorinated lipids, such as ω -fluoromyristic acid, in their seeds. Their biosynthesis is explained by the condensation of fluoroacetyl-CoA instead of acetyl-CoA with malonyl acyl carrier protein (malonyl-ACP) in the early stages of fatty acid biosynthesis.⁹² Furthermore, fluoroacetyl-CoA enters the citric acid

cycle and is converted to (2*R*,3*R*)-fluorocitrate, which is the actual toxic metabolite. Its conversion to (*R*)-hydroxy-*trans*-aconitic acid due to defluorination subsequent to hydroxylation by aconitase results in inhibition of this enzyme. The shutting down of the citric acid cycle due to fluoroacetate uptake is the lethal event because the cell is cut off from its energy supply, which, for example, leads to cardiac arrest in humans and animals.⁹³

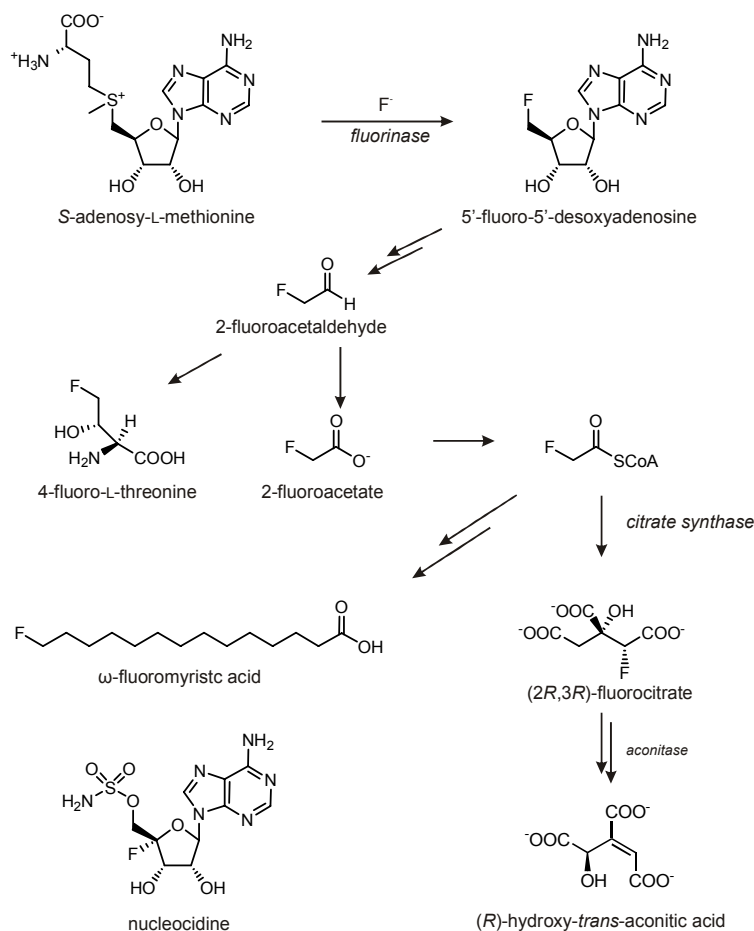


Figure 2.10 Biosynthesis of fluoroacetate, its metabolites, and the structure of nucleocidine.

The initial step of fluoroacetate biosynthesis, i.e. enzymatic C–F bond formation, was resolved only recently.^{94–96} In *Streptomyces cattleya* an enzyme termed ‘fluorinase’ catalyses the formation of a C–F bond through promotion of a nucleophilic attack by fluoride at C-5’ of S-adenosyl methionine (SAM). The resulting 5’-fluoro-5’-desoxyadenosine then undergoes a myriad of still unidentified reactions to form 2-fluoroacetaldehyde, which is finally oxidized to give 2-fluoroacetate. Nucleocidine has been isolated from *Streptomyces calvus*. The position of the fluorine atom at C-4’, in contrast to the other fluorinated natural biomolecules shown in Figure 2.10, led to the conclusion that this highly toxic antibiotic does not stem from fluoroacetate. However, to the present day, its biosynthesis has not been clarified.

3 Fluorinated Amino Acids in Peptide and Protein Engineering

Considering the often large beneficial impact of fluorination on the biological properties of small molecules, the modification of peptides and proteins with fluorinated analogues of the canonical amino acids holds great promise in peptide and protein engineering.²⁰ Interestingly, most studies published in recent years deal with fluorinated analogues of aliphatic or aromatic hydrophobic amino acids as well as fluorinated methionines and prolines, although syntheses of other fluorinated amino acids have been described as well.^{97,98} This may in part be explained by the fact that the consequences of fluorination on a molecule's hydrophobicity/lipophilicity are very well understood and thus far less controversially discussed than its impact on polar interactions. On the other hand, lacking additional functional groups, hydrophobic amino acids are also easier to synthesize and some of them are commercially available today. With emphasis on aliphatic side chains, which are relevant to the present study, the following sections will give a brief survey of the application of fluorinated hydrophobic amino acids to protein engineering.

3.1 Incorporation of fluorinated amino acids into peptides and proteins

Chemical peptide synthesis practically enables the incorporation of any amino acid into polypeptide chains, the precondition being that it is stable under the reaction conditions applied and in particular that it does not racemize. In this regard, special care must be taken with fluorinated amino acids since the strong negative inductive effect of fluorine may first reduce nucleophilicity of the amino function and second increase acidity of the α -proton. To overcome such difficulties, protocols to prevent racemization, especially during segment condensation, and to enhance coupling efficiency have been established and are now standard.^{99,100} Moreover, the automation of solid-phase peptide synthesis (SPPS)¹⁰¹ provides fast routine access to most peptides. It is the method of choice for small peptides because compared to protein expression, its flexibility regarding building blocks remains unmatched. For example, expressing a protein that is completely made up of D-amino acids is extremely difficult, since the reversed stereochemistry at the α -carbon is not tolerated by the enzymes involved.¹⁰² The chemical reactivity of an amino acid is in turn not affected and thus SPPS of "mirror image proteins", as shown for HIV-1 protease,¹⁰³ becomes possible. Nevertheless, linear SPPS is restricted to chain lengths of roughly 50 amino acids.¹⁰⁴ Longer sequences may be synthesized via condensation of multiple protected fragments. Moreover, many efforts have been undertaken to expand the repertoire of methods for chemoselective ligation of native peptide fragments^{104,105} so that syntheses of smaller proteins such as erythro-

poietin analogues (166 amino acids) are feasible today. The thioester-mediated peptide ligation (native chemical ligation) has undergone a variety of advancements in recent years.¹⁰⁵ One of them is a biochemical approach to protein thioesters that can be condensed to chemically synthesized fragments, e.g. those that contain non-coded amino acids (expressed protein ligation, EPL).¹⁰⁶

Production of larger proteins containing non-coded amino acids requires some manipulation of the natural protein expression apparatus.^{107,108} Both aminoacyl-tRNA synthetases and the ribosome are to an extent flexible regarding their recognition of side chains, i.e. they can accommodate non-natural amino acids and incorporate them into proteins. Several biosynthetic methods to globally replace an amino acid by a non-natural analogue are available. One method exploits auxotrophic bacterial strains that cannot biosynthesize the amino acid that is to be replaced. Overexpression of the protein of choice by growing these bacteria in media containing an unnatural analogue instead of the native amino acid yields a mutant, in which the specific residues are globally replaced. An early application of this method used an *E. coli* strain auxotrophic for phenylalanine to synthesize a protein in which the latter was partly replaced by *para*-fluorophenylalanine.¹⁰⁹ Degradation of cellular proteins during expression, however, may release the corresponding natural amino acid thus prohibiting quantitative replacement in most cases. Another limitation is given by the restriction to amino acids that are structurally very similar to the one they are supposed to replace. An extension of this method that in part overcomes this drawback is provided by employing engineered aminoacyl-tRNA synthetases with higher substrate specificity due to mutations within or close to the binding pocket.¹¹⁰⁻¹¹² Using auxotrophic bacterial strains may be circumvented when biosynthesis of the amino acid that is to be substituted can be inhibited. For example, tryptophane biosynthesis is disabled by 3-indoleacrylic acid. Adding this inhibitor during expression was used to incorporate 5-fluorotryptophane into a protein as an NMR probe.¹¹³

Notwithstanding these outstanding scientific achievements, several applications require the site-specific incorporation of non-native amino acids. This, in turn, requires extension of the genetic code to more than 20 amino acids. The basis for the latter was provided by Noren *et al.* in 1989.¹¹⁴ They took advantage of the fact that there exist three nonsense codons (UAA, UAG, and UGA) that normally signal termination of protein expression. As only one stop codon is required, the other two can be used to recognize so-called nonsense suppressor-tRNAs. These tRNAs carry the respective anti codon and thus suppress termination of protein biosynthesis when acylated with an amino acid. Applying, or rather optimizing the established protocols for acylation of tRNA¹¹⁵⁻¹¹⁷ as well as mutating the codon for the residue of interest to one of the stop

codons, allows incorporation of the residue into a specified position within a protein using *in vitro* translation. One major drawback of this method is that the misacylated suppressor-tRNA is consumed but not regenerated. The next step in expanding the genetic code was to engineer aminoacyl-tRNA synthetases that specifically acylate suppressor-tRNAs with the non-natural amino acid *in vivo* without interfering with other tRNA/synthetase pairs. Applying this approach more than 30 amino acids have now been added to the genetic code of, for example, *E. coli* and the continuing efforts in the field of genetic code engineering will certainly provide access to a large variety of modified proteins with improved properties and novel functions in the future.¹⁰⁷ More examples of fluorinated proteins that have been synthesized or expressed using one of the methods described above will be indicated in the following.

3.2 Fluorinated amino acids as NMR probes

As stated in section 2.1.1 the ¹⁹F isotope is a formidable NMR label that can be used to study the structure, interactions, and folding of proteins.^{26,27} Interestingly, the majority of studies deal with fluorinated analogues of aromatic amino acids such as phenylalanine, tyrosine, and tryptophane (Figure 3.1). These residues are often found in the hydrophobic binding pockets of proteins. Since single fluorine substituents cause minimal steric perturbations of the aryl moieties, they are easily accommodated in protein expression. Due to the high sensitivity of the ¹⁹F nucleus, the binding of substrates such as peptides, DNA, or small molecules can readily be monitored by NMR using these modified proteins.

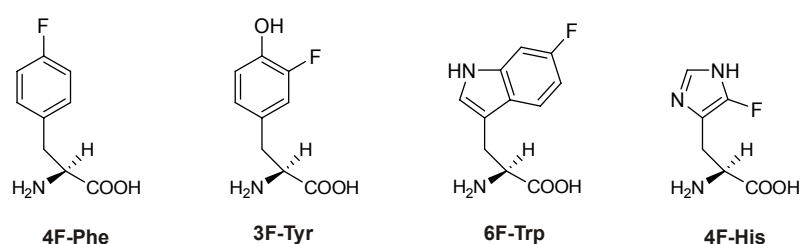


Figure 3.1 Structures of some frequently applied ¹⁹F NMR labels for proteins. From left to right: 4-fluorophenylalanine, 3-fluorotyrosine, 6-fluorotryptophane and 4-fluorohistidine. (Note that the numbering of the fluorine atoms neglects the amino acid backbone.)

Fluorinated analogues of histidine are also of interest, since the fluorine label, either at position 2 or 4, strongly lowers the pK_a of the side chain. Recently published procedures to biochemically integrate fluorohistidines into large proteins now pave the way towards exploring general acid/base catalysis in enzymes by applying ¹⁹F NMR.¹¹⁸

Another very interesting application of ^{19}F NMR is the investigation of membrane active peptides.¹¹⁹ As these peptides hold promise as antimicrobial agents (antimicrobial peptides, AMPs)¹²⁰ as well as transport systems (cell penetrating peptides, CPPs)^{121,122} it is of special interest to elucidate how these peptides interact with lipids, i.e. how they disrupt or translocate through membranes, respectively. One of the most important preconditions for a fluorinated amino acid to serve as a probe to study the binding and orientation of a peptide within a membrane is conformational rigidity. This is because flexibility of the side chain may hamper data analysis due to splitting of the fluorine signals. The chemical shift anisotropy results from the fluorine reporter not being fixed within one well-defined position with respect to the peptide backbone, which is the case for most fluorinated analogues of the canonical amino acids. Thus, specially designed amino acids are commonly used to study membrane active peptides by ^{19}F NMR (Figure 3.2). Derivatives of phenylglycine, for example, lack the β -methylene group thus fixing the orientation of the side chain. Fluorine substitutions *para* with respect to C_α keep the label (F^{123} or CF_3^{124}) in one defined position, since the side chains are then axially symmetric. The same is true for F_3 -Ala as well as TfmAla. However, phenylglycine derivatives are highly prone to racemization,¹²⁵ F_3 -Ala easily eliminates HF under basic conditions,¹²⁶ and incorporation of TfmAla into peptides is challenging, which is due to steric hindrance as well as reduced nucleophilicity of the α -amino group. At this point it is essential to note that incorporation of TfmAla is difficult but not impossible. In a recent study alamethicin labeled with either of the two stereoisomers in replacement for the native aminoisobutyric acid residue provided valuable insight into its membrane-associated structure.¹²⁷

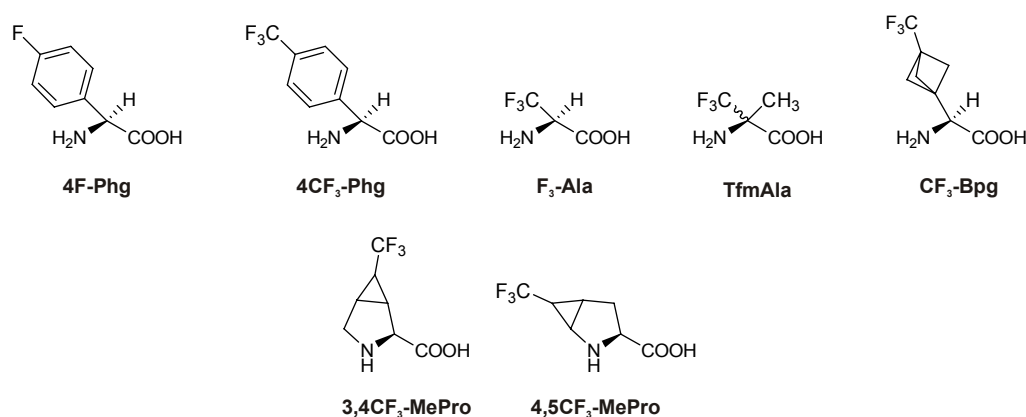


Figure 3.2 Structures of some frequently used NMR labels to study membrane active peptides and polyproline-II conformation. Upper panel from left to right: 4-fluorophenylglycine, 4-(trifluoromethyl)phenylglycine, trifluoroalanine, trifluoromethylalanine, and 3-(trifluoromethyl)-bicyclopent-[1.1.1]-1-yl glycine. Lower panel: 3,4- and 4,5-metanoprolines.

In the search for an ideal and broadly applicable label to study membrane-bound peptides, very interesting and uncommon structures that overcome the drawbacks men-

tioned above have recently emerged (see for example CF₃-Bpg).¹²⁸ In line with these studies, structurally unique fluorinated proline analogues to study the polyproline II conformation have been synthesized as well (Figure 3.2).¹²⁹

3.3 Fluorinated analogues of leucine, isoleucine, and valine in protein engineering

The most commonly used among the fluorinated analogues of aliphatic amino acids are those of leucine, isoleucine, and valine (Figure 3.3). Since a full review of their applications is beyond the scope of this thesis, some important studies that demonstrate the diversity of fluorine's effects will be summarized in the following sections.

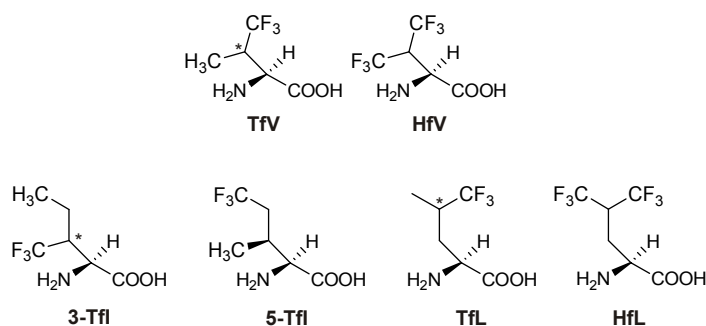


Figure 3.3 Structures of fluorinated analogues of native aliphatic amino acids. Upper panel form left to right: 4,4,4-trifluorovaline and 4,4,4,4',4',4'-hexafluorovaline. Lower panel 3,3,3'-trifluoroisoleucine, 5,5,5-trifluoroisoleucine, 5,5,5-trifluoroleucine, and 5,5,5,5',5',5'-hexafluoroleucine. The asterisk indicates stereochemical heterogeneity of the respective amino acid at this center.

3.3.1 Modification of membrane-active peptides by fluorinated amino acids

As stated above, membrane active peptides hold great promise as antimicrobial agents and thus offer a starting point for developing peptide-based antibiotics. Their ability to interact with or penetrate cell membranes mostly results from their amphiphilic, often helical structure, in which hydrophobic and hydrophilic residues are spatially separated.¹²⁰ They directly interact with lipid bilayers and do not require a receptor. Thus, it seems reasonable to assume that replacing native hydrophobic residues such as Leu and Val by more hydrophobic fluorinated analogues might increase the activity of such peptides.¹³⁰ The substitution of Leu and Ile in pexiganan by HfL, for example, stabilizes the dimeric structure of this peptide within lipid membranes.¹³¹ In this example, fluorination enhances the interaction with bacterial membranes and thus mostly conserves antimicrobial activity while the peptide remains hemolytically inactive. As opposed to pexiganan, fluorogainin is not digested trypsin and chymotrypsin when bound to the

membrane. However, this effect is a result of its increased tendency to self-assemble within the lipid bilayer rather than an effect of fluorination *per se*. In the absence of a membrane, the peptide is as rapidly degraded as its non-fluorinated analogue.¹³¹

An enhancement in membrane affinity was also shown for the bee venom mellitin,¹³² whose toxicity is a result of inducing membrane leakage. In this particular study, up to four leucine residues were substituted by both diastereomers of TfL. The authors describe a non-trivial impact of stereochemistry on hydrophobicity of the peptide. However, one main result of this investigation is that fluorination again enhances self-association of the peptide in membranes. Although the biological activity of these melittins has not been tested, the study points to the same important conclusion: the increased membrane binding behavior cannot be explained by an increase in hydrophobicity alone, but an enhancement in self-association due to hydrocarbon-fluorocarbon segregation. Thus, the 'fluorous effect' (section 2.3) has to be taken into account; while the lipophobic character of highly fluorinated alkyl side chains enhances self-association, the direct interaction with lipids, apparently, is less favorable. The significance of this finding has been shown for a gramicidin S (GS) variant in which the two Val residues were replaced by HfV.¹³³ Although the activity profile of GS is maintained, the fluorinated analogue exhibits an eight- to sixteen-fold lower activity, which the authors attribute to weaker peptide-membrane interactions due to the lipophobicity of the highly fluorinated side chain.

Meng *et al.* have studied the effects of fluorination on the two antimicrobial peptides buforin-2 and magainin-2, which have very distinct modes of action.¹³⁴ While buforin-2 translocates through membranes and is believed to kill bacteria by interacting with nucleic acids, magainin-2 causes cell lysis by forming pores in the membrane. Different variants, in which HfL replaces mainly Leu, Ile, and Val (but also Gly and Ala) that also vary in length in the case of buforin-2 were synthesized. All the fluorinated buforin-2 variants are equally or more active than the native analogue. More importantly, truncated buforin-2 variants that were found inactive regain activity upon fluorination. On the other hand, magainin-2 does not generally benefit from fluorination. While the hemolytic activity of buforin-2 remains unchanged, some of the fluorinated magainin-2 variants exhibit increased hemolytic potential. In addition, an analogue in which the apolar surface was completely fluorinated shows increased self-assembling behavior in solution that apparently reduces antimicrobial activity. The peptides were furthermore tested for stability against hydrolysis by trypsin. In contrast to the fluorinated pexiganans described above, the peptides investigated here are proteolytically stable in the absence of a membrane.

The above-described fluorination-activity and -stability relationships do not exclusively apply to membrane active peptides. HfL substitutions in glucagon-like peptide-1 revealed comparable effects.¹³⁵ Most of the fluorinated variants were active in stimulating cAMP production, albeit with reduced efficiency due to their lowered affinity towards their receptor. Again, fluorination confers considerable proteolytic stability (against the protease dipeptidyl peptidase IV, DPP IV) to the peptide, which contrasts the results for free pexiganan.

In summary these investigations show that the correlation between side chain fluorination and proteolytic stability as well as activity of biologically active peptides is complex. This finding points to the important conclusion that the impact of fluorine highly depends not only on the immediate environment of the peptide but more importantly on the environment of the fluorine substitution within the polypeptide sequence. However, these studies indicate that there are interesting consequences of fluorination on the phase-segregation behavior of peptides. As will be highlighted in the next section, these properties have been extensively studied in recent years.

3.3.2 Global fluorination of hydrophobic residues

As indicated above, fluorination makes a distinct contribution to the phase-segregation of membrane active peptides. This property is especially pronounced for peptides that form oligomeric helical structures (coiled coils, see chapter 6), in which the fluorinated residues constitute the helical interface. The formation of coiled coils is driven by the hydrophobic effect, i.e. segregation of hydrophobic side chains from water to form an interhelical hydrophobic surface. Thus, it is expected that substitution of native aliphatic residues by highly fluorinated analogues within the hydrophobic core stabilizes these structures. An early study was published by the group of David Tirrel, in which the workers incorporated TfL into the d-positions of the hydrophobic core of a designed coiled-coil dimer by means of expression using leucine-auxotrophic *E. coli* grown in media depleted of native leucine.⁵⁰ They found that both isomers of TfL, (2*S*,4*S*)-TfL and (2*S*,4*R*)-TfL, are activated by leucyl-tRNA synthetase (LeuRS). In contrast, attempts to also incorporate HfL, at that time, failed. Despite the fact that both diastereomers of TfL were present in the structure it was shown that fluorination increases thermal stability of the coiled-coil assembly, which was attributed to the increased hydrophobicity of TfL. The peptide with the highest fluorine content exhibited a by 13 K increased melting point compared to the native variant. A few years later, the same group published a follow-up study, in which they separately expressed the coiled coil with either of the two diastereomers.¹³⁶ Both analogues of the native coiled coil

exhibited enhanced stability ($\Delta T_m = 10$ K for both), albeit the extent of stabilization was lower than in the previous example, in which both isomers were mixed. Interestingly, the stability of the equimolar mixture of both fluorinated peptides was higher and nearly identical ($\Delta T_m = 14$ K) to the one that contains both diastereomers equally distributed within the helical interface at the same time. The reasons for the latter finding remain to be clarified. The authors also accomplished expression of a coiled coil in an engineered bacterial host containing HfL.¹³⁷ They found that their early attempts failed because the activation of HfL by LeuRS is 4000-fold slower compared to leucine. It is important to note at this point that the fidelity of aminoacyl-tRNA synthetases is a crucial factor during the synthesis of fluorinated proteins, as shown for isoleucine-tRNA synthetase. Though 100-fold less effective, isoleucine-auxotrophic bacterial strains readily incorporate 5-Tfl into murine dihydrofolate reductase, while 3-Tfl is not at all accepted.¹³⁸ Nevertheless, in agreement with their previous findings, increasing the degree of fluorination and thus hydrophobicity of the hydrophobic core by formally adding a second CF_3 group to leucine side chains results in even higher stability of the coiled coil ($\Delta T_m = 22$ K).

Comparable studies have been carried out using *bzip* proteins derived from the GCN4-transcription factor, a native coiled-coil dimer that has DNA binding activity. Regardless of whether the peptide is synthesized¹³⁹ or expressed,¹⁴⁰ fluorination effectuates an increase in stability and leaves the DNA-binding affinity unchanged. Furthermore, the general conclusion remains the same, no matter whether substitutions occur at position a¹⁴⁰ or d¹³⁹ of the coiled coil. However, the position of the CF_3 group was shown to have an impact on the magnitude of stabilization. It was found that the stabilizing effect of TfV is much smaller compared to that of TfL, which is explained by the β -trifluoromethyl group in TfV engaging in unfavorable steric interactions with the peptide backbone. Taking these results together, it was no surprise that complete fluorination of a GCN4 hydrophobic core (position a with TfV and position d with TfL at the same time) studied in the group of Krishna Kumar showed equal effects.¹⁴¹ However, Kumar's group highlighted a very important finding in their follow-up studies. They compared two helical assemblies, one that carried Leu in all a- and d-positions (peptide HH) and one that carried its hexafluorinated analogue (peptide FF).^{142,143} The heteromeric disulfide-bridged HF peptide shows only a marginal increase in melting temperature compared to HH ($\Delta T_m = 2$ K), while the FF coiled coil, due to the increased hydrophobicity of HfL, was 48 K more stable. This finding indicated that mixed hydrocarbon-fluorocarbon cores are disfavored, which points to a strong impact of the 'fluorous effect'; the property of highly fluorinated alkyl groups to be hydrophobic *and* lipophobic at the same time.

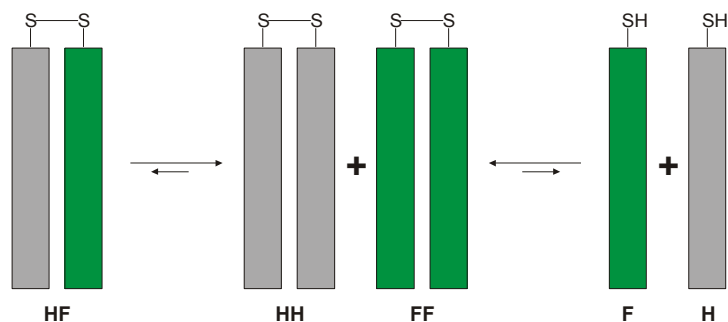


Figure 3.4 Self-sorting of a highly fluorinated and a native coiled coil. Oxidation of two individual monomers each carrying a terminal cysteine selectively forms a fluorinated (FF) and a non-fluorinated (HH) assembly (left to right), whereas a mixed hydrocarbon-fluorocarbon heteromer disproportionates to form HH and FF (according to Bilgicer et al.).¹⁴²

In this specific study, the ‘fluorous effect’ is exemplified by the fact that a mixture of reduced H and F specifically form HH and FF when subjected to oxidation (Figure 3.4). In turn, an oxidized HF heterooligomer disproportionates to form HH and FF in solution. Furthermore, the fluorinated peptides were shown to form higher oligomers (tetramers instead of dimers). The interpretation that the ‘fluorous effect’ drives the self-sorting of helical peptides that present fluorinated residues on the helical interface gained support from a study on a designed transmembrane helix. Extensive fluorination of leucine, here, resulted in an enhancement of oligomerization in the environment of micelles¹⁴⁴ as well as lipid bilayers,¹⁴⁵ which points to their tendency to segregate from the lipophilic environment. Thus, extensive fluorination of coiled-coil hydrophobic cores leads to hyperstable assemblies that segregate the fluorinated residues from both water and lipids due to the increased hydrophobicity and the fluorous effect.

As convincing as these results and their interpretations are, they are not undisputed. The group of Neil Marsh extensively investigated the stability of four- α -helix bundles containing variable levels of HfL instead of Leu within the hydrophobic core, claiming that the stabilization they observed is an effect of increased hydrophobicity only rather than the ‘fluorous effect’, or as the authors call it “specific fluorous interactions”.¹⁴⁶ This interpretation is based on the finding that the partitioning free energies for Leu and HfL into *n*-1,1-dihydroperfluoroheptanol are identical. Thus, compared to Leu, there is no apparent preference for HfL to partition into a perfluorinated environment. On the other hand, its preference to partition into *n*-heptanol is 0.4 kcal/mol larger. Furthermore, the stabilization of the coiled-coil assembly on a per HfL basis is 0.3 kcal/mol, a value that corresponds well to its increased free energy of partitioning into *n*-heptanol.

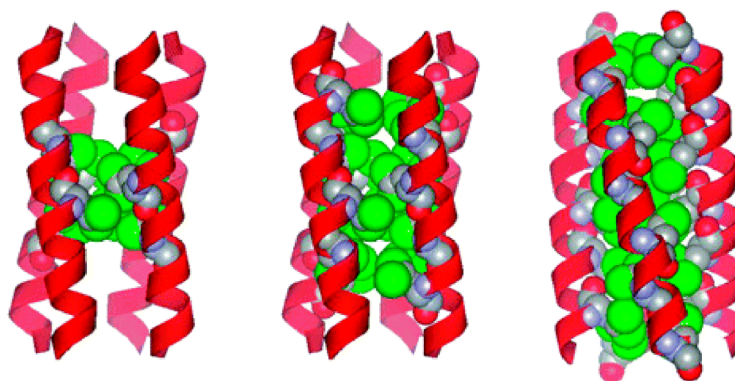


Figure 3.5 Modeled structures of different antiparallel four- α -helix bundles in which two, four, and six leucine residues per monomer were substituted by HfL. Fluorinated side chains are shown in green (reproduced from Lee et al.¹⁴⁷ with permission, Copyright © 2009 American Chemical Society).

Different variants of the antiparallel tetrameric coiled-coil peptide that contained increasing Leu to HfL substitutions at positions a and d were investigated (Figure 3.5).¹⁴⁷ Interestingly, the per-HfL stabilization was shown to decrease from 0.3 kcal/mol to 0.12 kcal/mol as the number of HfL residues increased from two to four, and six per monomer, respectively; hence, the author's conclusion that 'interactions' between the fluorinated residues do not seem to add stability to the coiled coil. Moreover, adding highly fluorinated solvents to the buffer, which might have been expected to selectively disrupt these interactions, were shown to have the same effect on both, the native and the fluorinated peptide. Comparison of the native peptide and the highest fluorinated variant showed that both peptides were equally disrupted into helical monomers by high concentrations of trifluoroethanol (TFE). In contrast, the fluorinated peptide remained a stable tetramer in ethanol, whereas the native coiled coil was disrupted.¹⁴⁸ As the fluorinated alcohol does not preferentially disrupt the fluorinated oligomer, the authors conclude that the 'fluorous effect' plays a minor role in the stabilization of highly fluorinated coiled-coil assemblies. However, this interpretation is disputable, since TFE is known to induce diverse peptides to adopt a monomeric α -helical conformation.^{149,150} Thus, the significance of the latter finding requires additional proof. The authors furthermore studied different helical bundles, in which Leu and HfL alternately pack against each other.¹⁵¹ They found that the per-HfL substitution in these peptides is greater than in the fully fluorinated variant, which is explained by a more favorable packing. Indeed, fluorination significantly increases the size of the side chain resulting in "overpacking" of the hydrophobic core. This effect can be partly attenuated by the alternate packing pattern as shown by ¹⁹F-NMR. This conclusion again highlights the fact that fluorine is not a conservative substitution in terms of size, especially when multiple hydrogens are displaced. However, an indication for self-sorting, i.e. the 'fluorous effect', was only found for the fully fluorinated peptide.

In contrast to coiled-coil proteins, in which the fluorinated residues constitute one distinct interface between several helical peptides, globular proteins, which usually exhibit a broader distribution of hydrophobic residues, are destabilized by side chain fluorination of these amino acids. Although enhancing secondary structure formation at ambient temperature, the thermal stability of chloramphenicol acetyltransferase (CAT), for example, decreased along with increasing Leu to TfL substitutions, which was shown by a drop in activity.¹⁵² Similarly, the green fluorescent protein (GFP) lost fluorescence upon global replacement of leucine by TfL due to poor structure formation.¹⁵³ In one of the papers, the authors note that one reason for the destabilizing effect, among others, may be the propensity of fluoroalkyl groups to “...exist near other fluorines”. In other words, the ‘fluorous effect’ may also promote misfolding when fluorinated residues cluster in non-native folding states of the protein.¹⁵²

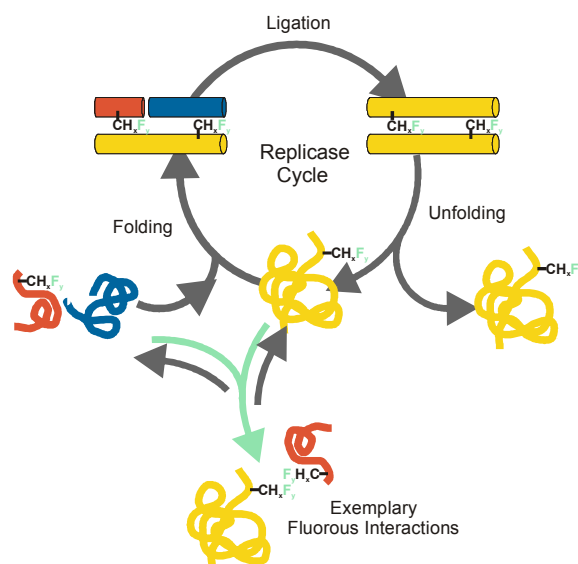


Figure 3.6 Catalytic cycle of a self-replicating peptide: the ligation between two fragments is catalyzed through coiled-coil formation with a full-length peptide, which brings the reactive functional groups (a thioester and a cysteine) in close proximity. The ligation of fluorinated peptides is retarded, presumably by forming fluorous ‘clusters’ that stabilize the unfolded state (reproduced from Jäckel *et al.*¹⁵⁴ with permission, Copyright © 2009 Wiley-VCH Verlag GmbH & Co. KGaA, Weinheim).

Although this interpretation is speculative, it does not stay without support. The same conclusion was drawn by Jäckel *et al.* before to explain the decreasing rates of product formation of a self-replicating coiled-coil peptide.¹⁵⁴ As the fluorine content in the side chain is increased from zero to two or three the rate of product formation over time decreased. In this example, fluorous ‘clusters’ in the unfolded state of the peptide are thought to inhibit the formation of the reactive complex between the template and the two peptide fragments (Figure 3.6). Further studies on both CAT and GFP, however, revealed that it is possible to evolve fluorinated proteins with distinct function and fold-

ing.^{153,155} Combining protein expression in the presence of TfL with directed evolution¹⁵⁶ yielded a CAT variant with improved thermostability. Interestingly, when the fluorinated protein served as the parent protein for mutagenesis no mutations were found in close proximity to the fluorinated residues and the binding site. Moreover, none of the leucines within the protein were removed. In a comparable study, a fluorinated GFP mutant with recovered and even 650-fold higher fluorescence intensity was generated.¹⁵³

In summary, stabilization of helical interaction motifs by global fluorination can be achieved, when the fluorinated residues constitute distinct interaction cores of the protein. However, while this mostly applies to homotypic interactions, most protein ligand interactions, which are important for drug development, are heterotypic. Globular proteins usually do not tolerate global fluorination and require reorganization, i.e. evolution of their primary structure to compensate for the loss in stability and activity. These results indicate that fluorine exerts its effects in a strongly environment-dependent manner, a fact that is now increasingly being recognized not only for aliphatic fluorinated amino acids but also for fluorinated aromatic residues.^{157,158} The application of phage display to screen for fluorophilic residues from within the pool of 20 encoded amino acids revealed that these prefer bulky hydrophobic residues such as leucine and isoleucine in a coiled-coil environment.¹⁵⁹ However, less is known about the molecular interactions with these amino acids. The main question that remains to be answered is as to what extent the polarity and size of fluorinated alkyl side chains affect interactions with native hydrophobic amino acids. Furthermore, it is important to systematically study the impact of hydrophobic side chain packing, i.e. the immediate environment. Such studies provide a basis for a more profound understanding of the rather divergent effects described above and for a directed application of fluorinated amino acids in modulating protein-protein interactions, such as those of small peptides (e.g. as drugs) with receptors.

4 Aim of the Work

Although there is a large body of literature dealing with peptides and proteins that are modified with fluorinated amino acids, the specific interactions by which these building blocks affect their structure and activity are not yet fully understood. Many investigations have been based on global fluorination and these have revealed interesting results such as the stabilizing impact of the 'fluorous effect' on coiled-coil peptides. Also, suitably designed amino acids have proven valuable for studying the structure and function of proteins by ^{19}F -NMR. Fewer studies considering substitutions of single native residues have been published but these revealed that the effects of fluorination can be rather diverse, since they appear to be highly dependent on the environment and thus difficult to predict. Therefore, complete characterization of the properties of fluorinated amino acids within a native protein environment is required to enable their directed application in peptide and protein engineering. To this end, model systems developed in the group of Prof. Dr. Beate Kokschi based on the α -helical coiled-coil folding motif have proven rather informative, since they adopt a very well defined and predictable three-dimensional structure. The coiled coil's well-established design principles enable a variety of folding studies that provide a detailed insight into the interactions of different peptides at the molecular level.

Based on previous findings gained with such a coiled coil, a new model system was developed in line with the present study to provide for an interaction between a fully native peptide and a complement containing various single fluoroamino acid substitutions. The goal of the study is to investigate the consequences of altering fluorine content and, thus, steric effects and hydrophobicity of the side chain on the structure and thermodynamics of folding applying circular dichroism spectroscopy. Analogous to earlier investigations of coiled-coil self-replication, a surface plasmon resonance based assay was developed to allow for a detailed investigation of fluorine's effects on coiled-coil folding kinetics. With the objective of elucidating how subtle differences in the environment of the substitution, such as packing preferences of the side chains, would affect fluorine's impact, two different positions within the hydrophobic core of the coiled coil were studied.

5 Applied Methods

The central objective of the present thesis is the thermodynamic and kinetic investigation of the effects that varying degrees of fluorination at a single site within a coiled-coil assembly have on its folding. The two most important methods - circular dichroism (CD) spectroscopy and surface plasmon resonance (SPR) - applied here are described in detail below. Brief accounts of additional methods that were used to characterize the peptides are given in the publications presented in chapter 6.

5.1 Circular dichroism spectroscopy

CD spectroscopy is one of the most important methods for investigating the global structure of biological macromolecules such as peptides and proteins as well as DNA.^{160,161} Since the common secondary structural motifs of polypeptides exhibit characteristic CD spectra in the UV range (see section 5.1.2), measuring CD allows assessing the proportionate contributions to the overall structure, albeit with low resolution. Nevertheless, the specific signals can be used to monitor structure formation or conversely denaturation as well as bimolecular interactions, for example, of peptides and membranes or nucleic acids, which are often associated with distinctive structural rearrangements. Thus, CD spectroscopy can be employed for a variety of investigations ranging from simple structural up to high level thermodynamic and kinetic studies.¹⁶²

5.1.1 Physical background

CD, also termed 'Cotton effect', is a physical phenomenon that occurs when two oppositely circularly polarized light beams are absorbed by an optically active molecule. Both light beams interact with the molecule but the extent to which they are absorbed is different. CD is defined as the difference in absorption between right- and left-circularly polarized light that can be written according to Lambert-Beer's law as:

$$\Delta A = A_L - A_R = \epsilon_L c l - \epsilon_R c l = \Delta \epsilon c l \quad (5.1)$$

where A is the absorption, ϵ the absorption coefficient, c the molar concentration of the analyte, and l the path length. The term $\Delta \epsilon$ is defined as the decadic molar CD.

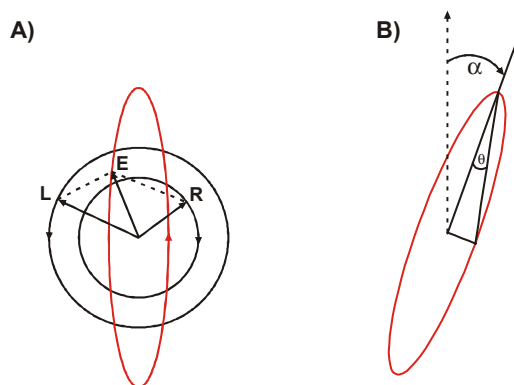


Figure 5.1 A) Elliptically polarized light visualized as a combination of two oppositely circularly polarized light beams of unequal intensity after absorption of plane-polarized light by an optically active molecule. In case the absorption of right-circularly polarized light is greater than that of left-circularly polarized light, then the result will be a left-elliptically polarized light beam. B) Definition of ellipticity θ as the angle between the minor and major axis of the ellipse whose ratio is equal to $\tan\theta$. The angle α is the optical rotation, i.e. the angle between the major axis of the ellipse and the initial plane of the incident plane-polarized light beam.

Plane-polarized light can be envisioned as a combination of a left- and a right-circularly polarized light beam of equal intensity. Thus when plane polarized light passes through an optically active sample the differential absorption of the two components results in an elliptically polarized light beam (Figure 5.1 A). The difference of magnitudes of the two components gives the semiminor axis, whereas their sum gives the semimajor axis of the ellipse. Other than directly reporting $\Delta\epsilon$ or the very small differences in absorption ellipticity θ is commonly used to discuss CD data. It is defined as the angle between the minor and major axis (Figure 5.1 B). Using equation 5.2, CD and ellipticity are readily interconvertible.¹⁶⁰

$$\theta(\text{deg}) = 180 \cdot \ln 10 \cdot \frac{\Delta A}{4\pi} = 32.98 \Delta A \quad (5.2)$$

To enable a comparison of spectra of different proteins ellipticity θ is usually converted into mean molar residual ellipticity $[\theta]$, which removes the linear dependence of the signal on path length, analyte concentration, and chain length. All CD data discussed in this thesis are reported in terms of $[\theta]$ that has the dimension $[10^3 \text{ deg cm}^2 \text{ dmol}^{-1} \text{ residue}^{-1}]$. Normalization is based on equation 5.3

$$[\theta] = \frac{\theta}{10000 \cdot c \cdot l \cdot n} \quad (5.3)$$

where n is the number of residues, θ the measured ellipticity in mdeg, c the analyte concentration in mol/l, and l the path length in cm. Here, c refers to the overall peptide concentration and n to the average number of residues both based on monomers.

5.1.2 Protein structure analysis

Being most abundant in polypeptides the amide group is the most important chromophore for CD spectroscopy of these biomolecules. It has three π centers and thus three π orbitals (π_+ , π_0 , and π^*) filled with four electrons. In addition, there are two lone pairs of electrons sitting in two n orbitals (n and n') located at the carbonyl oxygen (Figure 5.2 A). The π_+ π^* as well as the n' π^* transitions have not yet been identified. The π_0 π^* transition occurs at 190 nm and is marginally solvent dependent. The lower energy $n\pi^*$ transition usually occurs at 220 nm but shifts ± 10 nm depending on the solvent and molecular interactions of the amide group.

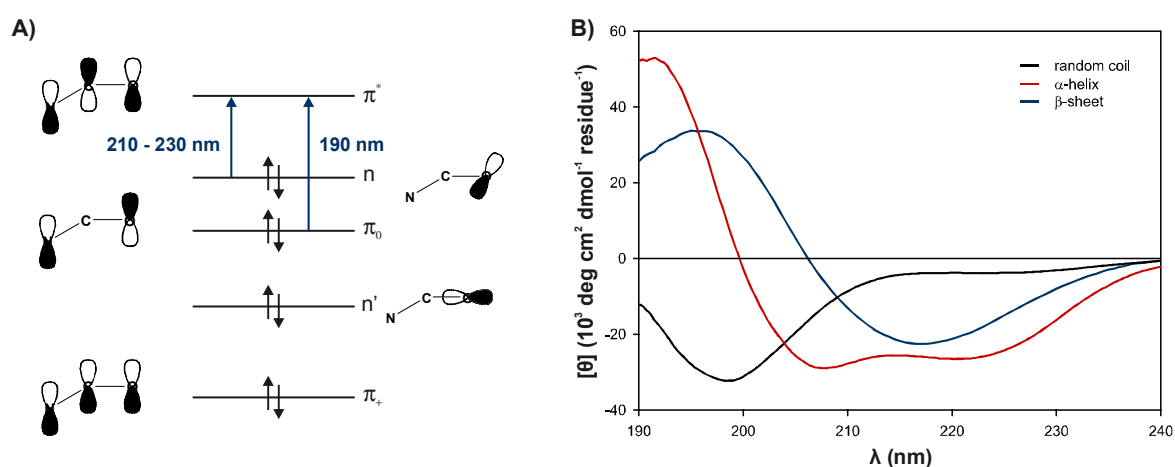


Figure 5.2 A) Electronic structure of the amide group with the two identified transitions in the UV range (according to ref. 160). B) Characteristic CD spectra of a random coil, an α -helix, and a typical β -sheet. (The helix and random coil spectra were taken from samples discussed in this thesis. The β -sheet spectrum has been drawn from data provided by Sara Wagner with her kind permission¹⁶³).

The characteristic far UV CD spectra of an unstructured peptide, an α -helix, and a β -sheet are shown in Figure 5.2 B. The α -helix spectrum is characterized by a minimum at 222 nm that has been assigned to the amide $n\pi^*$ transition. The strong minimum at 208 nm as well as the maximum at 190 nm result from excitation splitting of the $\pi\pi^*$ transition. β -sheets, in turn, usually show a broad minimum centered around 215 nm ($n\pi^*$ transition), a maximum at approximately 198 nm and a minimum at 175 nm (not shown) that were assigned to the $\pi\pi^*$ transition. The prediction of random coil spectra is problematic in that it is a combination of different unordered structures that rapidly interconvert. Thus, the spectra of unordered peptides can be rather different. While all of them exhibit a negative band just below 200 nm some random coils show a positive band in the long wavelength region and some do not (see Figure 5.2 B). Nevertheless, the spectra of the two most common secondary structures and random coils

are easily distinguishable. Many programs are available to deconvolute CD spectra of complex proteins, i.e. to assess the individual contribution of each of the three as well as other secondary structures such as polyproline II and β -turns.¹⁶⁴ The spectra of the latter two structural motifs, however, are less easily distinguishable. Polyproline-II spectra, for example, resemble those of random coils while β -turns exhibit spectra that are easily confused with α -helix (type I) and β -sheet (type II). However, these secondary structures are not an issue for the present investigations and are thus not discussed any further.

For the present study a simpler approach using the normalized signal intensity at 222 nm to calculate the helical content of the peptide assemblies was applied. The basis on which helical content is calculated was provided by Chen *et al.* who found that the chain length dependence of the $n\pi^*$ transition intensity fits the following equation:¹⁶⁵

$$[\theta]_{222nm} = [\theta]_{222nm}^{\infty} \cdot \left(1 - \frac{k}{r}\right) \quad (5.4)$$

where $[\theta]_{222nm}$ is the theoretical normalized signal intensity at 222 nm, $[\theta]_{222nm}^{\infty}$ the signal intensity at this given wavelength for an infinite helix and r the number of backbone amides. The values for k as well as $[\theta]_{222nm}^{\infty}$ vary in literature and depend on the method applied. An investigation by Gans *et al.* however gave a k value of 4.6, which, as the authors state, approximately corresponds the four C-terminal carbonyls that cannot participate in backbone hydrogen bonding,¹⁶⁶ a phenomenon termed “helix end-fraying”. Using this value for k , the ellipticity of an infinite helix is $-40 \cdot 10^3 \text{ deg cm}^2 \text{ dmol}^{-1} \text{ residue}^{-1}$. Accordingly, the fraction of a given peptide being in an α -helical conformation (f_{helix}) can now be expressed as the ratio of the measured normalized ellipticity and the theoretical value:

$$f_{helix} = \frac{[\theta]_{222nm}}{-40000 \cdot \left(\frac{4.6}{r}\right)} \quad (5.5)$$

Equation 5.5 does not consider the contribution of aromatic side chains to the CD signal at 222 nm. However, it has been shown that, since they are UV active, they may have a significant impact.¹⁶⁷ The magnitude to which they affect CD signals has unfortunately not yet been clearly quantified. Therefore, the contribution of the aromatic (*ortho*-aminobenzoic acid, Abz) label used for the present investigations is neglected. It has been shown that phenylalanine tends to reduce signal intensity at 222 nm. Taking the structural resemblance of Phe and Abz in terms of the aromatic ring into account

the values for f_{helix} reported here should, thus, be considered as relative values that, possibly, are underestimated.

5.1.3 Thermodynamic analysis of protein folding applying CD spectroscopy

Protein denaturation can be investigated by any kind of spectroscopy since it is usually associated with distinctive changes in absorption or fluorescence of chromophores that are buried in the native state. Thus, monitoring the CD signals as a function of temperature or denaturant concentration (urea or guanidinium hydrochloride) provides an option for monitoring the transition from the native fold to random coil. For α -helical structures the signal at 222 nm is most distinctive and thus commonly used to monitor denaturation. Also, more complex protein structures that contain α -helices can be investigated using this signal, since protein unfolding usually is a cooperative process, i.e. the transition of the folded to the unfolded state occurs simultaneously at every position of the protein. Fitting the data to an appropriate model then allows calculating thermodynamic data. In the following the equations used for data fitting of the peptides investigated in line with this thesis will be derived.

Although not undisputable in the case of coiled-coil peptides,¹⁶⁸ many proteins exhibit unfolding that apparently proceeds via a reversible two-state mechanism. This means that there is no accumulation of intermediates on the way from the native to the unfolded state. The equilibrium can be described by the simple relationship:

$$\Delta G = \Delta G^\circ + RT \ln K \quad (5.6)$$

where ΔG is the free energy of unfolding at a given temperature and K the equilibrium constant. ΔG° is the difference in free energy between the purely native and the purely unfolded protein under standard conditions (1M, 101325 Pa, 298.15 K). For the unfolding of a dimeric peptide assembly D into two monomers M , as is the case for the coiled-coil peptides investigated here, the concentrations of D and M at any temperature can be described in terms of fraction unfolded f_u :

$$[D]_T = [D]_0 - f_u [D]_0 \quad (5.7)$$

$$[M]_T = 2f_u [D]_0 \quad (5.8)$$

where $[D]_0$ is the initial concentration of the native protein assembly. Thus, with K at a given temperature defined as:

$$K_T = \frac{[M]_T^2}{[D]_T} \quad (5.10)$$

K can now be described in terms of fraction unfolded and peptide concentration:

$$K_T = \frac{4f_u^2 [D]_0^2}{[D]_0 - f_u [D]_0} \quad (5.11)$$

which in turn provides a definition of f_u at any temperature in terms of K_T :

$$f_u = \frac{\sqrt{16K_T [D]_0 + K_T^2} - K_T}{8K_T [D]_0} \quad (5.12)$$

For data fitting a reference temperature is chosen, at which a definition of f_u is available. The melting point T_m is defined as temperature where half of the protein is unfolded. Thus, with f_u at T_m being 0.5, ΔG° can be written combining equations 5.6 and 5.11 as:

$$\Delta G^\circ = \Delta G_T - RT \ln 2 [D]_0 \quad (5.13)$$

where ΔG_T is the free energy of unfolding as a function of temperature that can also be expressed by the Gibb's-Helmholtz relationship:

$$\Delta G_T = \Delta H_T - T \Delta S_T \quad (5.14)$$

The temperature dependence of the enthalpy of unfolding (ΔH_T) and the entropy of unfolding (ΔS_T) can be defined using T_m as the reference temperature:

$$\Delta H_T = \Delta H_{T_m} + \Delta C_p (T - T_m) \quad (5.15)$$

$$\Delta S_T = \Delta S_{T_m} + \Delta C_p \ln \left(\frac{T}{T_m} \right) \quad (5.16)$$

where ΔC_p is the difference in heat capacity between native and unfolded protein that is assumed to be temperature independent within the transition range. Since at the melting point ΔG_T must be zero the temperature dependence of ΔS can be rewritten using equation 5.14 as:

$$\Delta S_T = \frac{\Delta H_{T_m}}{T_m} + \Delta C_p \ln \left(\frac{T}{T_m} \right) \quad (5.17)$$

Combining equations 5.14, 5.15, and 5.17 gives:

$$\Delta G_T = \Delta H_{T_m} \left(1 - \frac{T}{T_m} \right) + \Delta C_p \left(T - T_m - T \ln \frac{T}{T_m} \right) \quad (5.18)$$

K_T in equation 5.12 can be expressed using the relationship:

$$K_T = e^{-\frac{\Delta G_T}{RT}} \quad (5.19)$$

where ΔG_T is represented by equation 5.18, which then gives a theoretical description of f_u when combined in equation 5.12.

Fraction unfolded may also be expressed in terms of ellipticity $[\theta]$ for the two-state transition. The temperature dependence of $[\theta]$ can be described as the sum of the temperature dependence of the ellipticities of the pure monomer and dimer that are related to fraction unfolded as follows:

$$[\theta]_T^M = f_u [\theta]^M \quad (5.20)$$

$$[\theta]_T^D = [\theta]^D - f_u [\theta]^D \quad (5.21)$$

where $[\theta]^M$ and $[\theta]^D$ are the temperature dependencies of the fully monomeric and dimeric peptides, respectively.

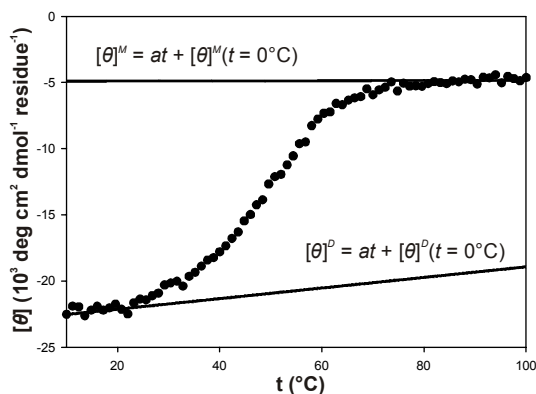


Figure 5.3 Example of a melting curve showing the linear baselines for the native dimeric state and the denatured monomeric state, where a and b are the slopes and t the temperature in $^{\circ}\text{C}$.

Thus, f_u can be written as:

$$f_u = \frac{[\theta] - [\theta]^D}{[\theta]^M - [\theta]^D} \quad (5.22)$$

with $[\theta]^M$ and $[\theta]^D$ represented by the linear baselines of the unfolding profile (Figure 5.3). Since the enthalpy strongly depends on ΔC_p it is not reasonable to fit both values simultaneously. Therefore, the change in heat capacity is initially assumed to be zero for the purpose of fitting. The observed dependence of f_u from temperature as described by equation 5.22 is then fit to the combined equations 5.18 and 5.19 to yield a ,

b , K_T , ΔH_{T_m} , and T_m . These values can then be used to calculate ΔG° using equation 5.13 when ΔC_p is known (see section 7.2).

5.2 Surface plasmon resonance

The equations describing SPR are not trivial. Since a complete understanding of their derivation, however, is not needed to understand the principle, only a phenomenological account of SPR will be given prior to a description of its applications in biophysics.

4.2.1 Physical background

When light passes from a material with a high refractive index (glass) into another with a low refractive index (water/buffer) some light is reflected. As the angle at which the light strikes the surface reaches a critical value, almost 100% of the incident light is reflected (total internal reflection). If, however, the glass surface is coated with a thin noble metal film such as gold, a further increase of the angle will result in “loss” of light into the metal. This phenomenon is explained by the light exciting surface plasmons at the glass metal interface. A surface plasmon can be described as a charge density wave (collective oscillation of the mobile electrons at the surface of the metal) that propagates parallel to the metal dielectric interface. When the wave vector of the incident light matches the wavelength of the surface plasmons, the electrons resonate, i.e. SPR occurs. This coupling of the incident light to the surface plasmons reduces the intensity of the reflected light (Figure 5.4). There exists one angle θ , the SPR angle, at which the intensity of the reflected light reaches a minimum.

The evanescent optical electric field of the surface plasmons decays exponentially away from the surface (~ 200 nm).¹⁶⁹ Within that range any change in refractive index and surface thickness will affect the SPR angle. Refractive index and dielectric constant are related as follows:

$$n = \sqrt{\frac{\varepsilon}{\varepsilon_0}} \quad (5.23)$$

where ε is the dielectric constant of the respective medium and ε_0 that of vacuum. For a clean metal surface evaporated onto a glass surface θ can be approximated by equation 5.24:

$$\theta \approx \arcsin \left[\frac{\varepsilon \varepsilon_m}{(\varepsilon + \varepsilon_m) \varepsilon_g} \right] \quad (5.24)$$

where, at the given wavelength, ε is the real part of the dielectric function of the metal, ε_m the dielectric constant of the medium above the surface, and ε_g that of glass. Given these relations, any adsorptive process near the surface that changes n is detected in terms of a change in θ . These changes can be monitored in real time, which allows assessing the kinetics of the processes at the surface.

There are different experimental setups to measure SPR. One, which measures $\Delta\theta$ in terms of resonance units (RU) has been described above. To a rough approximation one RU corresponds to 1 pg/mm² of material (protein) bound to the surface.¹⁷⁰ Alternatively, it is possible to measure the wavelength dependence of reflectivity (R) in a fixed angle experiment. Here, the minimum of R is a function of wavelength. In line with the present thesis the experiments were based on a fixed wavelength experiment (Figure 5.4) applying the BIAcore[®] technology.¹⁷¹ Usually, low-power laser light such as HeNe (632.8 nm) is used for investigation of protein-protein as well as protein-ligand interactions since polypeptides usually do not absorb light in the visible region. However, methods based on near-IR irradiation have been developed as well.¹⁶⁹

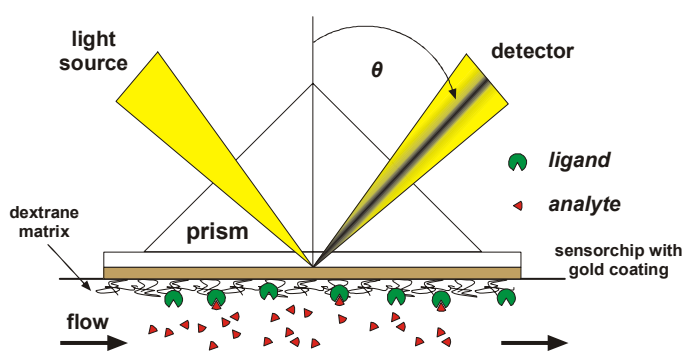


Figure 5.4 Typical experimental setup: Light of a constant wavelength strikes a surface at an array of different angles (a prism is used for dispersion) and the angle at which reflectivity is minimal is detected using a diode array detector.

5.2.2 Application of SPR in biomolecular interaction analysis

One of the major advantages of SPR is that it does not require labeling of the interacting partners since the quantity of surface bound material as well as surface thickness directly translate into a change in SPR angle. Thus, protein interactions with peptides, DNA and small molecule ligands can be monitored using the native biomolecules. Bio-specific interaction analysis (BIA) applying SPR has been commercialized towards the end of the last century by combining this highly sensitive detection principle with sensor chip technology.¹⁷² In the setup applied in BIAcore[®] experiments an approximately 50 μm gold surface is brought onto a glass chip that consists of several flow-channels al-

lowing parallel analyses of several interactions as well as on-line reference subtraction. In principle, proteins containing sulfhydryl groups can be directly immobilized on gold. However, the chips used for BIA today are coated with an extended coupling matrix composed of carboxymethylated dextrane. Such a hydrogel like matrix has several advantages over pure gold surfaces.¹⁷³ It does not only provide for higher levels of immobilization, it also prevents steric crowding of ligands on the surface thereby enhancing availability. A good availability of the binding sites is necessary to prevent limitation of binding by diffusion. Furthermore, the dextrane, being a polysaccharide, provides a hydrophilic surrounding that presents a favorable environment for most biomolecular interactions. The carboxyl group itself serves two purposes. First, it is used as a chemical handle that provides for chemical immobilization of the ligand. Second, given an appropriate pH, its negative charge can be used to enhance immobilization by drawing the proteins towards the surface under conditions where they are positively charged.

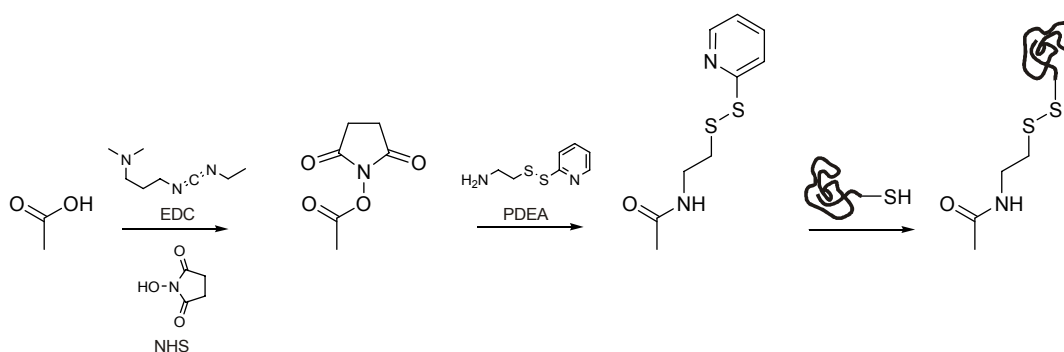


Figure 5.5 Activation of the surface carboxyl groups and ligand thiol capture.

The first critical step in each SPR experiment is immobilization of the ligand. The carboxyl groups at the surface, as stated above, provide for a variety of immobilization chemistries. Moreover, BIAcore[®] offers a variety of modified sensorchips such as those coated with streptavidine for biotiny based immobilization or hydrophobic surfaces for lipid immobilization.¹⁷⁰ However, one needs to ensure that first, immobilization does not inactivate the ligand and second that all ligands are equally oriented on the surface since heterogeneous surfaces may seriously hamper data analysis. This is presumably due to unequal availability or blocking of binding sites. Chemically assembled peptides and DNA can easily be endowed with biotiny that may then be used to capture the ligand on streptavidine coated sensor chips. Ligands that are modified with sulfhydryl groups (e.g. cysteine) remote from the binding site are immobilized through disulfide bridge formation after adequate chemical modification of the surface carboxyl groups. Moreover, proteins may be directly immobilized via amine coupling subsequent to activation of the carboxyl moieties (e.g. as succinimidyl esters). However, since peptides and proteins contain a large number of amino groups, direct immobilization may result

in heterogeneous surface coating. In the present work an indirect technique has been applied. Here, the surface is chemically activated prior to introducing a thiol for ligand thiol capture (Figure 5.5). Since the ligand used for the investigations presented here contains a single C-terminal cysteine, heterogeneous immobilization is prevented.

Usually a range of analyte concentrations is used in several experiments that are then globally analyzed to calculate most precise kinetic parameters. Applying high flow rates (100 $\mu\text{l}/\text{min}$) ensures that the analyte concentration is constant during the association phase, which results in pseudo first order binding kinetics. Subsequently, the flow of analyte is switched to a flow of pure buffer and dissociation of the complex is monitored. The final step is appropriate data analysis that can only be performed when the stoichiometry of the interaction is known. BIAcore[®] offers a software package containing a variety of interaction models ranging from simple 1:1 Langmuir binding up to more complex models considering heterogeneity of the ligand or analyte as well as multistep interactions. Further interaction models can be implemented. It is however necessary to validate the results by comparing the calculated equilibrium constants to results gained from other experiments as will be further discussed in sections 6.7 and 6.8.

6 Results and Discussion

The results presented in this chapter have partly been published in the following peer-reviewed reports:

- S. Samsonov, M. Salwiczek, G. Anders, B. Kokschi, M. T. Pisabarro; Fluorine in Protein Environments: A QM and MD Study; *J. Phys. Chem. B* **2009**, *113*, 16400-16408. **(Section 6.2)**
- M. Salwiczek, S. Samsonov, T. Vagt, E. Nyakatura, E. Fleige, J. Numata, H. Cölfen, M. T. Pisabarro, B. Kokschi; Position-Dependent Effects of Fluorinated Amino Acids on the Hydrophobic Core Formation of a Heterodimeric Coiled Coil; *Chem. Eur. J.* **2009**, *15*, 7628-7636. **(Section 6.3)**
- M. Salwiczek, P. K. Mikhailiuk, I. V. Komarov, S. Afonin, A. S. Ulrich, B. Kokschi; Compatibility of the Conformationally Rigid CF₃-Bpg Side Chain with the Hydrophobic Coiled-Coil Interface; *Amino Acids*, accepted **2010**. **(Section 6.5)**
- M. Salwiczek, B. Kokschi; Effects of Fluorination on the Folding Kinetics of a Heterodimeric Coiled Coil; *ChemBioChem* **2009**, *10*, 2867-2870. **(Section 6.7)**

Results that are not part of these publications as well as further considerations and interpretations are presented in additional sections.

6.1 The Coiled Coil as a model for a natural polypeptide environment

A model system that is suitable for systematically studying the interactions of a library of non-native amino acids with native residues in a natural protein environment at the molecular level must fulfill some key conditions: 1) a predictable, defined, and structurally well characterized fold that determines the interacting residues; 2) substitutions should be easily accommodated, i.e. the model should be structurally and thermodynamically stable towards modifications; while 3) being sensitive enough to detect them; and 4) quick and efficient to synthesize. However, the resolution of the 'protein-folding problem',¹⁷⁴ i.e. our limited ability to accurately predict polypeptide and protein folding based on knowledge of their primary structure, is undoubtedly one of the most ambitious aims in biological chemistry. Statistical analyses of many protein structures lead to a scale that lists the propensity of the canonical amino acids to be found in a certain conformation.^{175,176} In addition, thermodynamic scales have been established, at least for the two most common secondary structural motifs, the α -helix¹⁷⁷ and the β -sheet.¹⁷⁸ Based on these progresses supported by computer-aided structure prediction, solving

the problem seems no longer as big a challenge as it appeared a few decades ago.¹⁷⁹ Nevertheless, the *de novo* design of proteins that adopt a desired fold usually is expensive in labor and time. The α -helical coiled-coil folding motif represents a major exception. Because its structural features are well understood, rules for its design have been established.¹⁸⁰ Therefore, it almost perfectly fulfills the conditions given above and has already proven valuable for studying the interactions of fluorinated amino acids with their native counterparts.^{154,181} The next two sections summarize the basic structural features and some important biological functions of coiled-coil based proteins. Furthermore, the design of the VPE-VPK model system employed in this study will be described.

6.1.1 *The coiled-coil folding motif: Structure and function*

With the objective to unravel an at that time unusual X-ray diffraction pattern belonging to α -keratin, the coiled coil was first hypothesized as a folding motif in 1952 by Francis Crick.¹⁸² While some of the reflexions could not be explained in terms of a regular, straight α -helix, taking into account oligomerization of several helices through side-by-side packing with a 20° left-handed superhelical twist rationalized the findings.¹⁸³ Furthermore, it was postulated that α -keratin's primary structure must follow a repetitive amino acid sequence comprising seven residues¹⁸⁴ of which every third and fourth is hydrophobic. This pattern is well-known today as the heptad repeat (abcdefg)_n. The first complete sequencing of such a repeat pattern was accomplished in 1972 for tropomyosin.¹⁸⁵ Comparison of the sequences of some DNA-binding domains¹⁸⁶ and the first high-resolution crystal structure of an isolated coiled coil in 1991 (Figure 6.1 A)¹⁸⁷ eventually revealed the sophistication of the coiled-coil primary structure.

Hydrophobic residues such as leucine, isoleucine, valine, and methionine are clearly preferred in the a- and d-positions,^{188,189} whereas all the other positions primarily harbor polar and charged amino acids such as lysine, glutamic acid, glutamine, and asparagine. In contrast to isolated α -helices, in which each complete turn comprises 3.6 residues, the number is reduced to 3.5 in coiled-coil helices. Thus, one heptad makes up two turns of the helix. Projection onto an idealized helical wheel shows that the a- and d-positions are arranged on one side of the helix, spatially separating them from the polar and charged residues (Figure 6.1 C). This arrangement of polar and non-polar residues renders the individual helices highly amphiphilic and provides an interface for recognition as well as the driving force for oligomerization. Through zipper-like 'knobs-into-holes' packing of a- and d- against a'- and d'-positions of the opposite strand (Figure 6.2 C), a hydrophobic core that provides most of a coiled coil's stability is formed.

Interhelical Coulomb interactions between the e-/g- and e'-/g'- positions, respectively, provide for folding specificity, e.g. parallel vs. antiparallel orientation¹⁹⁰ and homo- vs. heterooligomerization.¹⁹¹ These Coulomb interactions furthermore contribute to the overall stability of the assembly.¹⁹²⁻¹⁹⁴ Therefore, depending on whether these interactions are attractive or repulsive, a specific orientation and oligomerization state can be favored.

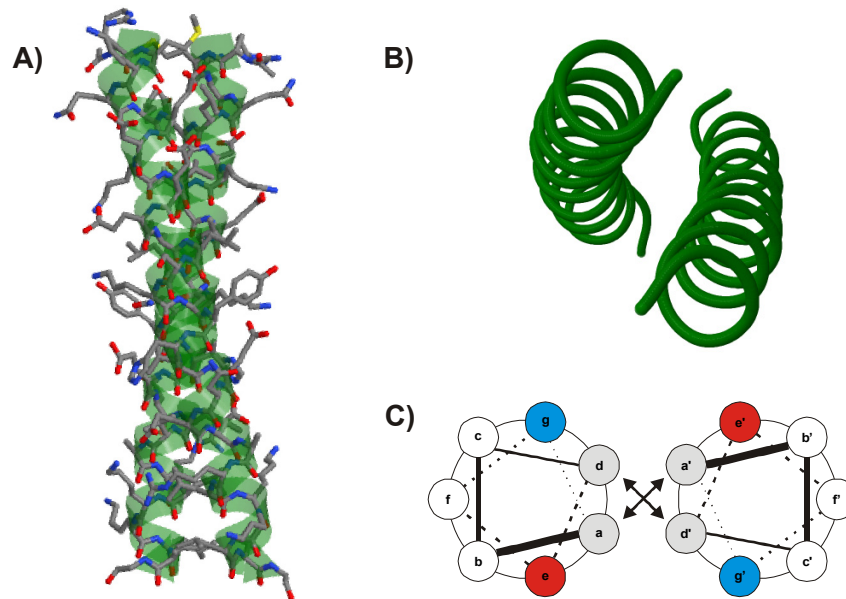


Figure 6.1 A) Crystal structure of the GCN4 leucine zipper (PDB code 2ZTA), B) GCN4 backbone viewed from the N- to the C-terminus along the superhelical axis, C) helical wheel representation of B depicting the heptad repeat pattern.

Oligomerization state and helix orientation are also affected by the hydrophobic core. It was found that the burial of polar residues such as asparagine within the hydrophobic core favors dimerization.¹⁹⁵ Hydrogen-bonding between two asparagines may furthermore direct helix orientation.^{196,197} The β -branched amino acid valine at position a favors parallel dimers and trimers whereas complete leucine cores favor an antiparallel helix orientation.¹⁸⁰ In coiled-coil dimers the remaining positions are mainly solvent-exposed and mediate solubility in water. However, intramolecular interactions between these residues may account for additional stability of the individual helices.^{198,199}

Classical coiled coils, i.e. those based on the heptad repeat, are usually composed of two to five α -helices. Recently, also a synthetic seven-helix coiled coil was reported.²⁰⁰ They can be as short as two heptads in synthetic models^{199,201} and as long as 200 in native proteins. Roughly 10% of all proteins contain coiled-coil domains that, depending on their length and architecture,²⁰² serve a multitude of biological functions.^{203,204} Long coiled coils, i.e. domains of several hundred amino acids in length,

usually have structural and mechanical functions. They build up the cytoskeleton (intermediate filament proteins) and function as motor proteins that assemble muscle filaments (e.g. myosin). Nuclear coiled coils are involved in chromatin organization and nuclear envelope assembly as well as transcription, mitosis, and apoptosis. Some of these long coiled coils also exhibit elastic properties that are in part responsible for hair flexibility (α -keratin) and muscle function (myosin). Many short coiled-coil domains have been identified as structural components as well as recognition domains of DNA binding proteins. Most prominent amongst these are Jun, Fos, and GCN4 which are important transcription factors. Viral fusion proteins such as gp41,^{205,206} which is part of an HIV-1 envelope glycoprotein, are also based on the heptad repeat. The vast structural changes that are associated with coiled-coil formation are believed to induce membrane fusion after binding of the virus to its host cells.

The vital functions of coiled coils and their involvement in pathogenic events such as viral fusion make them attractive candidates for drug development. Due to their interesting physical properties such as elasticity future applications in nanotechnology, e.g. as molecular springs, may be envisaged. Important for the purpose of the present study, however, are the coiled coil's basic structural features. Its folding is predictable and the interaction partners within the assembly are precisely defined. A design that provides for heterotypic oligomerization, therefore, enables a systematic investigation of the molecular interactions of fluorinated amino acids with native residues in a natural polypeptide environment.

6.1.2 Design of the model system

The model system VPE-VPK was designed to provide an environment for specific interactions between a fluorinated and a non-fluorinated peptide. The peptide model fulfills two important criteria: 1) specificity for one distinct orientation (parallel) of the peptide strands within the assembly and 2) heterodimerization, i.e. the interaction of a fully native with a complementary fluorinated peptide strand. Figure 6.2 illustrates the design of the model peptide.

The amino acid composition of the hydrophobic core is inspired by the GCN4 transcription factor, which has already been extensively characterized at high resolution.¹⁸⁷ Here, valine in all of the a- and leucine in all of the d-positions provide for a parallel orientation of the peptide strands in the coiled-coil dimer. Most important for the purpose of this study, heterodimerization is required to guarantee that the observed effects trace back to a single fluoroamino acid substitution per dimer. This condition is accomplished by introducing e-g' and g-e' pairs that engage in favorable electrostatic interac-

tions in the heterodimer but would repel one another in both possible homodimers. In addition, the g22-e'27 and e27-g'22 substitution pattern (E instead of K and K instead of E) supports the parallel orientation. These interactions are favorable for the parallel alignment, while they would be repulsive for an antiparallel coiled coil.

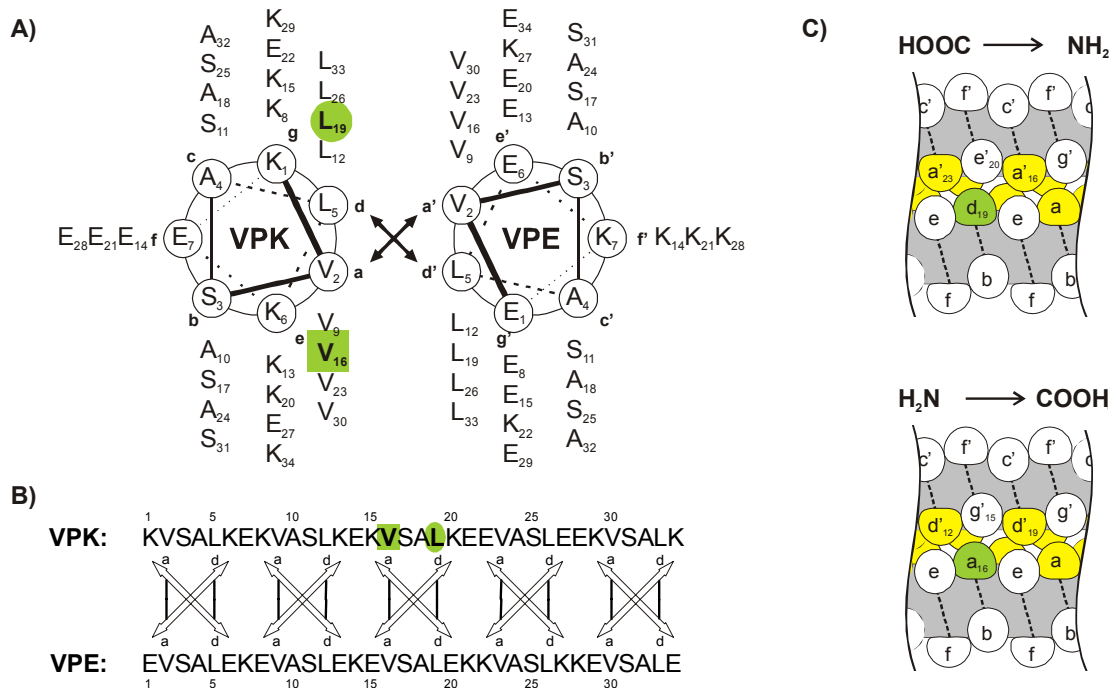


Figure 6.2 A) Helical wheel model viewed from the N- to the C-terminus and B) sequence of the VPE-VPK dimer. The substitution positions are highlighted in green. C) Cutout of the rod model illustrating the packing of the residues at the substitution sites.

The GCN4 crystal structure shows that, in contrast to antiparallel coiled coils, the packing characteristics of the a- and d-positions in parallel coiled-coil dimers are different (Figure 6.3).²⁰⁷ The a-positions pack against a' whereas d-positions pack against d'-positions. Due to the parallel alignment of the helices the C_α-C_β bond vectors point out of the hydrophobic core (parallel packing), away from each other at position a while they point into the core, towards each other at position d (perpendicular packing). This packing pattern results in two different packing layers within the hydrophobic core. In the case of antiparallel helix orientation the packing of a against d' and d against a' is very similar (acute packing) resulting in two equally packed layers within the hydrophobic core. The differences in packing of a- and d-residues in parallel coiled-coil dimers, therefore, allow the evaluation of the impact of fluorination within two different hydrophobic microenvironments, in which the side chains adopt distinctly different orientations. Based upon these observations, the VPK strand contains the fluorinated amino acids either at position a16 or d19. Peptides containing leucine, the largest and most

hydrophobic of the canonical amino acids, at the respective substitution site serve as a reference.

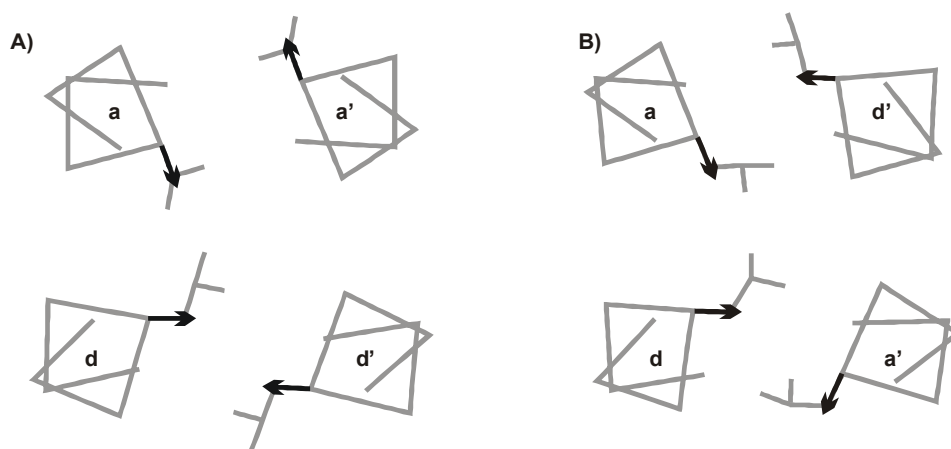


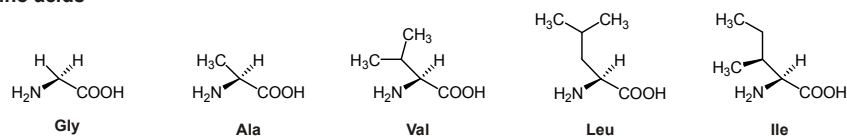
Figure 6.3 Schematic demonstration of the packing of *a*- and *d*-positions in A) a parallel and B) an antiparallel coiled coil dimer (according to ref. 207). The C_{α} - C_{β} bond vectors are represented by a black arrow.

6.2 Hydrophobicity of the fluorinated amino acids

The hydrophobic effect plays an important role in protein structure formation, since the large entropy gain upon the liberation of water molecules is a major driving force for folding.²⁰⁸ The hydrophobicity of a molecule is usually evaluated on the basis of partitioning coefficients between water and organic solvents, micelles, or vapor. In addition, many HPLC based methods have been developed.²⁰⁹ However, the numerous scales and the resulting hydrophobicity rankings of amino acids often poorly correlate.^{209,210} Furthermore, it is questionable as to how far an organic solvent, vapor, or an RP-column relate to protein hydrophobic cores in terms of polarity and structure. Thus, in rational protein design these scales should be used with caution, especially when attempting to quantitatively relate differences in partitioning free energy to the thermodynamic stability of proteins. Nevertheless, given the interest in a characterization of fluorinated organic molecules in this respect (see chapter 2) the goal of the present investigation was to compare the fluorinated side chains to purely hydrocarbon congeners on the basis of an HPLC assay. The goal was to assess the correlation between hydrophobicity and steric size as well as the degree of fluorination. To this end, the retention time of all amino acids relevant to this study (Figure 6.4) on a hydrophobic C18-column has been determined using their N^{α} -Fmoc protected analogues. The van der Waals volumes of the side chains were estimated starting from the β -carbon by summation of atomic increments and bond contributions.²¹¹ This method has proven a good approximation since the volumes are readily comparable to those derived from

standard computational methods. However, it cannot distinguish between Leu and Ile. These two amino acids represent a special case because their side chains have an identical chemical composition while their constitution is different. Their ranking in hydrophobicity scales depends on the method applied, e.g. on whether it is shape-sensitive or not, and a comparison of different scales reveals that there is an almost even split to which of them is more hydrophobic.²⁰⁹

Canonical amino acids



Non-canonical amino acids

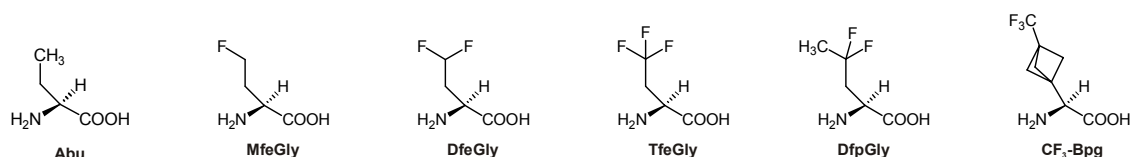


Figure 6.4 Chemical structures of the relevant natural hydrophobic amino acids (upper panel), Abu, its fluorinated analogues MfeGly, DfeGly, and TfeGly as well as DfpGly and CF₃-Bpg (lower panel). Except for Abu the non-canonical amino acids are regarded as alkyl-substituted glycines.

Amino acids carrying pure hydrocarbon side chains (except Phe) are practically homologous since they are exclusively based on aliphatic frameworks of carbon and hydrogen. Thus, their hydrophobicity can be assumed to be determined by size only, because no other functional groups that may be, for example, pH sensitive, are present. Furthermore, it has been shown before that relative hydrophobicity of uncharged side chains is not affected by their chemical environment.²¹²

Indeed, the retention time of native aliphatic amino acids and Abu increases, albeit not linearly, with increasing side chain volume (Figure 6.5 A). The non-linearity may be explained by the fact that as the side chain is elongated the polarizing effect of the α -amide as well as the carboxy group on the alkyl group progressively decreases.²¹² Thus, for example, the contribution of the γ -methyl group of leucine to overall hydrophobicity is larger than that of the β -methyl group of aminobutyric acid. The present method is furthermore validated by the observation that the generated hydrophobicity scale is well comparable to scales based on partitioning of the side chains between cyclohexane or octanol and water although the latter are usually measured at physiological pH. In contrast, the scale shown here has been generated under acidic conditions (pH 2). The correlation coefficients between retention time and partitioning free energies are 0.99 for cyclohexane/water and 0.97 for octanol/water, respectively (Fig-

ure 6.5 B). These excellent correlations validate the present assay. However, Kovacs *et al.* pointed out that, in order to determine the intrinsic hydrophobicity of the side chains that has significance in a polypeptide or protein context, one should apply a method based on peptide retention times.²¹² Accordingly, they employed a *de novo* designed decapeptide in an extensive assay to determine hydrophobicity of the canonical amino acids at various conditions.

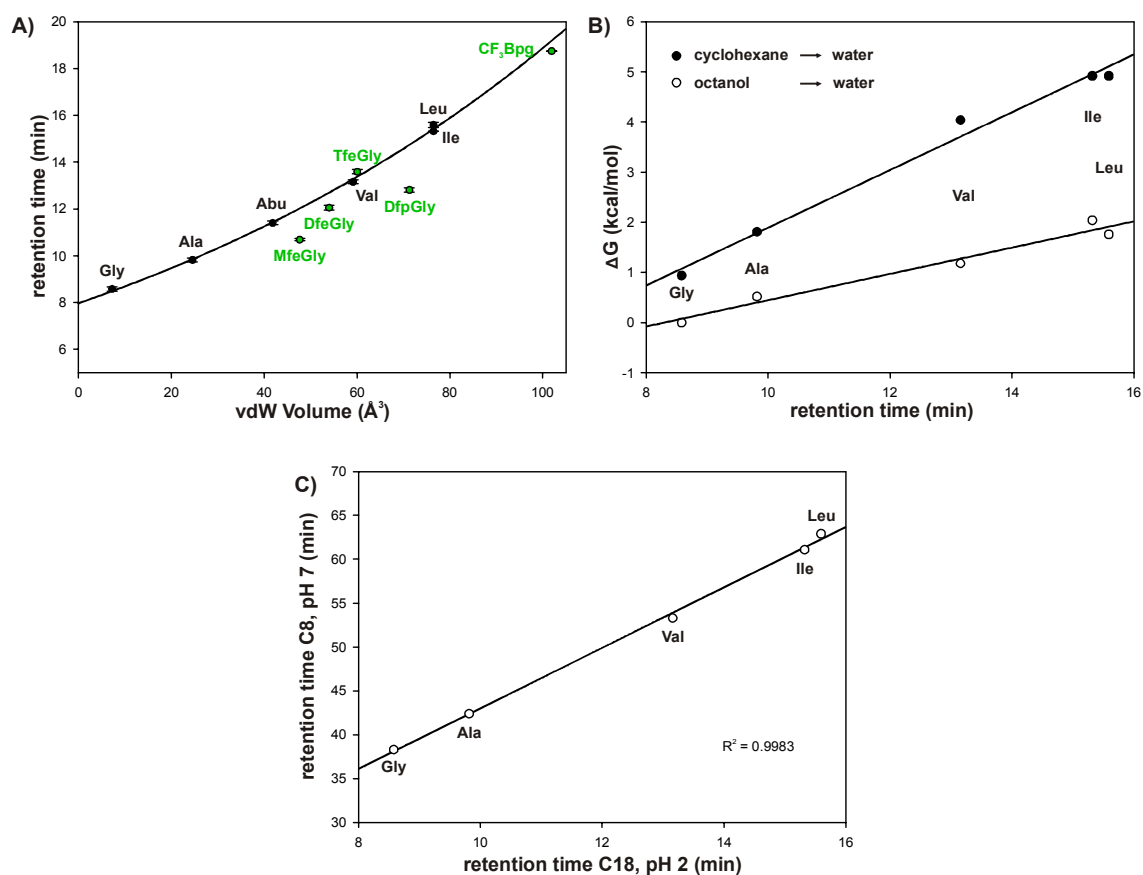


Figure 6.5 A) Retention times of the N^α -Fmoc-protected amino acids plotted against the vdW-volume of the side chains. The solid line represents the fit ($rt = 8 \exp[0.009 \cdot V_{vdW}]$, $R^2 = 0.9984$); B) correlation of retention time of the Fmoc-analogues and free energies of partitioning between water and cyclohexane or octanol, respectively; and C) correlation of retention times of hydrophobic Fmoc-amino acids at pH 2 on a Capcell PAK C18 column with retention times of the peptide Ac-XGAKGAGVGL-NH₂, in which X represents the substitution position, determined by Kovacs *et al.* at pH 7 on a Zorbax XDB C8 column.²¹²

Figure 6.5 C shows the correlation of the retention times of the Fmoc-amino acids at pH 2 with their peptide retention times determined on a C8 column at pH 7. The values obtained using Fmoc-amino acids at pH 2 on a C18 column perfectly correlate with their values although they were determined at rather different conditions. Therefore, the RP-HPLC assay developed here can be regarded as a very quick and reliable method that generates a hydrophobicity scale that compares well to those published. Furthermore, the present method is rather convenient since it employs Fmoc-amino acids that

are easily available in every peptide chemist's laboratory. These advantages notwithstanding, it is important to note that this assay is applicable to non-ionizable side chains only. For any other amino acid whose side chain is sensitive towards pH it would likely produce misleading results if not carried out under conditions (pH) relevant to the protein studies that may follow.

The retention times of the fluorinated amino acids do not fit into the correlation between side chain volume and retention time shown for their pure hydrocarbon analogues. Although larger than Abu, both MfeGly and DfeGly are less hydrophobic than one might expect regarding their size. Also, DfpGly that is close to leucine in size is even more polar than the much smaller valine. Solely TfeGly is comparable to valine in both, size and hydrophobicity. Comparison of the three fluorinated analogues of Abu (MfeGly, DfeGly, and TfeGly) reveals that hydrophobicity increases much more progressively with fluorine content than it does with size. The results for the Abu analogues and DfpGly are consistent with the general finding that partial aliphatic fluorination decreases hydrophobicity, while perfluorination generally brings about a pronounced increase in hydrophobicity.⁶⁹ These results were furthermore supported by a quantum mechanical investigation that revealed potential hydrogen bonds of the fluorinated side chains with water.²¹³ Based on these data, two effects of side chain fluorination must be considered: 1) partial fluorination renders the amino acids more polar, but 2) hydrophobicity increases more progressively with fluorine content than with side chain volume. This observation can be explained by fluorine being a weak hydrogen bond acceptor⁸¹ and by the impact of fluorination on the overall polarizability of the molecules. Because fluorine is itself a very weakly polarizable atom and at the same time very electronegative (see Table 2.1), it also reduces the polarizability of adjacent C–C and C–H bonds.²¹⁴ As a consequence, hydrogen bond, dipole-dipole, as well as London dispersion interactions of the side chains with water are progressively weakened as the number of fluorine atoms increases. Beyond a certain threshold, which is reached for three fluorine atoms in the side chain of Abu, fluorinated amino acids become more hydrophobic than size alone would suggest. Consequently, perfluorocarbons are what may be called hyperhydrophobic. CF₃-Bpg, the most hydrophobic amino acid in this series, is, due to its unique structure, not comparable to the other fluorinated amino acids and is, therefore, not discussed further here. In order to assess the impact of fluorine it would need to be compared to an analogue that carries a methyl group instead of a trifluoromethyl group.

Size and hydrophobicity of side chains play an important role in coiled-coil formation. Having summarized these general properties of fluorinated amino acids, the next sections give an insight into the stereoelectronic effects of fluorination on the molecular

interactions of these building blocks within a native protein environment by applying the model system VPE-VPK.

6.3 Effects of size and hydrophobicity of fluorinated amino acids at two different positions within the hydrophobic core

The results presented in this section have been originally published as: M. Salwiczek, S. Samsonov, T. Vagt, E. Nyakatura, E. Fleige, J. Numata, H. Cölfen, M. T. Pisabarro, B. Kokschi; Position-Dependent Effects of Fluorinated Amino Acids on the Hydrophobic Core Formation of a Heterodimeric Coiled Coil; *Chemistry – A European Journal* **2009**, *15*, 7628-7636.

The original paper with supporting information is available at:

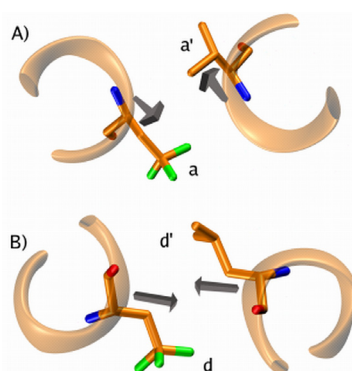
<http://dx.doi.org/10.1002/chem.200802136>

Paper summary

The model system VPE-VPK served two different studies in the group of Prof. Kokschi and, therefore, its design was developed in cooperation with Toni Vagt who employed it in a phage display based screen for preferred interaction partners of fluorinated amino acids.²¹⁵ All experimental investigations (SPPS, CD spectroscopy, thermodynamic analysis, analytical ultracentrifugation, and FRET) are part of this thesis. MD simulations were conducted by Sergey Samsonov (BIOTEC, TU Dresden). Data evaluation of sedimentation velocity and sedimentation equilibrium experiments was supported by Dr. Helmut Cölfen. Jorge Numata provided assistance in setting up an Excel table for fitting the thermal unfolding data. Elisabeth Nyakatura and Emanuel Fleige synthesized four of the VPK analogues during practical/bachelor internships in the group of Prof. Kokschi that were supervised by the author.

The goal of this study was to establish a new coiled-coil model that fulfills the requirement to tolerate fluoroamino acid substitutions within the hydrophobic core while allowing for sensitive detection of their effects (see section 6.1). The paper describes the optimization of the synthesis and the structural characterization of the VPE-VPK coiled coil applying CD spectroscopy (secondary structure), analytical ultracentrifugation (oligomerization state), and FRET (strand orientation). As intended by design VPE and VPK form stable α -helical assemblies with parallel strand orientation. Analytical ultracentrifugation furthermore indicates the exclusive formation of heterodimers that undergo cooperative unfolding transitions from α -helix to random coil in the temperature range from 20 to 100 °C (temperature dependant CD spectroscopy).

The objective was then to evaluate the effects that substitutions of native residues within two different hydrophobic core positions (a16 and d19) within VPK have on the interactions with native amino acids in the corresponding VPE strand. The question was, whether the different orientation of the side chains at these positions would have a detectable impact on the effects that the size and hydrophobicity of the fluorinated amino acids provoke. Two series of peptides that contain Abu, its fluorinated analogues DfeGly and TfeGly as well as DfpGly at either position a16 or position d19 of VPK were synthesized. By the time of publication MfeGly was unavailable. Its effects are therefore discussed in section 6.4. For the VPK-a16 series and additional variant containing Leu was synthesized since Leu served as the control substitution in this study. The structure of the coiled coils was investigated by CD spectroscopy and molecular dynamics simulations. The thermodynamic stability of all variants was furthermore evaluated on the basis of temperature induced unfolding monitored by CD spectroscopy as well as at the theoretical level applying MM-PBSA calculations.



GRAPHICAL ABSTRACT: Picking up the fluorine trail Example showing the orientation of TfeGly at A) position a16 and B) position d19 (reproduced from the table of contents of *Chem. Eur. J.* 2009, 15, issue 31 with permission, Copyright © 2009 Wiley-VCH Verlag GmbH & Co. KGaA, Weinheim).

Both, the experimental and theoretical investigations allow for the same conclusion. The different orientations of the fluorinated side chains imposed by the coiled-coil backbone at position a16 and d19 (see graphical abstract) have an impact on their effects on stability folding. While at position a16 mainly size and hydrophobicity of the fluorinated side chain determine stability, the polarity induced by fluorine, due to the different orientation of the local dipole at the β -carbon, diminishes the stabilizing impact of increasing size and overall hydrophobicity at position d19. The main conclusion of this study, therefore, is that the impact of fluorination on protein stability does to a non-negligible extent depend on the microenvironment of the substitution, i.e. on whether the locally induced dipoles are oriented towards interacting hydrophobic residues or not. While it may be difficult to transfer this knowledge to the design of folding motifs

other than the coiled coil, it helps to understand why the impact of fluorination on protein folding is hardly ever predictable; since it is hard to predict local side chain orientations it is also difficult to pre-estimate the impact of fluorine-induced polarity and its impact on hydrophobic interactions at the substitution site.

6.4 Evaluation of the interactions of (S)-4-fluoroaminobutyric acid

The preceding section described the position-dependent effects of two aminobutyric acid analogues (DfeGly and TfeGly) as well as DfpGly on structure formation of the heterodimeric coiled-coil model. At the time of publication, the monofluorinated analogue MfeGly was not available. Therefore, these results are discussed in this additional section.

Containing only one fluorine atom, MfeGly (Figure 6.4) completes the series of aminobutyric analogues that carry increasing numbers of fluorine atoms at the γ -position. Compared to DfeGly and TfeGly, however, it represents the only analogue that is actually more polar than Abu (see section 6.2). Although bulkier and more hydrophobic than Abu, DfeGly and TfeGly were not able to stabilize the coiled-coil assembly. Therefore, the initial expectation was that MfeGly would be the most destabilizing substitution at both positions because it is smaller and more polar than its analogues. Figure 6.6 A shows the CD-spectra of individual VPE and VPK-MfeGly16. Both spectra indicate that the individual peptides are predominantly random coil with residual helical structure as indicated by the low intensity double minimum of which the one at 208 nm is slightly shifted towards lower wavelengths. The equimolar mixture, in contrast, displays a defined double minimum at 208 and 222 nm indicating a well ordered α -helical structure. As discussed in the next section, the helical content (88%, see section 7.4) is the highest among all the investigated variants and shows that MfeGly is structurally well accommodated by the coiled coil. However, the analysis of thermal unfolding (Figure 6.6 B) reveals that this coiled coil is also the least stable a16-substituted variant. With a free energy of unfolding of 10.3 ± 0.2 kcal/mol it is 1.2 kcal/mol less stable than the Abu variant and by even 3.5 kcal/mol less stable than the Leu containing peptide.

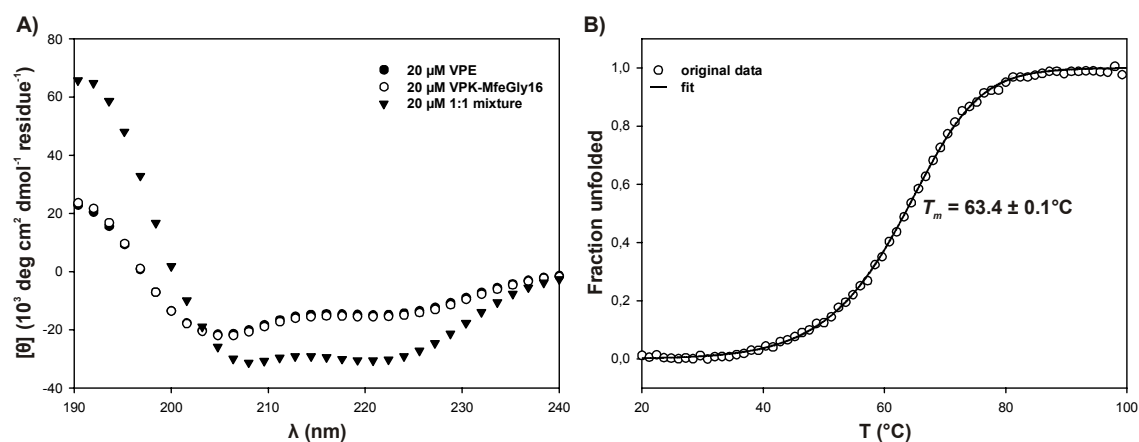


Figure 6.6 A) CD-spectra of 20 μM solutions of individual VPE, VPK-MfeGly16, and an equimolar mixture of both at 20 $^{\circ}\text{C}$ and B) melting curve of the equimolar mixture. All experiments were carried out at pH 7.4 (100 mM phosphate buffer).

At position d19, MfeGly imparts a comparable, albeit slightly less pronounced destabilizing effect, which is in accordance with the findings for the other analogues (section 7.2). Figure 6.7 shows the CD-spectral analysis and thermal unfolding profile of VPE-VPK-MfeGly19. The main difference is that the individual VPK-MfeGly19 analogue is completely random coil shown by the single minimum just below 200 nm. Again the mixture of VPE and VPK-MfeGly19 displays a strong double minimum that indicates high helical content (76%, see section 6.6). The standard free energy of unfolding for the coiled coil is 9.6 ± 0.1 kcal/mol which represents 0.7 kcal/mol destabilization compared to Abu and 2.8 kcal/mol compared to Leu at the same position.

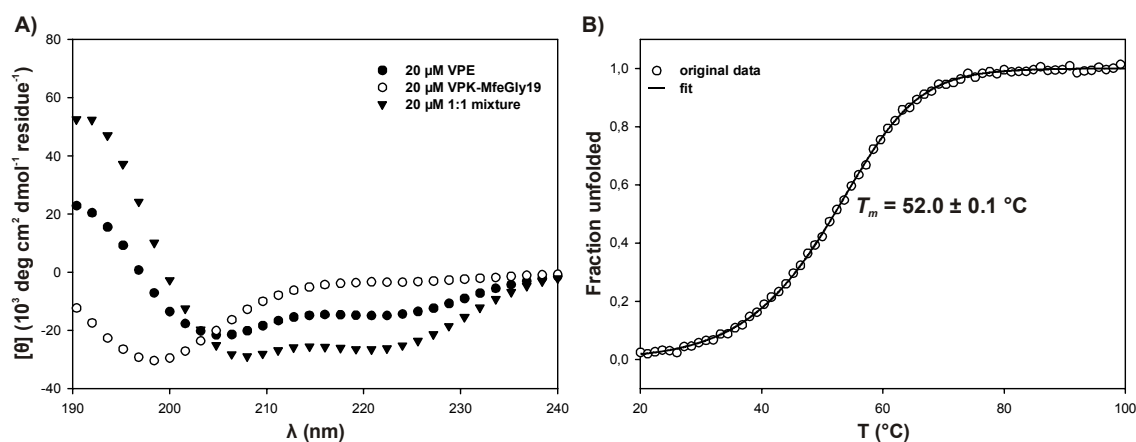


Figure 6.7 A) CD-spectra of 20 μM solutions of individual VPE, VPK-MfeGly19, and an equimolar mixture of both at 20°C and B) melting curve of the equimolar mixture. All experiments were carried out at pH 7.4 (100 mM phosphate buffer).

The strong destabilization compared to leucine may largely be attributed to the markedly smaller side chain of MfeGly ($\Delta V^{\text{vdw}} = 28.8 \text{ \AA}^3$). The size difference in side-chain volume between Abu and MfeGly is 5.8 \AA^3 , but size arguments may not explain the destabilization, since MfeGly is the larger of the two amino acids. Instead, the destabilizing effect must be attributed to the high polarity of MfeGly that strongly perturbs hydrophobic interactions at the substitution site. Furthermore, the driving force to bury such a polar residue within the core of the coiled coil should be rather low. Therefore, the initial assumption that MfeGly should destabilize the coiled coil compared to Abu and would accordingly be the most destabilizing of all substitutions investigated here is confirmed.

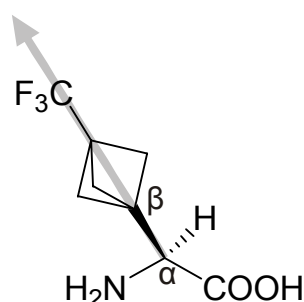
6.5 Evaluation of the interactions of the newly designed NMR label CF₃-Bpg

The results presented in this section have been accepted for publication in *Amino Acids* as: M. Salwiczek, P. K. Mikhailiuk, S. Afonin, I. V. Komarov, A. S. Ulrich, and B. Kokschi; Compatibility of the Conformationally Rigid CF₃-Bpg Side Chain with the Hydrophobic Coiled-Coil Interface. Pavel K. Mikhailiuk synthesized the amino acid under supervision of Igor V. Komarov. Anne S. Ulrich and Sergii Afonin contributed to interpreting the results from the viewpoint of an NMR specialist. The original paper with supplementary material is available under DOI: 10.1007/s00726-010-0581-8 at:

<http://dx.doi.org/10.1007/s00726-010-0581-8>

Paper summary

As described in section 2.1, ¹⁹F represents a formidable NMR label for a variety of analytical applications. However, as a label, fluorinated amino acids should fulfill some vital conditions such as rigidity, which prevents conformational anisotropy especially when NMR is used for distance measurements or for assessing the orientations of peptide segments in the context of larger assemblies such as those of proteins within tertiary and quaternary structures or in the environment of biological membranes. Since the orientation of the side chains within the coiled-coil model studied in this thesis is the fundament on which the interpretation is built up, one such label, CF₃-Bpg (see graphical abstract), was used to evaluate its suitability as a potential NMR probe in the context of coiled-coil hydrophobic cores.



GRAPHICAL ABSTRACT: A stubborn partner Structure of the rigid CF₃-Bpg demonstrating how the position of the CF₃ group directly translates into the orientation of the C_α-C_β vector (grey arrow).

The objective of this study was to assess the compatibility of the bulky and rigid CF₃-Bpg side chain with the coiled-coil hydrophobic core in terms of structure and stability. The effects were studied by CD spectroscopy and FRET as described in the preceding sections. CD spectroscopy revealed that incorporation of the amino acid at posi-

tion a16 or d19 has only minor structural consequences for the coiled coil as indicated by the practical identity of the spectra compared to the parental peptide that contains Val and Leu at these positions, respectively. Although CF₃-Bpg is more hydrophobic than Val and Leu the thermodynamic stability of the coiled coil, however, is markedly reduced especially when compared to Leu. The conclusion is thus, that its rigid and bulky side chain, despite its pronounced hydrophobicity, cannot engage in favorable packing interactions with the native residues of the interacting VPE strand. However, given the still sufficient stability and the fact that the CD spectra do not show major structural perturbations one may envisage its application to probe the orientation of the C_α-C_β vector of the side chains at both substitution positions. As shown in the graphical abstract above, the position of the CF₃-group directly traces back to the orientation of the C_α-C_β bond, which is due to its linkage via the conformationally rigid and axially symmetrical bicyclo[1.1.1]pentyl unit. Therefore, as far as coiled coils are concerned, CF₃-Bpg may not be an appropriate label to study side chain interactions. It may nevertheless prove useful to study local side chain orientations that are imposed by the peptide backbone.

6.6 Helix propensity and coiled-coil stability

As discussed in section 6.3, it can be assumed that helix propensity plays a less important role in the context of coiled-coil stability as it does in isolated helices.²¹⁶ The formation of coiled-coil helices is strongly determined by specific hydrophobic interactions between the monomers as well as intermolecular electrostatic interactions that are only possible in the helical state. Since these interactions stabilize the structure, they could have an impact on the measured helix propensity values. Therefore, helix propensity is evaluated using isolated helices, in which side-chain interactions are absent by design.¹⁷⁷ This section will give further support for the argument against a strong impact of helix propensity of the fluorinated amino acids on coiled-coil stability through a more detailed analysis and discussion of CD-structure data as well as dihedral angles derived from MD simulations.²¹⁷

Helix propensity (w) describes the tendency of an amino acid within a peptide assembly to adopt an α -helical conformation. The conformation of the peptide backbone can be described in terms of dihedral angles ϕ , ψ , and ω of the amino acid backbone. In the more common *trans*-peptide bond, ω is constant around $179 \pm 3^\circ$, i.e. the peptide bond may be considered planar.²¹⁸ Therefore, ϕ and ψ are sufficient to describe the peptide backbone conformation (Figure 6.8). In typical α -helices, ϕ and ψ are centered around -62° and -41° , respectively. Figure 6.9 A shows a Ramachandran plot of the dihedral angles of all residues in the VPE-VPK heterodimer that have been derived from molecular dynamics simulations. The plot shows that VPE-VPK adopts an almost ideal α -helical conformation. Approximately five residues per helix (see section 5.1.2), mainly those at the helix termini (see insert Figure 6.9 A) however, exhibit non-helical conformations, a common phenomenon known as helix end fraying due to the absence of hydrogen-bonding partners for the terminal residues.²¹⁹

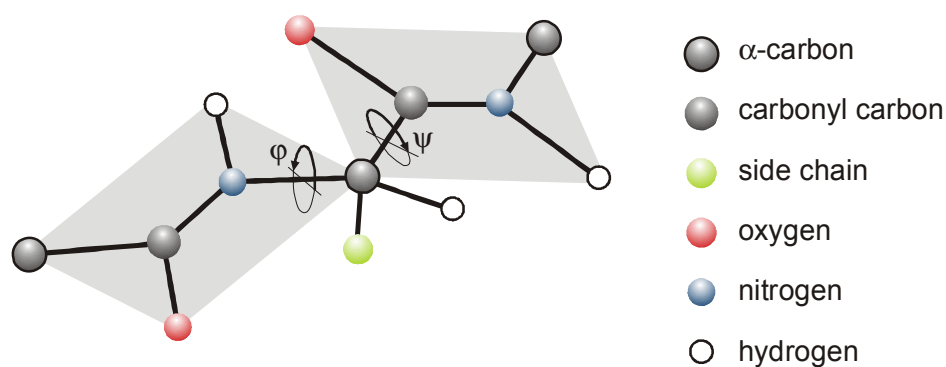


Figure 6.8 Cutout of a peptide backbone showing one residue and the two adjacent peptide bonds.

Regarding the low helix propensity of fluorinated aliphatic amino acids compared to native residues (Table 6.1),^{220,221} one may initially assume that the destabilization of the VPE-VPK model system due to the fluorination of position a16 or d19 results from unfavorable side-chain conformations of the fluorinated side chains.

Table 6.1 Helix propensity of fluorinated amino acids compared to hydrocarbon analogues.

Amino acid	w	
	Chiu <i>et al.</i> ^{220,221}	Chakrabartty <i>et al.</i> ¹⁷⁷
Val	n/d	0.23
Leu	1.06	0.96
Abu	1.22	n.d.
TfeGly	0.0513	n.d.
Qfl	0.445	n.d.
Hfl	0.128	n.d.

Theory, however, predicts that Abu, TfeGly, and DfpGly exhibit typical α -helical dihedral angles that are comparable to those of Leu within this coiled-coil environment (Figure 6.9 B). For DfeGly, ψ appears distorted, which, however, is not reflected by the thermodynamic stability of the coiled coil. Nevertheless, a first strong argument that partially rules out that helix propensity mainly determines coiled-coil stability can be drawn from comparing Leu and Abu. Despite the higher helix propensity of Abu, its substitution for Leu destabilizes the VPE-VPK dimer by 2.3 kcal/mol (position a16) and 2.1 kcal/mol (position d19). Thus, the decrease in stability is very likely to be caused by the reduced van der Waals volume and hydrophobicity of Abu.

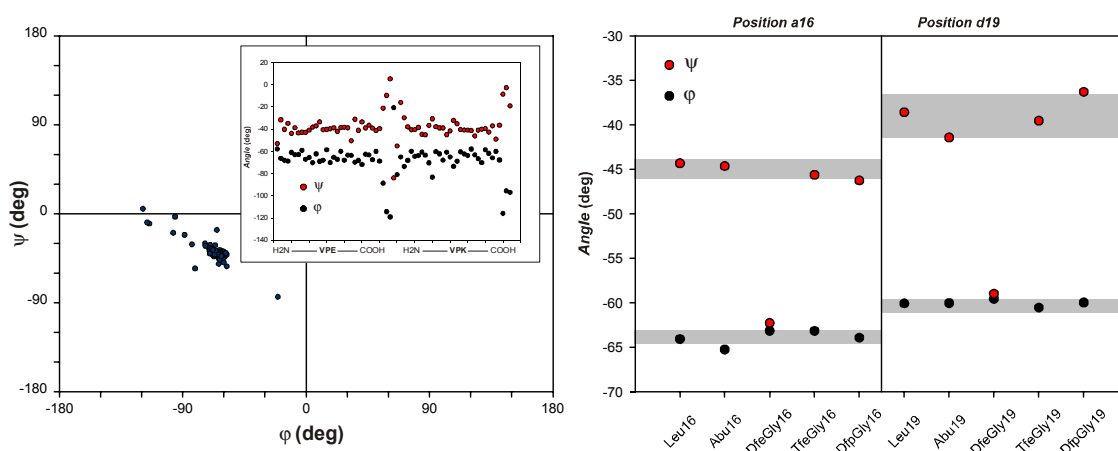


Figure 6.9 A) Ramachandran plot of the theoretically calculated dihedral angles ϕ and ψ for the parental VPE-VPK heterodimer and B) ϕ and ψ for the substituted variants.

Table 6.2, on the other hand, shows that the fluorinated peptides indeed exhibit lower helical content than their non-fluorinated counterparts. At a first glance this finding could be interpreted in such a way to support the argument that the low helix propensity of fluorinated amino acids destabilizes the coiled coil through unfavorable conformations. However, again the comparison between Abu and Leu indicates that the helix propensity cannot solely account for the structural as well as thermodynamic effects. While the Abu-substituted a16 variant is more helical than the Leu variant the trend is reversed for position d19. The same reversal in helicity trend was observed for DfeGly and TfeGly.

Table 6.2 Helical content of the VPE-VPK variants.

Amino acid	$[\theta]_{222\text{nm}}$	f_{H}^{a}	$[\theta]_{222\text{nm}}$	f_{H}^{a}
	[deg cm ² dmol ⁻¹]	[%]	[deg cm ² dmol ⁻¹]	[%]
	position a ₁₆		position d ₁₉	
Val	-26.274	76	n.d.	n.d.
Leu	-22.937	66	-26.274	76
Abu	-25.004	72	-21.929	63
MfeGly	-30.462	88	-26.288	76
DfeGly	-18.119	52	-21.582	62
TfeGly	-18.900	54	-20.122	58
DfpGly	-23.100	66	-22.449	65
CF ₃ -Bpg	-24.375	70	-22.962	66

^a calculated according to eq. 5.5

These results indicate that packing effects as well as side-chain interactions rather than helix propensity determine the structural and thermodynamic effects of the substitutions observed here. Since interhelical hydrophobic interactions are weaker for the more polar fluorinated amino acids the whole coiled-coil assembly loses stability and, thus, structural integrity. Another finding that may also be used to rebut the helix propensity argument is that the most helical of the VPE-VPK variants investigated, i.e. those containing MfeGly (a16: 88% and d19: 76% helix, respectively), are at the same time the least stable.

In summary, it should be noted that the low helix propensity of fluorinated amino acids is not completely ruled out as an argument to explain the destabilizing effects. Theoretical investigations show that fluorination may furthermore have diverse effects in this respect. While MfeGly and TfeGly were found to prefer α -helical conformations, DfeGly and DfpGly apparently favor β -sheets.²¹³ Recent experimental data indicate that some fluorinated amino acids are indeed well-suited to stabilize β -sheets.²²² However, as β -sheets do usually not exist as individual peptide strands, intrinsic β -sheet propensities are not easy to measure. Thus, these recent data may be insufficient to draw a

final conclusion. The present investigation indicates that hydrophobicity and van der Waals volume play a more important role in the context of coiled coils. Nevertheless, a more detailed structural and thermodynamic analysis may be necessary to deconvolute the contribution of all of these factors.

6.7 Effects of fluorine substitution at position d19 on folding kinetics

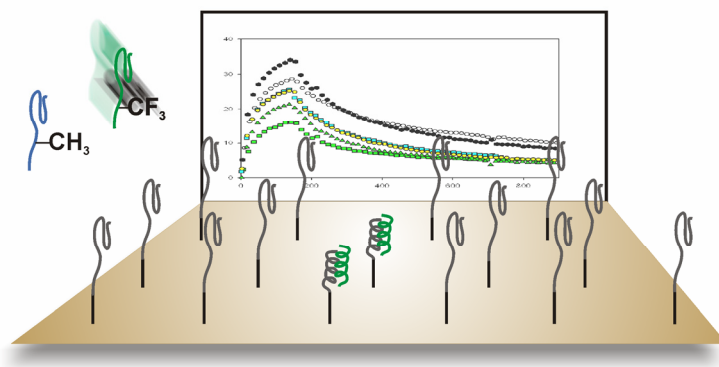
The results presented in this section have been originally published as: M. Salwiczek, B. Kokschi; Effects of Fluorination on the Folding Kinetics of a Heterodimeric Coiled Coil; *ChemBioChem* **2009**, 10, 2867-2870.

The original paper including supporting information is available at:

<http://dx.doi.org/10.1002/cbic.200900518>

Paper summary

As mentioned in section 3.3 earlier investigations on coiled-coil self-replication indicated that increasing the fluorine content may result in retardation of coiled-coil association although the increase in hydrophobicity would be expected to have the opposite effect.¹⁵⁴



GRAPHICAL ABSTRACT: The fast and the fluorous Schematic representation of a gold surface covered with VPE (grey bundles). Coiled-coil formation can be monitored in real time upon treatment with suitably buffered solutions of different VPK analogues (typical sensograms are shown in the background). Due to increasing hydrophobicity, fluorination increases the rate of association (green peptide compared to blue peptide on the left). The figure has been reproduced from the table of contents of *ChemBioChem* 2009, 10, issue 18 with permission (Copyright © 2009 Wiley-VCH Verlag GmbH & Co. KGaA, 69451 Weinheim).

However, since these investigations could not provide kinetic data the interpretation heretofore needed additional proof. The paper describes the application of SPR to probe the effects of Abu side chain fluorination on coiled-coil folding kinetics. To this

end, the interactions of surface bound VPE with VPK analogues containing Abu, DfeGly, TfeGly, and DfpGly at position d19 were investigated. At the time of the SPR investigations neither MfeGly nor CF₃-Bpg were available and, thus, were not part of this study.

Other than the thermal unfolding data, the kinetic data observed using SPR can only be analyzed assuming a three-state rather than a two-state folding mechanism, i.e. folding requires two steps and an intermediate accumulates along the folding pathway. However, the second folding step does contribute merely 10% to the overall free energy of folding and is very slow compared to the first step. Furthermore, it is hardly affected by substitutions. The thermodynamic data calculated from the kinetics of the first folding step are in excellent agreement with the data derived from analysis of equilibrium unfolding and the effects of fluorine substitutions are readily detected. Comparison of the data for association of the DfeGly and TfeGly substituted VPK variant with VPE confirm that increasing fluorine content of the side chain slightly retards coiled-coil association. Thus, the association does, indeed, not always correlate with size and hydrophobicity in the case of fluorinated amino acids. In contrast, the dissociation rates decrease with increasing size and hydrophobicity; the more hydrophobic the side chain, the less readily it is withdrawn from the hydrophobic environment. However, the fact that increasing fluorine content from DfeGly to TfeGly decreases the association rate could be an indication for the formation of fluorous 'clusters' between several unfolded peptide strands because fluorine tends to segregate from both, aqueous and hydrophobic environments.

In conclusion, SPR is able to detect kinetic effects of fluorination and readily reproduces the thermodynamic consequences. The results are consistent with earlier investigations, in which a different model system and a different method were applied. However, it is impossible to detect the postulated fluorous clusters with the methods applied here and thus, proving their existence remains an issue of future investigations using methods with high structural resolution such as NMR.

6.8 Effects of fluorine substitution at position a16 on folding kinetics

In analogy to the thermodynamic investigations presented in sections 6.2 through 6.7, the aim was to furthermore investigate the position-dependence of fluorine substitutions on coiled-coil folding kinetics. Again, aiming to evaluate the impact of a rather small structural change by introducing two or three fluorine atoms, or a methyl group, respectively, Abu was to be compared to its analogues DfeGly, TfeGly, and DfpGly at position a16.

While the results for position d19 are in excellent qualitative and reasonable quantitative agreement with the data derived from equilibrium unfolding (section 6.7),²²³ the kinetic investigation of position a16 substitutions posed major problems. Figure 6.10 shows the sensograms for the interaction of VPK-Abu16 with VPE analyzed by applying two different models.

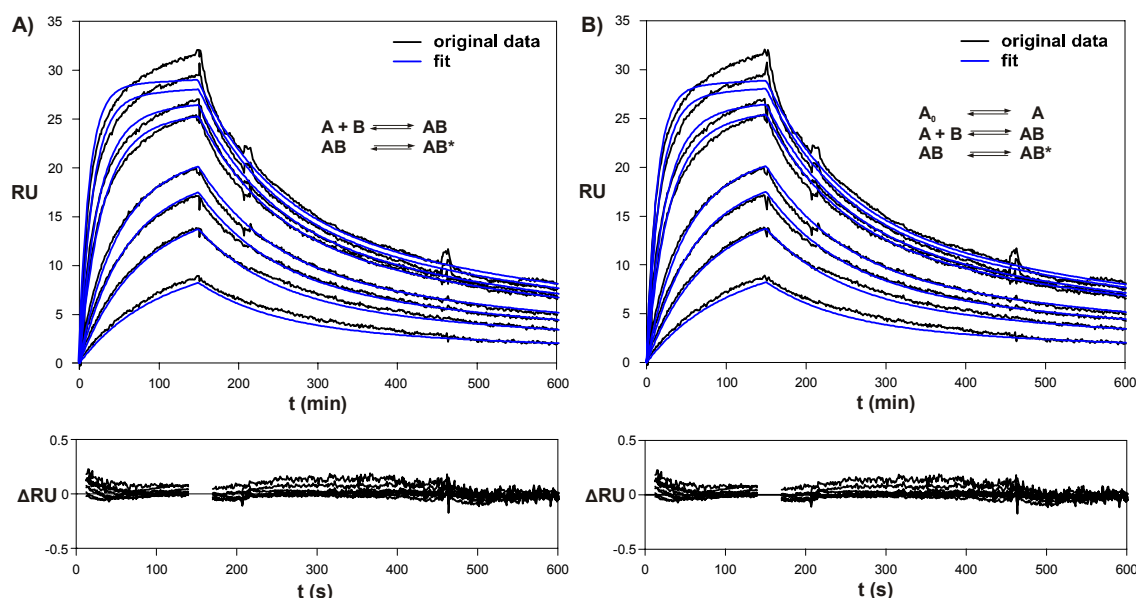


Figure 6.10 Upper panel: Global analysis of the VPK-Abu16 interaction with VPE at 25°C (pH 7.4, 100 mM phosphate buffer, 3.4 mM EDTA, 0.05 % Tween 20). Eight concentrations were injected over approximately 50 RUs of immobilized VPE ($C_{\text{VPK-Abu16}} = 5, 10, 15, 20, 40, 50, 75,$ and 100 nM). Lower panel: residuals from the fit to A) a simple association-dissociation model including a second conformational rearrangement step ($\chi^2 = 0.2$) and B) the same model considering mass transfer of VPK-Abu16 to the surface. Mass transfer is interpreted as diffusion of the analyte A_0 from the bulk solution to the surface ($\chi^2 = 0.2$).

Visual inspection of the sensograms and the corresponding residuals from each fit reveals the inadequacy of both models. Several reasons may account for unsuccessful data analysis in SPR.²²⁴ First, in order to adequately analyze SPR sensograms one has to make sure that the concentrations are determined as accurately as possible. However, as the experiments were carried out identically to those for position d19, concentration errors may be ruled out. Second, folding specificity, i.e. oligomerization state, of

these coiled coils could be concentration-dependent, which would cause a global fit over different concentrations to fail. Analytical ultracentrifugation of the original VPE-VPK peptides, on the other hand, has shown that folding specificity is identical within a large concentration range. In addition, the magnitude of fluorescence decrease in FRET analysis is equal for all coiled-coil assemblies investigated here (see section 6.3) suggesting that their folding specificity is equal. Although the fit to a simple association-dissociation equilibrium followed by a conformational change does not describe the interaction appropriately, the deviance χ^2 is rather low (Table 6.3). Thus, this analysis was performed for all the variants. Comparison of thermodynamic data derived from the kinetic analysis with those from equilibrium unfolding, interestingly, shows that they are within the same order of magnitude. However, the standard deviation of the free energy values is rather large for all the analogues, which makes a quantitative comparison impossible (Table 6.4). Accordingly, a detailed discussion of these kinetic and thermodynamic data is precluded.

Table 6.3 Kinetic parameters of the interaction of VPK-a16 analogues with VPE derived from the fit to the model shown in Figure 6.10 A.

Amino acid	k_{ass} [$10^5 \text{ mol}^{-1} \text{ s}^{-1}$]	k_{diss} [10^{-3} s^{-1}]	k_r [10^{-3} s^{-1}]	k_{-r} [10^{-3} s^{-1}]	χ^2
Abu	6.92 ± 0.02	8.01 ± 0.05	2.28 ± 0.03	1.74 ± 0.03	0.2
DfeGly	5.83 ± 0.03	9.04 ± 0.08	2.73 ± 0.05	1.82 ± 0.04	0.3
TfeGly	5.17 ± 0.03	8.76 ± 0.1	2.79 ± 0.05	0.96 ± 0.03	0.3
DfpGly	6.75 ± 0.03	8.31 ± 0.09	2.85 ± 0.06	1.97 ± 0.05	0.4

Table 6.4 Free energies of unfolding calculated from kinetic data compared to those from temperature induced unfolding.

Amino acid	ΔG_1° [kcal mol $^{-1}$]	ΔG_2° [kcal mol $^{-1}$]	ΔG_t° [kcal mol $^{-1}$]
Abu	10.8 ± 0.4	11.3 ± 0.8	11.5 ± 0.2
DfeGly	10.6 ± 0.5	11.2 ± 0.8	11.5 ± 0.2
TfeGly	10.6 ± 0.4	11.4 ± 1.0	11.5 ± 0.2
DfpGly	10.8 ± 0.5	11.3 ± 0.8	12.3 ± 0.2

¹ free energy of the association-dissociation; ² free energy of unfolding including the rearrangement step, ^t free energy of unfolding from temperature induced unfolding

A third explanation for unsuccessful data fitting may be that the association of the analyte and the ligand on the SPR surface is mass-transport limited. This phenomenon occurs when the association rate is comparable to or even larger than the diffusion rate of the analyte to the surface. However, including mass transfer in analyzing the senso-

grams (Figure 6.10 B) does not improve the fit. Most importantly, the value for the mass transfer constant k_m derived from this analysis is markedly larger than the association constant and its statistical error is by two orders of magnitude larger than the actual value, which is shown in a representative case for VPK-Abu16 (Table 6.5). Thus, this value does not have any interpretable significance. Furthermore, the thermodynamic data calculated from these kinetic constants strongly deviate from those derived from equilibrium unfolding (Table 6.6). Therefore, the analysis including mass transport limitation is not appropriate.

Table 6.5 Kinetic parameters of the interaction of VPK-a16 analogues with VPE derived from the fit to the model including mass transfer shown in Figure 6.10 B.

Amino acid	k_{ass} [$10^5 \text{ mol}^{-1} \text{ s}^{-1}$]	k_{diss} [s^{-1}]	k_r [s^{-1}]	$k_{r,r}$ [10^{-3} s^{-1}]	k_m [$10^{18} \text{ mol}^{-1} \text{ s}^{-1}$]	χ^2
Abu	6.92 ± 0.02	62.5 ± 0.4	17.8 ± 0.2	13.6 ± 0.2	$0.05 \pm 5,62$	0.2

Table 6.6 Free energies of unfolding calculated from kinetic data compared to those from temperature induced unfolding.

Amino acid	ΔG_1° [kcal mol $^{-1}$]	ΔG_2° [kcal mol $^{-1}$]	ΔG_t° [kcal mol $^{-1}$]
Abu	5.5 ± 0.4	6.0 ± 0.8	11.5 ± 0.2

The fourth, and in the case of coiled coils also most plausible reason, may be self-association of the analytes (VPK) in solution. SPR detects rather small changes in the refractive index just above the surface of the sensor chip. Any solution equilibrium that takes place in the supernatant cannot be detected because it does not change the refractive index close to the gold surface. If the isolated VPK variants self-associate then this additional equilibrium could be a limiting step prior to association with VPE. Assessing its contribution by means of rate constants by applying SPR, however, would be impossible.

Indeed, comparing the CD spectra of the isolated VPK variants in a position-dependent manner supports that self-association of the analyte may explain why data analysis failed. The simple visual inspection shows that the a16 substituted VPK analogues are largely helical, which suggests coiled-coil formation. In contrast, all d19 substituted variants are predominantly random coil. Coiled-coil formation of the individual a16 analogues is synonymous with self-association. Table 6.7 summarizes the helical content of the relevant VPK analogues in comparison to their mixtures with VPE. For position d19 the helical content is rather low with values between 11% and 20% while all position a16 variants are up to a maximum of 50% helical. The residual helicity of

the d19 analogues apparently does not affect SPR data analysis. In contrast, it was impossible to derive reliable data for VPK-a16 analogues.

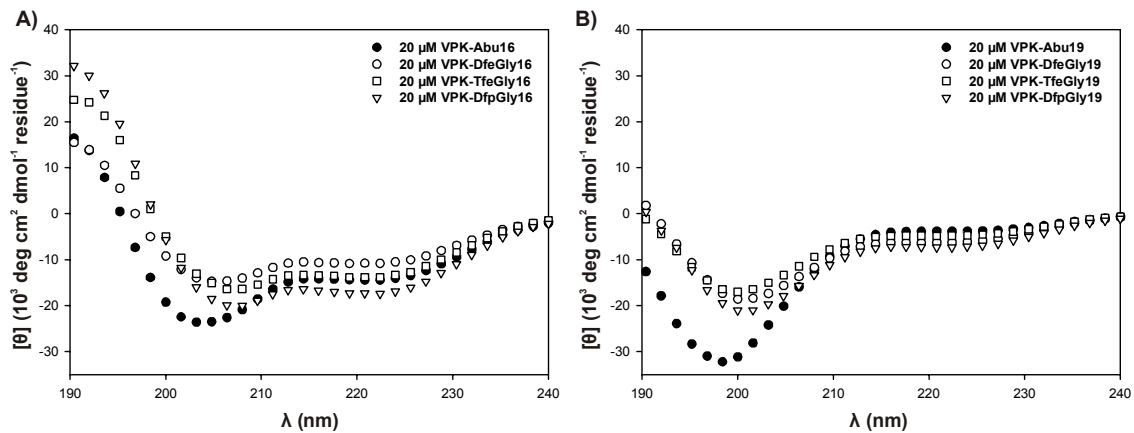


Figure 6.11 CD-spectra of 20 μM solutions of the isolated VPK-variants containing Abu and its analogues at A) position a16 and B) position d19. All spectra were recorded at 20°C at pH 7.4 (100 mM phosphate buffer).

Table 6.7 Helical content of the homomeric VPK variants compared to the heteromeric VPE-VPK variants.

Amino acid	Homomeric		Heteromeric		Homomeric		Heteromeric	
	f_H^a [%]	T_m [°C]	f_H^a [%]	T_m [°C]	f_H^a [%]	T_m [°C]	f_H^a [%]	T_m [°C]
	<i>position a₁₆</i>				<i>position d₁₉</i>			
Abu	42	39.8	72	65.9	11	n.a. ^b	63	53.7
DfeGly	31	40.6	52	66.9	18	n.a. ^b	62	56.9
TfeGly	40	44.6	54	69.0	14	n.a. ^b	58	55.3
DfpGly	50	49.3	66	69.3	21	n.a. ^b	65	57.5

^a calculated according to eq. 5.5, ^b For d19 analogues melting points could not be determined since these peptides were random coils and the CD signal at 222 nm did not change significantly upon heating.

To show that those VPK-a16 variants that exhibit helical CD spectra are not monomeric, one representative example, for which sedimentation velocity data were obtained, has been chosen to be discussed here. As shown in Figure 6.12 A, the original VPK sequence exhibits a CD spectrum that is comparable to all the VPK a16 analogues. SPR analysis of this peptide, accordingly, failed as well. The distribution of molecular weights (Figure 6.12 B) indicates equilibrium between two species, one at approximately 4700 g/mol and one at 7500 g/mol. Sedimentation velocity data may only give approximate values for molecular weight. However, these values roughly correspond to a monomer-dimer equilibrium proving that those VPK analogues that exhibit significantly helical CD spectra are not exclusively monomeric. On the other hand, the heteromers are entirely dimeric, since they are thermodynamically favored (see section 6.3).

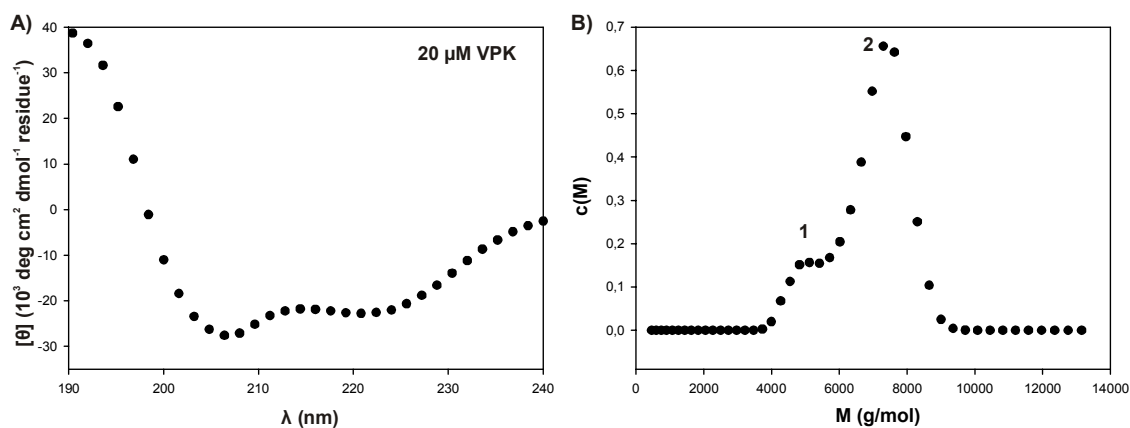


Figure 6.12 A) CD spectrum of a 20 μM solution of isolated VPK and B) molecular weight distribution of a 50 μM solution of isolated VPK indicating equilibrium between two species (1: 4700 g/mol and 2: 7500 g/mol). Measurements were performed at pH 7.4 (100 mM phosphate buffer).

For the thermodynamic investigation presented in section 6.3 the situation is different, since unfolding of the peptide starts from equilibrium when the heterodimers are fully formed. The condition that allows neglecting homooligomerization in analyzing temperature induced equilibrium unfolding is that the melting points of the heterooligomers are significantly higher.²²⁵ The markedly larger helix content and melting points of the heterodimers indicate that VPK homooligomers are strongly disfavored. At the temperatures, at which the heteromers unfold the much less stable homomers do not compete since it can be assumed that their equilibrium concentration at the melting point of the heterodimer is negligible. This condition is readily fulfilled by all VPE-VPK variants. The individual a16 analogues have melting points that are by more than 20 K lower than those of the heteromers. Since SPR, however, is an isothermal method the VPK analogues substituted at position a16 are stable in the absence of VPE under the conditions applied (25°C, 1 atm) and cannot be ignored. It may be noted at this point that the fact that the thermodynamic data resulting from the kinetic analysis without mass transport limitation are within the same order of magnitude as the equilibrium data (Table 6.4) indicates that the contribution of VPK self-association is not very pronounced. This is in agreement with the low melting points of the individual VPK analogues. A reliable calculation of the kinetics of their formation based on SPR, on the other hand, is impossible.

With that said, a quantitative analysis of the impact of Abu side chain fluorination on coiled-coil folding at position a16 is not available at present. This, in turn, points to a certain shortcoming of the current design. Although the effects were readily detectable for position d19 the actual position-dependence, therefore, remains an issue of future research. To this end, the design requires a slight modification such that the individual VPK peptides are all monomeric. Regarding the findings for position d19, however, this approach has a great chance of success.

7 Summary and Outlook

The aim of this study was a thermodynamic and kinetic characterization of the molecular interactions of fluorinated aliphatic amino acids with native hydrophobic residues. To this end, the hydrophobic core of a heterodimeric coiled-coil peptide served as a model for a natural polypeptide environment. The overarching objective was to assess the impact of altering fluorine content and therewith hydrophobicity and steric size on thermodynamic stability as well as kinetics of protein folding. In addition, this study intended to reveal as to how far subtle differences in the environment itself would affect the impact of fluorination. In this respect these investigations represent a complement to previous studies in the group of Prof. Kokschi, in which a different model system and different methods have been applied.

The parental coiled coil VPE-VPK has been structurally characterized to proof that it folds into a parallel heterodimer. Hereupon, thirteen variants of VPK were synthesized to provide an equal substitution pattern either at position a16 or position d19 through incorporation of Abu, its fluorinated analogues MfeGly, DfeGly, and TfeGly as well as DfpGly. This substitution scheme allowed for a systematic investigation of the impact of increasing fluorine content, and thus size and hydrophobicity of the side chain, on the stability of the VPE-VPK interaction. Furthermore, the two substitution sites exhibiting different packing preferences allowed assessing the impact of the microenvironment on the interactions of these building blocks. For each series of VPK peptides a variant containing leucine at the respective substitution position served as a reference.

Hydrophobicity of the amino acids was evaluated on the basis of their retention times on a reversed phase C18-column. While native aliphatic amino acids exhibit the expected correlation between side chain volume and retention time, increasing volume by fluorination has a different effect. Most of the fluorinated amino acids are less hydrophobic than expected based on size arguments, which is explained by fluorine-induced polarity. Increasing fluorine content, however, enhances hydrophobicity more vigorously than size alone, which points to fluorine's tendency to reduce polarizability and thus dispersive interactions of alkyl groups with water. Beyond a certain threshold, which is reached for three fluorine atoms in the series of the Abu analogues, fluorinated amino acids, thus, become hyperhydrophobic, i.e. more hydrophobic than expected based on size arguments alone.

Regardless of their position within the hydrophobic core, the amino acids studied here mostly retain secondary structure, while destabilizing the coiled-coil interaction compared to the much more bulky and hydrophobic leucine side chain. However, internal comparison of the fluorinated amino acids reveals distinct differences in their ef-

fects depending on whether they are present at position a16 or d19. At position a16 increasing the size of the side chain through addition of fluorine atoms (in the series MfeGly, DfeGly and TfeGly) or a methyl group (DfpGly) increases the stability of the coiled-coil assembly. Apart from MfeGly, the same substitutions at position d19, in contrast, reveal no noticeable impact on stability among them. The observed differences of position a and d are explained by their distinctly different packing preferences. While position d exposes the strongly polarized β -methylene group to the interacting β -methylene groups of the VPE-strand, position a16 exposes the bulk of the side chain and turns the β -methylene groups away from the hydrophobic core. Thus, fluorine-induced polarity apparently has a stronger destabilizing effect at position d19 while at position a16 the size of the side chain is the prevailing factor that determines stability. These results indicate that although both positions are part of the same hydrophobic environment, their packing has a strong impact on the effect of side chain fluorination; hence the conclusion that the microenvironment of fluorinated amino acids itself directs their impact on molecular interactions.

Abu and MfeGly furthermore represent two hallmarks in the discussion of the impact of helix propensity on coiled-coil interactions. Although it is not possible to thermodynamically quantify helix propensity using coiled-coil models, the fact that MfeGly substitutions yield the most helical and at the same time least stable dimers supports the conclusion that helix propensity is a less important factor to control the thermodynamic stability of coiled-coil peptides. Conversely, the slightly more helix favoring Abu heavily destabilizes the coiled coil compared to Leu, since its reduced size and hydrophobicity effectuate much weaker packing within the hydrophobic core.

The investigation of a recently developed ^{19}F -NMR label, the amino acid CF_3 -Bpg, which carries a very bulky and conformationally rigid side chain, furthermore revealed that conformational flexibility of hydrophobic side chains is important to gain efficient packing within the hydrophobic core. Both, at position a16 and d19, this amino acid despite its pronounced hydrophobicity, strongly destabilizes the VPE-VPK interaction. Although it retains secondary structure, these results indicate that packing interactions of this amino acid with other side chains are strongly disfavored.

Further investigations applying the coiled-coil model may include fluorinated building blocks that have a completely different substitution pattern. All the multiply fluorinated amino acids studied in this thesis carry fluorine substituents at the same carbon. However, vicinal substitution may also have an impact on side chain conformation (see the *gauche* effect, section 2.2.1) that may affect side chain packing as well as the preference for secondary structures. In addition, the *gauche* effect may also have an impact on the conformation of the Abu analogues investigated here. Studying the conforma-

tional effects of fluorination applying high-resolution methods such as NMR and crystal structure analysis in the context of protein-protein interactions, however, is essential to provide a full insight. Furthermore, a quantification of the helix propensities applying the model proposed by Chiu *et al.* (see section 6.6) would provide a complete set of data that fully characterizes the properties of these building blocks in the context of α -helical protein-protein interactions. The differences in thermodynamic values that describe helix propensity could be subtracted from the stability differences observed for the coiled-coil interactions. These adapted values would then exclusively trace back to intermolecular interactions between the side chains, which would provide an even deeper insight into the effect of size and polarity of the fluorinated side chains.

The kinetic investigations applying the SPR based biosensor were successful for peptides carrying Abu, DfeGly, TfeGly, and DfpGly at position d19. Since VPK has a tendency to also form homooligomers, the less destabilizing substitutions at position a16 resulted in formation of weakly assembled homotypic coiled coils in the absence of VPE. While this did not hamper the thermodynamic equilibrium studies by CD, kinetic data could not be derived from the respective SPR experiments. The VPK variants that carried substitutions at position d19, however, exhibited predominantly random coil structures and kinetic data could be computed from their sensograms. The thermodynamic data calculated from SPR are in good agreement with those from the CD equilibrium studies. The kinetic data reveal that difluorination (DfeGly) of Abu accelerates coiled-coil association due to increasing hydrophobicity of the side chain thus promoting desolvation and burial within the hydrophobic core. On the other hand, addition of a third fluorine (TfeGly) atom leads to a decrease in association rate. This finding corresponds well to earlier findings with a self-replicating coiled coil that exhibited a decrease in product formation rate along with increasing fluorine content. Thus, the same behavior of coiled-coil peptides has been shown applying a completely different technique. Accordingly, SPR supports the significance of these earlier results. Although awaiting direct experimental proof, the conclusion that formation of fluorous 'clusters' in the unfolded state of a protein, i.e. the 'fluorous effect', may complicate folding can therefore be held up.

The dissociation rate shows a good correlation with hydrophobicity. Along with increasing hydrophobicity the amino acids are less readily withdrawn from the hydrophobic core. Thus, the dissociation rate decreases in the order Abu, DfeGly and TfeGly. DfpGly does not follow this trend, which may be explained by its structural dissimilarity to the Abu analogues. Since MfeGly and CF₃-Bpg were not available at the time these investigations were carried out, assessing their kinetic effects remains an issue of future work. The detection of the postulated fluorous 'clusters' may be approached by

NMR (by measurement of ^{19}F NOE). However, regarding the large association rates of the coiled coils studied here, it may not be possible to detect these clusters since they are kinetically unstable on the NMR time scale. Thus, these studies require the design of a short random coil peptide that shows unspecific aggregation due to the fluororous effect. If it were possible to prove that this aggregation is due to the fluororous effect this would indirectly prove that the formation of fluororous clusters may stabilize the unfolded state of polypeptides.

The future SPR studies using the coiled-coil model should furthermore consider an improvement of the model design so as to prevent the formation of even weakly assembled homooligomers, since these unfortunately hamper the kinetic analysis (position a16 variants). Incorporation of two Asn residues placed at opposite sites of the hydrophobic core is known to have a strong impact on folding specificity through formation of intermolecular hydrogen bonds (see section 6.1.1). At the same time its polarity destabilizes the homooligomeric assemblies. This effect, however, will also be present in the heterodimers. Therefore, the coiled coil may need some additional structural alterations since the reduced stability could render the model too sensitive for substitutions. Moreover, the polar Asn should not interact with the fluorinated residues, since this may give rise to polar interactions such as hydrogen bonds that, albeit of utmost interest, were not present in the former design. It would, therefore, be advisable to elongate the monomers by one heptad. The Asn should then be placed in one of the outer heptads while the central core positions could be used for fluorine modifications. Provided that the adapted design retains the parallel heterodimeric folding specificity, the effects of fluorine substitutions will be identical to those presented here. In an additional study the coiled coil may be used to study the polar interactions named above. Placing polar residues opposite to the fluorinated residues could be used to probe such interactions, for example, by NMR.

Having a picture of the effects of side chain fluorination within the hydrophobic core, one of the most important next steps would be the characterization of fluorine's impact within the charged interaction domain (positions e and g) of the coiled coil, since salt-bridges are equally important in directing protein-protein interactions. Fluorination of charged amino acids such as Glu (fluoroGlu) is expected to alter hydrophobicity of their side chains in line with having a strong impact on pK_a . One may prophesy these individual contributions, whereas the net effect on the stability and kinetics of coiled-coil interactions is difficult to predict. The coiled-coil based model system described here will provide an ideal target for these studies. The position-dependence (e-position vs. g-position) and different combinations would have to be studied (e.g. fluoroGlu-Lys,

fluoroGlu-Arg) to find the optimal interaction partners. A rough quantification of the contribution of these fluorinated amino acids to the stability of the coiled coil may be envisioned to provide the basis for fine-tuning of protein-protein interactions. For example, fluorine is expected to stabilize the anionic state of the Glu side chain and may therefore be used to stabilize protein-protein interactions or substrate binding under more extreme pH conditions, which could, for example, be useful for developing tailor-made industrial enzymes that are active under relatively harsh conditions.

One may expect that taking all the data available today together with those that will be generated in the future will certainly add value to our current understanding of fluorine's effects within a natural protein environment. It may then be possible to establish rules for the design of fluorinated peptides and proteins with superior properties that have great potential in analytical, clinical, and industrial applications.

8 Literature

1. S. H. Gellman, *Chem. Rev.* **1997**, *97*, 1231-1232.
2. R. E. Babine, S. L. Bender, *Chem. Rev.* **1997**, *97*, 1359-1472.
3. A. L. Weber, S. L. Miller, *J. Mol. Evol.* **1981**, *17*, 273-284.
4. C. W. Valerie, J. C. Stuart, C.-P. Anne, X. Y. Jun, A. G. Andrew, R. W. Marc, W. D. Mark, H. Ray, L. W. Keith, H.-S. Ian, *Electrophoresis* **1995**, *16*, 1090-1094.
5. V. Bellotti, F. Chiti, *Curr. Opin. Struct. Biol.* **2008**, *18*, 771-779.
6. C. W. Lee-Jun, *Muscle & Nerve* **2007**, *36*, 279-293.
7. E. Lang, J. Bléhaut, *Specialty Chemicals Magazine* **2008**, *28*, 46-48.
8. T. Matthews, M. Salgo, M. Greenberg, J. Chung, R. DeMasi, D. Bolognesi, *Nat. Rev. Drug Discov.* **2004**, *3*, 215-225.
9. A. Hüther, U. Dietrich, *AIDS Rev.* **2007**, *9*, 208-217.
10. M. Morishita, N. A. Peppas, *Drug Discovery Today* **2006**, *11*, 905-910.
11. A. Giannis, T. Kolter, *Angew. Chem. Int. Ed.* **1993**, *32*, 1244-1267.
12. J. T. Welch, in *Fluorine and Health*, 1 ed. (Eds.: A. Tressaud, G. Haufe), Elsevier, Amsterdam, **2008**, pp. 699-735.
13. J. Chatterjee, C. Gilon, A. Hoffman, H. Kessler, *Acc. Chem. Res.* **2008**, *41*, 1331-1342.
14. D. Seebach, M. Overhand, F. N. M. Kühnle, B. Martinoni, L. Oberer, U. Hommel, H. Widmer, *Helv. Chim. Acta* **1996**, *79*, 913-941.
15. J. Frackenpohl, P. Arvidsson, I. , J. Schreiber, V , D. Seebach, *ChemBioChem* **2001**, *2*, 445-455.
16. K. Hamamoto, Y. Kida, Y. Zhang, T. Shimizu, K. Kuwano, *Microbiol. Immunol.* **2002**, *46*, 741-749.
17. B. Kokschi, N. Sewald, H.-J. Hofmann, K. Burger, H.-D. Jakubke, *J. Pept. Sci.* **1997**, *3*, 157-167.
18. K. Müller, C. Faeh, F. Diederich, *Science* **2007**, *317*, 1881-1886.
19. N. C. Yoder, K. Kumar, *Chem. Soc. Rev.* **2002**, *31*, 335-341.
20. C. Jäckel, B. Kokschi, *Eur. J. Org. Chem.* **2005**, *2005*, 4483-4503.
21. A. F. Hollemann, *Lehrbuch Der Anorganischen Chemie, Vol. 101*, 34 ed., de Gruyter, Berlin, New York, **1995**, 432-435; 829.
22. D. B. Harper, D. O'Hagan, *Nat. Prod. Rep.* **1994**, *11*, 123-133.
23. A. Bondi, *J. Phys. Chem.* **1964**, *68*, 441-451.
24. L. Pauling, *The Nature of the Chemical Bond and the Structure of Molecules and Crystals; an Introduction to Modern Structural Chemistry*, 3d ed., Cornell University Press, Ithaca, New York, **1960**, 85.

25. M. Hesse, H. Meier, B. Zeeh, *Spektroskopische Methoden in Der Organischen Chemie, Vol. 5*, Thieme, Stuttgart, New York, **1995**, 202.
26. M. A. Danielson, J. J. Falke, *Annu. Rev. Biophys. Biomol. Struct.* **1996**, *25*, 163-195.
27. S. L. Cobb, C. D. Murphy, *J. Fluorine Chem.* **2009**, *130*, 132-143.
28. G. Brix, M. E. Bellemann, U. Haberkorn, L. Gerlach, W. J. Lorenz, *Nucl. Med. Biol.* **1996**, *23*, 897-906.
29. J. F. Schenck, *J. Magn. Res. Imaging* **2000**, *12*, 2-19.
30. C. Heidelberger, N. K. Chaudhuri, P. Danneberg, D. Mooren, L. Griesbach, R. Duschinsky, R. J. Schnitzer, E. Plevin, J. Scheiner, *Nature* **1957**, *179*, 663-666.
31. E. P. Cormier, M. Das, I. Ojima, in *Fluorine in Medicinal Chemistry and Chemical Biology* (Ed.: I. Ojima), Wiley-Blackwell, Chichester, **2009**, p. 548.
32. O. Couturier, A. Luxen, J. F. Chatal, J. P. Vuillez, P. Rigo, R. Hustinx, *Eur. J. Nucl. Med. Mol. Imaging* **2004**, *31*, 1182-1206.
33. M. Reivich, D. Kuhl, A. Wolf, J. Greenberg, M. Phelps, T. Ido, V. Casella, J. Fowler, E. Hoffman, A. Alavi, P. Som, L. Sokoloff, *Circ. Res.* **1979**, *44*, 127-137.
34. N. D. Volkow, J. S. Fowler, S. J. Gatley, J. Logan, G.-J. Wang, Y.-S. Ding, S. Dewey, *J. Nucl. Med.* **1996**, *37*, 1242-1256.
35. S. M. Ametamey, M. Honer, P. A. Schubiger, *Chem. Rev.* **2008**, *108*, 1501-1516.
36. S. M. Okarvi, *Eur. J. Nucl. Med. Mol. Imaging* **2001**, *28*, 929-938.
37. S. Guhlke, H.-J. Wester, C. Bruns, G. Stöcklin, *Nucl. Med. Biol.* **1994**, *21*, 819-825.
38. G. Vaidyanathan, M. R. Zalutsky, *Nucl. Med. Biol.* **1997**, *24*, 171-178.
39. M. Berndt, J. Pietzsch, F. Wuest, *Nucl. Med. Biol.* **2007**, *34*, 5-15.
40. J. Marik, J. L. Sutcliffe, *Tetrahedron Lett.* **2006**, *47*, 6681-6684.
41. M. R. Kilbourn, X. Shao, in *Fluorine in Medicinal Chemistry and Chemical Biology* (Ed.: I. Ojima), Wiley-Blackwell, Chichester, **2009**, pp. 361-388.
42. J. Becaud, L. Mu, M. n. Karramkam, P. A. Schubiger, S. M. Ametamey, K. Graham, T. Stellfeld, L. Lehmann, S. Borkowski, D. Berndorff, L. Dinkelborg, A. Srinivasan, R. Smits, B. Koks, *Bioconjugate Chemistry* **2009**, *20*, 2254-2261.
43. O. N. Sharts, L. P. Avakyants, in *229th ACS National Meeting*, American Chemical Society, San Diego, CA, USA, **2005**.
44. C. M. Sharts, V. S. Gorelik, A. M. Agoltsov, L. I. Zlobina, O. N. Sharts, in *Proceedings of SPIE-The International Society for Optical Engineering*, SPIE-The International Society for Optical Engineering, San Diego, CA, USA, **1999**, pp. 317-326.
45. V. S. Gorelik, A. V. Chervyakov, L. I. Zlobina, C. M. Sharts, in *Proceedings of SPIE-The International Society for Optical Engineering*, SPIE-The International Society for Optical Engineering, Moscow, Russia, **1999**, pp. 16-27.

46. C. W. Thornber, *Chem. Soc. Rev.* **1979**, *8*, 563-580.
47. L. M. Lima, E. J. Barreiro, *Curr. Med. Chem.* **2005**, *12*, 23-49.
48. S. Purser, P. R. Moore, S. Swallow, V. Gouverneur, *Chem. Soc. Rev.* **2008**, *37*, 320-330.
49. D. O'Hagan, H. S. Rzepa, *Chem. Commun.* **1997**, 645-652.
50. Y. Tang, G. Ghirlanda, W. A. Petka, T. Nakajima, W. F. DeGrado, D. A. Tirrell, *Angew. Chem. Int. Ed.* **2001**, *40*, 1494-1496.
51. T. Nagai, G. Nishioka, M. Koyama, A. Ando, T. Miki, I. Kumadaki, *J. Fluorine Chem.* **1992**, *57*, 229-237.
52. G. Bott, L. D. Field, S. Sternhell, *J. Am. Chem. Soc.* **1980**, *102*, 5618-5626.
53. R. J. Abraham, S. L. R. Ellison, P. Schonholzer, W. A. Thomas, *Tetrahedron* **1986**, *42*, 2101-2110.
54. T. Allmendinger, P. Furet, E. Hungerbühler, *Tetrahedron Lett.* **1990**, *31*, 7297-7300.
55. T. Yamazaki, T. Taguchi, I. Ojima, in *Fluorine in Medicinal Chemistry and Chemical Biology* (Ed.: I. Ojima), Wiley-Blackwell, Chichester, **2009**, pp. 22-24.
56. T. Allmendinger, E. Felder, E. Hungarbühler, *Tetrahedron Lett.* **1990**, *31*, 7301-7304.
57. J. J. Urban, B. G. Tillman, W. A. Cronin, *J. Phys. Chem. A* **2006**, *110*, 11120-11129.
58. S. Couve-Bonnaire, D. Cahard, X. Pannecoucke, *Org. Biomol. Chem.* **2007**, *5*, 1151-1157.
59. X. Wang, J. , F. Etzkorn, A. , *Pept. Sci.* **2006**, *84*, 125-146.
60. S. Oishi, H. Kamitani, Y. Kodera, K. Watanabe, K. Kobayashi, T. Narumi, K. Tomita, H. Ohno, T. Naito, E. Kodama, M. Matsuoka, N. Fujii, *Org. Biomol. Chem.* **2009**, *7*, 2872-2877.
61. H. Senderowitz, P. Aped, B. Fuchs, *Tetrahedron* **1993**, *49*, 3879-3898.
62. J.-P. Bégué, D. Deplon-Bonnet, in *Bioorganic and Medicinal Chemistry of Fluorine*, John Wiley & Sons, Inc., Hoboken, New Jersey, **2008**, pp. 180-222.
63. L. Goodman, H. Gu, V. Pophristic, *J. Phys. Chem. A* **2005**, *109*, 1223-1229.
64. K. B. Wiberg, M. A. Murcko, K. E. Laidig, P. J. MacDougall, *J. Phys. Chem.* **1990**, *94*, 6956-6959.
65. C. R. S. Briggs, D. O'Hagan, J. A. K. Howard, D. S. Yufit, *J. Fluorine Chem.* **2003**, *119*, 9-13.
66. C. R. S. Briggs, D. O'Hagan, H. S. Rzepa, A. M. Z. Slawin, *J. Fluorine Chem.* **2004**, *125*, 19-25.
67. C. R. S. Briggs, M. J. Allen, D. O'Hagan, D. J. Tozer, A. M. Z. Slawin, A. E. Goeta, J. A. K. Howard, *Org. Biomol. Chem.* **2004**, *2*, 732-740.

68. W. Kim, K. Hardcastle, I., V. Conticello, P., *Angew. Chem. Int. Ed.* **2006**, *45*, 8141-8145.
69. B. E. Smart, *J. Fluorine Chem.* **2001**, *109*, 3-11.
70. A. Avdeef, *Curr. Top. Med. Chem.* **2001**, *1*, 277-351.
71. B. Cornils, *Angew. Chem. Int. Ed.* **1997**, *36*, 2057-2059.
72. V. Montanari, K. Kumar, *J. Fluorine Chem.* **2006**, *127*, 565-570.
73. A. Garcia-Bernabé, Carl C. Tzschucke, W. Bannwarth, R. Haag, *Adv. Synth. Catal.* **2005**, *347*, 1389-1394.
74. S. K. Mamidyala, K.-S. Ko, F. A. Jaipuri, G. Park, N. L. Pohl, *J. Fluorine Chem.* **2006**, *127*, 571-579.
75. T. Takayuki, N. Aya, Y. Tomoko, N. Hajime, M. Koichi, *Eur. J. Org. Chem.* **2008**, 1331-1335.
76. E. T. Kool, H. O. Sintim, *Chem. Commun.* **2006**, 3665-3675.
77. R. Paulini, K. Müller, F. Diederich, *Angew. Chem. Int. Ed.* **2005**, *44*, 1788-1805.
78. M. Schlosser, *Angew. Chem. Int. Ed.* **1998**, *37*, 1496-1513.
79. A. Donetti, E. Cereda, A. Ezhaya, R. Micheletti, *J. Med. Chem.* **1989**, *32*, 957-961.
80. M. B. van Niel, I. Collins, M. S. Beer, H. B. Broughton, S. K. F. Cheng, S. C. Godacre, A. Heald, K. L. Locker, A. M. MacLeod, D. Morrison, C. R. Moyes, D. O'Connor, A. Pike, M. Rowley, M. G. N. Russell, B. Sohal, et al., *J. Med. Chem.* **1999**, *42*, 2087-2104.
81. J. D. Dunitz, R. Taylor, *Chem. Eur. J.* **1997**, *3*, 89-98.
82. L. H. Takahashi, R. Radhakrishnan, R. E. Rosenfield, E. F. Meyer, D. A. Trainor, *J. Am. Chem. Soc.* **1989**, *111*, 3368-3374.
83. E. Carosati, S. Sciabola, G. Cruciani, *J. Med. Chem.* **2004**, *47*, 5114-5125.
84. P. Zhou, J. Zou, F. Tian, Z. Shang, *J. Chem. Inf. Model.* **2009**, *49*, 2344-2355.
85. F. Hof, D. Scofield, M., W. B. Schweizer, F. Diederich, *Angew. Chem. Int. Ed.* **2004**, *43*, 5056-5059.
86. J. A. Olsen, D. W. Banner, P. Seiler, U. Obst Sander, A. D'Arcy, M. Stihle, K. Muller, F. Diederich, *Angew. Chem. Int. Ed.* **2003**, *42*, 2507-2511.
87. C. B. Justin, K. Hong Woo, G. D. Stephen, *ChemBioChem* **2004**, *5*, 622-627.
88. B. K. Park, N. R. Kitteringham, P. M. O'Neill, *Annu. Rev. Pharmacol. Toxicol.* **2003**, *41*, 443-470.
89. J.-P. Bégué, D. Bonnet-Delpon, in *Bioorganic and Medicinal Chemistry of Fluorine*, John Wiley & Sons, Hoboken, New Jersey, **2008**, pp. 84-89.
90. J. Fried, D. K. Mitra, M. Nagarajan, M. M. Mehrotra, *J. Med. Chem.* **1980**, *23*, 234-237.

91. K. Bannai, T. Toru, T. Oba, T. Tanaka, N. Okamura, K. Watanabe, A. Hazato, S. Kurozumi, *Tetrahedron* **1983**, *39*, 3807-3819.
92. M. C. Walsh, W. E. Klopfenstein, J. L. Harwood, *Phytochemistry* **1990**, *29*, 3797-3799.
93. H. Lauble, M. C. Kennedy, M. H. Emptage, H. Beinert, C. D. Stout, *Proc. Natl. Acad. Sci. USA* **1996**, *93*, 13699-13703.
94. D. O'Hagan, C. Schaffrath, S. L. Cobb, J. T. G. Hamilton, C. D. Murphy, *Nature* **2002**, *416*, 279-279.
95. C. Dong, F. Huang, H. Deng, C. Schaffrath, J. B. Spencer, D. O'Hagan, J. H. Naismith, *Nature* **2004**, *427*, 561-565.
96. X. Zhu, D. A. Robinson, A. R. McEwan, D. O'Hagan, J. H. Naismith, *J. Am. Chem. Soc.* **2007**, *129*, 14597-14604.
97. A. Sutherland, C. L. Willis, *Nat. Prod. Rep.* **2000**, *17*, 621-631.
98. X.-L. Qiu, W.-D. Meng, F.-L. Qing, *Tetrahedron* **2004**, *60*, 6711-6745.
99. J. M. Humphrey, A. R. Chamberlin, *Chem. Rev.* **1997**, *97*, 2243-2266.
100. S.-Y. Han, Y.-A. Kim, *Tetrahedron* **2004**, *60*, 2447-2467.
101. R. B. Merrifield, *J. Am. Chem. Soc.* **1963**, *85*, 2149-2154.
102. J. A. Ellman, D. Mendel, P. G. Schultz, *Science* **1992**, *255*, 197-200.
103. R. C. Milton, S. C. Milton, S. B. Kent, *Science* **1992**, *256*, 1445-1448.
104. S. B. H. Kent, *Chem. Soc. Rev.* **2009**, *38*, 338-351.
105. C. P. R. Hackenberger, D. Schwarzer, *Angew. Chem. Int. Ed.* **2008**, *47*, 10030-10074.
106. R. David, M. P. Richter, A. G. Beck-Sickinger, *Eur. J. Biochem.* **2004**, *271*, 663-677.
107. L. Wang, P. G. Schultz, *Angew. Chem. Int. Ed.* **2005**, *44*, 34-66.
108. N. Budisa, *Angew. Chem. Int. Ed.* **2004**, *43*, 6426-6463.
109. G. N. Cohen, R. Munier, *Biochim. Biophys. Acta* **1956**, *21*, 592-593.
110. M. Ibba, P. Kast, H. Hennecke, *Biochemistry* **1994**, *33*, 7107-7112.
111. V. Doring, H. D. Mootz, L. A. Nangle, T. L. Hendrickson, V. de Crecy-Lagard, P. Schimmel, P. Marliere, *Science* **2001**, *292*, 501-504.
112. Y. Tang, D. A. Tirrell, *Biochemistry* **2002**, *41*, 10635-10645.
113. M. Leone, R. A. Rodriguez-Mias, M. Pellecchia, *ChemBioChem* **2003**, *4*, 649-650.
114. C. J. Noren, S. J. Anthony-Cahill, M. C. Griffith, P. G. Schultz, *Science* **1989**, *244*, 182-188.
115. T. G. Heckler, L. H. Chang, Y. Zama, T. Naka, M. S. Chorghade, S. M. Hecht, *Biochemistry* **1984**, *23*, 1468-1473.

116. G. Baldini, B. Martoglio, A. Schachenmann, C. Zugliani, J. Brunner, *Biochemistry* **1988**, *27*, 7951-7959.
117. S. A. Robertson, J. A. Ellman, P. G. Schultz, *J. Am. Chem. Soc.* **1991**, *113*, 2722-2729.
118. J. F. Eichler, J. C. Cramer, K. L. Kirk, J. G. Bann, *ChemBioChem* **2005**, *6*, 2170-2173.
119. A. S. Ulrich, *Prog. Nucl. Magn. Reson. Spectrosc.* **2005**, *46*, 1-21.
120. M. Zasloff, *Nature* **2002**, *415*, 389-395.
121. P. Lundberg, Ü. Langel, *J. Mol. Recognit.* **2003**, *16*, 227-233.
122. J. Fernández-Carneado, M. Kogan, J., S. Pujals, E. Giralt, *Pept. Sci.* **2004**, *76*, 196-203.
123. S. Afonin, R. W. Glaser, M. Berditchevskaia, P. Wadhvani, K.-H. Gührs, U. Möllmann, A. Perner, A. S. Ulrich, *ChemBioChem* **2003**, *4*, 1151-1163.
124. P. Wadhvani, J. Bürck, E. Strandberg, C. Mink, S. Afonin, A. S. Ulrich, *J. Am. Chem. Soc.* **2008**, *130*, 16515-16517.
125. L. A. Carpino, *J. Org. Chem.* **1988**, *53*, 875-878.
126. F. Weygand, W. Steglich, W. Oettmeier, *Chem. Ber.* **1970**, *103*, 1655-1663.
127. D. Maisch, P. Wadhvani, S. Afonin, C. Bolttcher, B. Kokschi, A. S. Ulrich, *J. Am. Chem. Soc.* **2009**, *131*, 15596-15597.
128. P. K. Mykhailiuk, S. Afonin, A. N. Chernega, E. B. Rusanov, M. O. Platonov, G. G. Dubinina, M. Berditsch, A. S. Ulrich, I. V. Komarov, *Angew. Chem. Int. Ed.* **2006**, *45*, 5659-5661.
129. P. K. Mykhailiuk, S. Afonin, G. V. Palamarchuk, O. V. Shishkin, A. S. Ulrich, I. V. Komarov, *Angew. Chem. Int. Ed.* **2008**, *47*, 5765-5767.
130. E. N. G. Marsh, B. C. Buer, A. Ramamoorthy, *Mol. Biosyst.* **2009**, *5*, 1143-1147.
131. L. M. Gottler, H. Y. Lee, C. E. Shelburne, A. Ramamoorthy, E. N. Marsh, *ChemBioChem* **2008**, *9*, 370-373.
132. A. Niemz, D. A. Tirrell, *J. Am. Chem. Soc.* **2001**, *123*, 7407-7413.
133. T. Arai, T. Imachi, T. Kato, H. I. Ogawa, T. Fujimoto, N. Nishino, *Bull. Chem. Soc. Jpn.* **1996**, *69*, 1383-1389.
134. H. Meng, K. Kumar, *J. Am. Chem. Soc.* **2007**, *129*, 15615-15622.
135. H. Meng, S. T. Krishnaji, M. Beinborn, K. Kumar, *J. Med. Chem.* **2008**, *51*, 7303-7307.
136. J. K. Montclare, S. Son, G. A. Clark, K. Kumar, D. A. Tirrell, *ChemBioChem* **2009**, *10*, 84-86.
137. Y. Tang, D. A. Tirrell, *J. Am. Chem. Soc.* **2001**, *123*, 11089-11090.
138. P. Wang, Y. Tang, D. A. Tirrell, *J. Am. Chem. Soc.* **2003**, *125*, 6900-6906.

139. Y. Tang, G. Ghirlanda, N. Vaidehi, J. Kua, D. T. Mainz, W. A. Goddard, W. F. DeGrado, D. A. Tirrell, *Biochemistry* **2001**, *40*, 2790-2796.
140. S. Son, I. C. Tanrikulu, D. A. Tirrell, *ChemBioChem* **2006**, *7*, 1251-1257.
141. B. Bilgicer, A. Fichera, K. Kumar, *J. Am. Chem. Soc.* **2001**, *123*, 4393-4399.
142. B. Bilgicer, X. Xing, K. Kumar, *J. Am. Chem. Soc.* **2001**, *123*, 11815-11816.
143. B. Bilgicer, K. Kumar, *Tetrahedron* **2002**, *58*, 4105-4112.
144. B. Bilgicer, K. Kumar, *Proc. Natl. Acad. Sci. USA* **2004**, *101*, 15324-15329.
145. N. Naarmann, B. Bilgicer, H. Meng, K. Kumar, C. Steinem, *Angew. Chem. Int. Ed.* **2006**, *45*, 2588-2591.
146. K.-H. Lee, H.-Y. Lee, M. M. Slutsky, J. T. Anderson, E. N. G. Marsh, *Biochemistry* **2004**, *43*, 16277-16284.
147. H.-Y. Lee, K.-H. Lee, H. M. Al-Hashimi, E. N. G. Marsh, *J. Am. Chem. Soc.* **2006**, *128*, 337-343.
148. L. M. Gottler, R. de la Salud-Bea, E. N. G. Marsh, *Biochemistry* **2008**, *47*, 4484-4490.
149. P. Luo, R. L. Baldwin, *Biochemistry* **1997**, *36*, 8413-8421.
150. D. Roccatano, G. Colombo, M. Fioroni, A. E. Mark, *Proc. Natl. Acad. Sci. USA* **2002**, *99*, 12179-12184.
151. B. C. Buer, R. de la Salud-Bea, H. M. Al Hashimi, E. N. G. Marsh, *Biochemistry* **2009**, *48*, 10810-10817.
152. T. Panchenko, W. W. Zhu, J. K. Montclare, *Biotechnol. Bioeng.* **2006**, *94*, 921-930.
153. T. H. Yoo, A. J. Link, D. A. Tirrell, *Proc. Natl. Acad. Sci. USA* **2007**, *104*, 13887-13890.
154. C. Jäckel, M. Salwiczek, B. Koksich, *Angew. Chem. Int. Ed.* **2006**, *45*, 4198-4203.
155. J. K. Montclare, D. A. Tirrell, *Angew. Chem. Int. Ed.* **2006**, *45*, 4518-4521.
156. C. Jäckel, P. Kast, D. Hilvert, *Annu. Rev. Biophys.* **2008**, *37*, 153-173.
157. M. G. Woll, E. B. Hadley, S. Mecozzi, S. H. Gellman, *J. Am. Chem. Soc.* **2006**, *128*, 15932-15933.
158. N. Voloshchuk, A. Y. Zhu, D. Snyder, J. K. Montclare, *Bioorg. Med. Chem. Lett.* **2009**, *19*, 5449-5451.
159. T. Vagt, E. Nyakatura, M. Salwiczek, C. Jäckel, B. Koksich, *Org. Biomol. Chem.* **2010**, DOI: 10.1039/b917205j.
160. R. W. Woody, in *Circular Dichroism and the Conformational Analysis of Biomolecules* (Ed.: G. D. Fasman), Plenum Press, New York, **1996**, pp. 25-67.
161. S. Y. Venyaminov, J. T. Yang, in *Circular Dichroism and the Conformational Analysis of Biomolecules* (Ed.: G. D. Fasman), Plenum Press, New York and London, **1996**, pp. 69-107.

-
162. K. Kuwajima, in *Circular Dichroism and the Conformational Analysis of Biomolecules* (Ed.: G. D. Fasman), Plenum Press, New York, **1996**, pp. 159-199.
163. S. C. Wagner, Doctoral Thesis thesis, Freie Universität (Berlin), **2009**.
164. N. J. Greenfield, *Anal. Biochem.* **1996**, *235*, 1-10.
165. Y.-H. Chen, J. T. Yang, K. H. Chau, *Biochemistry* **1974**, *13*, 3350-3359.
166. P. J. Gans, P. C. Lyu, M. C. Manning, R. Woody, W. , N. R. Kallenbach, *Biopolymers* **1991**, *31*, 1605-1614.
167. R. Woody, W., *Biopolymers* **1978**, *17*, 1451-1467.
168. A. I. Dragan, P. L. Privalov, *J. Mol. Biol.* **2002**, *321*, 891-908.
169. J. M. Brockman, B. P. Nelson, R. M. Corn, *Annu. Rev. Phys. Chem.* **2003**, *51*, 41-63.
170. P. A. van der Merve, in *Surface Plasmon Resonance in Protein-Ligand Interactions: Hydrodynamics and Calorimetry* (Eds.: S. E. Harding, B. Z. Chowdhry), Oxford University Press, Oxford, **2001**, pp. 137-170.
171. M. Malmqvist, *Nature* **1993**, *361*, 186-187.
172. U. Jonsson, L. Fagerstam, B. Ivarsson, B. Johnsson, R. Karlsson, K. Lundh, S. Lofas, B. Persson, H. Roos, I. Ronnberg, et al., *Biotechniques* **1991**, *11*, 620-627.
173. S. Löfås, M. Malmqvist, I. Rönnerberg, E. Stenberg, B. Liedberg, I. Lundström, *Sensors and Actuators B: Chemical* **1991**, *5*, 79-84.
174. T. E. Creighton, *Science* **1988**, *240*, 267-344.
175. P. Y. Chou, G. D. Fasman, *Biochemistry* **1974**, *13*, 211-222.
176. P. Y. Chou, G. D. Fasman, *Biochemistry* **1974**, *13*, 222-245.
177. A. Chakrabarty, T. Kortemme, R. L. Baldwin, *Protein Sci.* **1994**, *3*, 843-852.
178. C. K. Smith, J. M. Withka, L. Regan, *Biochemistry* **1994**, *33*, 5510-5517.
179. K. A. Dill, S. B. Ozkan, M. S. Shell, T. R. Weikl, *Annu. Rev. Biophys.* **2008**, *37*, 289-316.
180. D. N. Woolfson, *Adv. Protein Chem.* **2005**, *70*, 79-112.
181. C. Jäckel, W. Seufert, S. Thust, B. Kocsch, *ChemBioChem* **2004**, *5*, 717-720.
182. F. H. C. Crick, *Nature* **1952**, *170*, 882-883.
183. F. Crick, *Acta Cryst.* **1953**, *6*, 689-697.
184. L. Pauling, R. B. Corey, *Nature* **1953**, *171*, 59-61.
185. J. Sodek, R. S. Hodges, L. B. Smillie, L. Jurasek, *Proc. Natl. Acad. Sci. USA* **1972**, *69*, 3800-3804.
186. W. H. Landschulz, P. F. Johnson, S. L. McKnight, *Science* **1988**, *240*, 1759-1764.
187. E. K. O'Shea, J. D. Klemm, P. S. Kim, T. Alber, *Science* **1991**, *254*, 539-544.

188. C. Cohen, D. Parry, A. D., *Proteins: Struct. Funct. Genet.* **1990**, 7, 1-15.
189. A. Lupas, M. Van Dyke, J. Stock, *Science* **1991**, 252, 1162-1164.
190. O. D. Monera, C. M. Kay, R. S. Hodges, *Biochemistry* **1994**, 33, 3862-3871.
191. T. J. Graddis, D. G. Myszka, I. M. Chaiken, *Biochemistry* **1993**, 32, 12664-12671.
192. N. E. Zhou, C. M. Kay, R. S. Hodges, *J. Mol. Biol.* **1994**, 237, 500-512.
193. W. D. Kohn, C. M. Kay, R. S. Hodges, *Protein Sci.* **1995**, 4, 237-250.
194. N. E. Zhou, C. M. Kay, R. S. Hodges, *Protein Eng.* **1994**, 7, 1365-1372.
195. L. Gonzalez, Jr., D. N. Woolfson, T. Alber, *Nat. Struct. Biol.* **1996**, 3, 1011-1018.
196. M. G. Oakley, P. S. Kim, *Biochemistry* **1998**, 37, 12603-12610.
197. D. L. McClain, H. L. Woods, M. G. Oakley, *J. Am. Chem. Soc.* **2001**, 123, 3151-3152.
198. M. Meier, P. Burkhard, *J. Struct. Biol.* **2006**, 155, 116-129.
199. P. Burkhard, S. Ivaninskii, A. Lustig, *J. Mol. Biol.* **2002**, 318, 901-910.
200. J. Liu, Q. Zheng, Y. Deng, C.-S. Cheng, N. R. Kallenbach, M. Lu, *Proc. Natl. Acad. Sci. USA* **2006**, 103, 15457-15462.
201. P. Burkhard, M. Meier, A. Lustig, *Protein Sci.* **2000**, 9, 2294-2301.
202. E. Moutevelis, D. N. Woolfson, *J. Mol. Biol.* **2009**, 385, 726-732.
203. A. Rose, I. Meier, *Cell. Mol. Life Sci.* **2004**, 61, 1996-2009.
204. J. M. Mason, K. M. Arndt, *ChemBioChem* **2004**, 5, 170-176.
205. W. Weissenhorn, A. Dessen, S. C. Harrison, J. J. Skehel, D. C. Wiley, *Nature* **1997**, 387, 426-430.
206. D. C. Chan, D. Fass, J. M. Berger, P. S. Kim, *Cell* **1997**, 89, 263-273.
207. O. D. Monera, N. E. Zhou, C. M. Kay, R. S. Hodges, *J. Biol. Chem.* **1993**, 268, 19218-19227.
208. G. D. Rose, R. Wolfenden, *Annu. Rev. Biophys. Biomol. Struct.* **1993**, 22, 381-415.
209. K. M. Biswas, D. R. DeVido, J. G. Dorsey, *J. Chromatogr. A* **2003**, 1000, 637-655.
210. M. C. J. Wilce, M.-I. Aguilar, M. T. W. Hearn, *Anal. Chem.* **1995**, 67, 1210-1219.
211. Y. H. Zhao, M. H. Abraham, A. M. Zissimos, *J. Org. Chem.* **2003**, 68, 7368-7373.
212. J. M. Kovacs, C. T. Mant, R. S. Hodges, *Pept. Sci.* **2006**, 84, 283-297.
213. S. A. Samsonov, M. Salwiczek, G. Anders, B. Koksich, M. T. Pisabarro, *J. Phys. Chem. B* **2009**, 113, 16400-16408.
214. J. C. Biffinger, H. W. Kim, S. G. DiMagno, *ChemBioChem* **2004**, 5, 622-627.
215. T. Vagt, Doctoral thesis, Freie Universität Berlin (Berlin), **2009**.

-
216. S. C. Kwok, C. D. Mant, R. S. Hodges, in *25th European Peptide Symposium* (Eds.: S. Bajusz, F. Hudecz), Akadémiai Kiadó, Budapest, **1998**, pp. 34-35.
217. M. Salwiczek, S. Samsonov, T. Vagt, E. Nyakatura, E. Fleige, J. Numata, H. Cölfen, M. T. Pisabarro, B. Kocsch, *Chem. Eur. J.* **2009**, *15*, 7628-7636.
218. D. J. Barlow, J. M. Thornton, *J. Mol. Biol.* **1988**, *201*, 601-619.
219. A. J. Doig, *Biophysical Chemistry* **2002**, *101-102*, 281-293.
220. H. P. Chiu, Y. Suzuki, D. Gullickson, R. Ahmad, B. Kokona, R. Fairman, R. P. Cheng, *J. Am. Chem. Soc.* **2006**, *128*, 15556-15557.
221. H. P. Chiu, R. P. Cheng, *Org. Lett.* **2007**, *9*, 5517-5520.
222. H.-P. Chiu, B. Kokona, R. Fairman, R. P. Cheng, *J. Am. Chem. Soc.* **2009**, *131*, 13192-13193.
223. M. Salwiczek, B. Kocsch, *ChemBioChem* **2009**, *10*, 2867-2870.
224. D. G. Myszka, *Curr. Opin. Biotechnol.* **1997**, *8*, 50-57.
225. D. Krylov, I. Mikhailenko, C. Vinson, *EMBO J.* **1994**, *13*, 2849-2861.

